An analytical examination of retirement strategies in South Africa

by A.J. van Niekerk

Submitted in partial fulfilment of the requirements for the degree
Philosophiae Doctor

Faculty of Natural and Agricultural Sciences
Department of Actuarial Science
University of Pretoria

Supervisor: Professor Eben Maré
March 18, 2025

Andries J. van Niekerk

An analytical examination of retirement strategies in South Africa

March 18, 2025

Supervisor: Professor Eben Maré

University of Pretoria
Faculty of Natural and Agricultural Sciences
Department of Actuarial Science
Corner of Lynnwood Road and Roper Street, Hatfield
Pretoria
0083

Abstract

A typical retirement strategy requires a multifaceted approach, considering various products like annuities and a well-structured investment portfolio. Balancing risks like mortality and longevity, along with factors such as healthcare costs, inflation, and tax implications, is essential for ensuring a secure retirement. Most retirees in South Africa face the challenge of either outliving their retirement savings or living below their means. Studies suggest a 'safe' withdrawal/spending rate of between 4% and 5%, which is below the average fund size-weighted drawdown rate of approximately 6.7% experienced in South Africa.

The success rates of hybrid retirement strategies are evaluated, and the primary aim of these strategies is to enhance the overall success rate and sustainability of retirement portfolios. We assess the success rates of retirement strategies that incorporate foreign exposure by converting any gains in the S&P 500 back to South African Rand (ZAR), factoring in the exchange rate, which is modelled stochastically to simulate real-world currency fluctuations.

Both US and South African inflation rates (CPI) are incorporated to ensure that success rates are evaluated in real terms, capturing the impact of inflation on retirees' income. A core aspect of this study is the incorporation of stochastic correlation and volatility modelling. Using the hyperbolic tangent Ornstein-Uhlenbeck process, we capture the dynamic, complex relationships between relevant asset classes, enabling realistic simulations of asset behaviour under varied market conditions. We analyse the success rates and fugits[1]of living annuities and various retirement strategies, within a South African context.

[1]A fugit is defined as the expected time until portfolio failure.

This page has been intentionally left blank

Acknowledgments

I would like to express my deepest gratitude to my supervisor, Prof. Eben Maré, whose expertise, guidance, and encouragement have been instrumental in the successful completion of this thesis. Throughout this journey, he has been an extraordinary mentor, providing not only academic advice but also unwavering support and motivation. It has been an honour and privilege to work under his supervision, and I am deeply indebted to him for his invaluable contributions to my academic and personal growth.

I am grateful to my family and friends for their unwavering encouragement and support throughout the past few years.

I am deeply grateful to my amazing parents, Dries and Hanlie. Thank you for everything you have done for me, especially for your unwavering support and encouragement throughout my PhD journey. I would not be the person I am today without you. To my sister, Cornitha, thank you for being a pillar of support throughout my journey.

I extend my heartfelt thanks to the anonymous reviewers and editorial staff for their valuable suggestions and constructive feedback on the article submissions, which have greatly enhanced the quality of the final product.

This page has been intentionally left blank

Declaration

I, A.J. van Niekerk, declare that this thesis, which I hereby submit for the degree Philosophiae Doctor at the University of Pretoria, is my own independent work and has not previously been submitted by me for a degree at this or any other tertiary institution.

Centurion, Pretoria, 6 January 2024

Andries J. van Niekerk

Contents

List of Figures

List of Figures

List of Tables

This page has been intentionally left blank

Abbreviations

Abbreviation	Description
ASISA	Association for Saving and Investment in South Africa
CIR	Cox-Ingersoll-Ross Model
CPI	Consumer Price Index
COVID	Coronavirus Disease 2019
EMM	Efficient Method of Moments
FX	Foreign Exchange
GAPM	Gompertz Annuity Pricing Model
gBm	Geometric Brownian Motion
GFC	Global Financial Crisis
JSE	Johannesburg Stock Exchange
JSE Top 40	Top 40 Index on the Johannesburg Stock Exchange
S&P 500	Standard & Poor's 500 Index
SARB	South African Reserve Bank
SARS	South African Revenue Service
Treasury	National Treasury of South Africa
US	United States
USD	United States Dollar
WHO	World Health Organization
ZAR	South African Rand

Notation

Symbol	Description
$\mathcal{N}(0,1)$	Standard normal distribution with mean 0 and variance 1
S_t	Price of the portfolio at time t
μ	Drift term (representing the return of the portfolio)
σ	Volatility (representing the standard deviation of the portfolio)
W_t	Wiener process (standard Brownian motion)
r_p	Portfolio's expected return
$\Pi(t)$	Value of the portfolio at time t
N	Initial investment
ω_{life}	Weight invested in the life annuity
ω_{living}	Weight invested in the living annuity
ω_{equity}	Weight invested in equities
ω_{bond}	Weight invested in bonds
r_{equity}	Monthly real return from equities
r_{bond}	Monthly real return from bonds
r_{living}	Monthly withdrawal required from the living annuity
$a(x,g,R)$	Upfront cost of R1 per year for life, starting at age x
$p(x,i)$	Survival probability from age x to $x+i$
R	Interest rate
φ	Oldest possible age attainable
I	Indicator function for portfolio value
sr	Success rate
M	Number of simulations
r_t	Instantaneous interest rate at time t
κ	Speed of mean reversion
θ	Long-term mean level of interest rates
Γ	Gamma function
F	Hypergeometric function

Definitions and terms

Bootstrap: A statistical method used to resample data with replacement to create numerous simulated samples. In retirement modelling, it is often employed to generate hypothetical return scenarios from historical market data to assess portfolio outcomes under uncertainty.

Conditional median life expectancy: The expected remaining lifespan for an individual at a given age, considering they have already survived to that age. It is used in retirement planning to estimate how long retirement income needs to last.

Diversification: The strategy of spreading investments across various asset classes, sectors, or geographies to reduce risk by limiting the impact of poor performance in any single investment.

Fees: Costs incurred in financial services, including administration, investment management, and advisory fees. These fees can significantly affect the net returns of retirement portfolios over time and are stated per annum.

Fugit: In retirement modelling, fugit refers to the expected time until portfolio failure, i.e., when the portfolio balance reaches zero under specified withdrawal rates and market conditions.

Foreign Exposure: The allocation of a portion of a retirement portfolio to investments outside the investor's home country, aimed at diversifying risks and potentially enhancing returns by accessing foreign markets.

Foreign Exchange (FX): The system of exchanging one currency for another. FX rates are important in retirement modelling when considering foreign exposure, as exchange rate volatility can impact portfolio performance.

Heston Model: The Heston model is a stochastic volatility model that describes the evolution of asset prices by allowing volatility to vary over time, driven by a mean-reverting square root process.

Hybrid strategy: A retirement strategy combining a living annuity (market-linked) and a life annuity (guaranteed income) to balance longevity

risk with growth potential, often improving overall success rates in retirement.

Inflation (CPI): The rate at which the general level of prices for goods and services rises over time, reducing the purchasing power of money. The Consumer Price Index (CPI) is commonly used to measure inflation.

Kurtosis: A statistical measure of the 'tailedness' of a distribution. In financial markets, high kurtosis indicates the potential for extreme market events, which can affect portfolio risk and retirement planning.

Life Annuity: A retirement product that provides a guaranteed income for life, purchased with a portion or full amount of retirement savings. It removes longevity risk but lacks flexibility and growth potential.

Living Annuity: A retirement product that allows retirees to draw an income from their invested savings, with the flexibility to adjust withdrawal rates and investment strategies. However, it exposes retirees to market and longevity risks.

Nominal return: The total percentage return on an investment without adjusting for inflation, reflecting the raw growth of the portfolio over time.

Real return: The inflation-adjusted return on an investment, showing the actual growth in purchasing power over time.

Skewness: A measure of the asymmetry of a distribution. In financial markets, positive skewness indicates the potential for large positive returns, while negative skewness reflects the likelihood of extreme losses.

Stochastic Correlation: A modelling approach that considers correlations between asset returns as dynamic and variable over time, often influenced by changing market conditions.

Success rate: The probability that a retirement portfolio will sustain withdrawals over the retiree's lifetime without depleting the funds, based on specified assumptions of market returns, longevity, and withdrawal rates.

Weight: The proportion of an asset or asset class in a portfolio. Adjusting weights can influence portfolio risk and return characteristics.

Withdrawal rate: The percentage of the initial portfolio balance that a retiree withdraws annually to meet living expenses. Sustainable withdrawal rates are key to ensuring retirement savings last throughout retirement.

This page has been intentionally left blank

Preamble

The purpose of the preamble is to emphasise the importance of retirement planning and discuss the current two-pot regulation and its possible future impact. The preamble is devided into four sections, the first section discusses the current South African retirement setting. Thereafter the two-pot regulation is introduced and its current popularity under working class South Africans. The third section defines two important performance metrics that we continually use throughout the thesis, namely success rate and fugit. Lastly, we stress the importance of asset allocations for retirement strategies.

Retirement in South Africa

In South Africa, retirees are confronted with the challenges from emerging market conditions. Only 6% of economically active South Africans are projected to retire comfortably, while many face the risk of experiencing a lower standard of living than they had before retirement (ASISA, 2022).

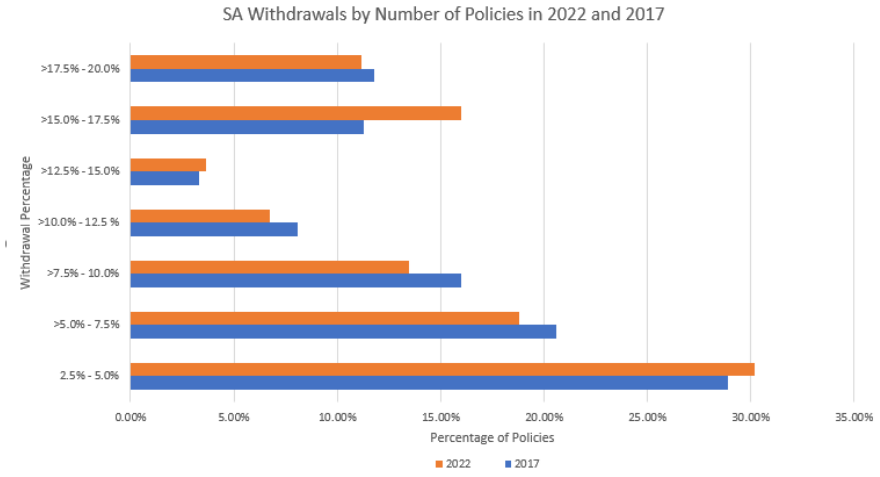

Figure 1: Withdrawal Rates from South African Retirement Policies (ASISA, 2022)

Figure 1 illustrates a shift in the annual withdrawal rates among South African retirees in 2022 compared to 2017, particularly in the 15%-17.5% bucket. The large increase in the proportion of retirees withdrawing be-

tween 15% and 17.5% of their retirement savings may be attributed to the economic difficulties experienced as a result of the Covid-19 pandemic and subsequent lockdowns. High inflation, increased unemployment, and sluggish economic growth have further intensified the financial pressure that many South African retirees experience.

These economic pressures are exacerbated by structural challenges in South Africa's labour market. With an unemployment rate exceeding 30% (Africa, 2024), only a small percentage of the population is part of the formal working class, which significantly limits the pool of individuals contributing to retirement savings. Early retirement, often induced by public sector policies aimed at 'creating jobs' through workforce restructuring, further compounds the issue. Many government employees are forced into early retirement with insufficient savings, pushing them to withdraw excessively from their retirement funds to meet their financial needs. This structural fragility underscores the difficulty of sustaining retirement income in such a challenging economic environment.

The two-pot dilemma

On 1 September 2024, South Africa implemented a reform (South African National Treasury, 2024) designed to address the challenge of providing for immediate financial needs while preserving funds for retirement. Under this system, retirement contributions are divided into two components: the savings pot, which accounts for one-third of contributions and can be accessed once a year before retirement, and the retirement pot, which constitutes the remaining two-thirds and is locked until retirement. This system was introduced to alleviate the pressure on individuals needing short-term liquidity while ensuring the majority of retirement savings remain untouched, fostering long-term financial security.

The 'two pot reform' has seen rapid uptake, with SARS reporting payouts of R21.4 billion in the first six weeks of implementation. This figure underscores the immediate financial relief provided to individuals facing economic pressures such as rising living costs and debt. However, this early surge in withdrawals has raised concerns among policymakers and financial analysts

about the potential depletion of the savings pot over time. If individuals withdraw funds regularly without replenishing them adequately, they may face a significant shortfall upon retirement (South African Revenue Service (SARS), 2024). Is South Africa deferring a more significant retirement issue to future generations?

Consider a theoretical scenario, where a person withdraws a fixed annual amount from their savings portion over an average working career of 30 years. The impact of these withdrawals over the 30-year period is illustrated in Figure 2, which represents the future savings values for annual withdrawals of R10 000, R20 000, and R30 000. According to Alexforbes (BusinessTech, 2024), the average withdrawal amount from the 'savings pot' is R19 000 p.a., impacting over 350 000 member policies.

A person withdrawing R10 000 from the two-pot system over a 30-year working career would possibly lose R660k in future value retirement savings. At a R20k and R30k per year withdrawal, the future value then grows to R1.3m and almost R2.0m, respectively, of possible future value savings that are lost, under the assumption of a mere 5% cash growth rate.

Figure 2: Future Value of Withdrawals, for a person withdrawing R10 000, R20 000, and R30 000 p.a. for 30 years.

While the system provides short-term financial relief, particularly in times of economic hardship, the early withdrawals can severely compromise long-

term retirement outcomes. Once funds are withdrawn, the ability to 'catch up' or replenish savings becomes increasingly difficult due to the compounding nature of investment returns. Individuals who withdraw early face the dual challenge of reduced savings balances and lost growth potential, which, when combined with rising inflation and market volatility, exacerbate the risk of insufficient retirement funds. This effect is particularly concerning in a country like South Africa, where many individuals already save too little for retirement and rely heavily on employer contributions or mandatory schemes(ASISA, 2022).

If retirement savings are insufficient in the coming decades due to early withdrawals and limited top-up contributions, the fiscal implications for South Africa could be profound. A large segment of the population reaching retirement age without adequate savings would likely increase dependency on the state's old-age pension system, placing additional strain on already stretched public finances. The government might face mounting pressure to intervene, either through expanded social grants or other welfare mechanisms, to support retirees who cannot meet their basic needs. This would not only divert funds from other critical areas like healthcare and education but could also lead to increased borrowing or taxation, placing further pressure on the economy. Over time, the financial sustainability of both individuals and the broader public system could be compromised, highlighting the importance of balancing immediate access to funds with long-term retirement security. While the Two-Pot Reform (South African National Treasury, 2024) may provide temporary relief by addressing immediate financial pressures, its long-term effects on retirement savings will likely become evident over the next decade, potentially eroding the retirement security of the working class.

Success Rate and Fugit

We define Π as the value of a retirement portfolio at a certain point in time and if $\Pi \leq 0$, then the value of the portfolio for all future time points is equal to 0. This indicates that the portfolio has defaulted and has reached the state of ruin. To define the success rate, we first introduce an indicator matrix $I_{\mathrm{M\times N}}$, where N denotes the number of time points and M denotes the number of simulations. The indicator matrix is obtained by populating

the elements of I as follows

$$I_{n,m} = \begin{cases} 1, & \Pi_{n,m} > 0, \quad \forall\, n \in \mathbb{N} \text{ and } m \in \mathbb{M}, \\ 0, & \Pi_{n,m} \leq 0, \quad \forall\, n \in \mathbb{N} \text{ and } m \in \mathbb{M}. \end{cases} \tag{1}$$

The success rate (SR) can then be defined as

$$SR = \frac{1}{M} \sum_{j=1}^{M} \min(I_{\tau,j}), \quad \forall\, \tau \in t, \tag{2}$$

where M denotes the number of simulations and t denotes the time horizon for portfolio simulations.

The term 'fugit' was first defined by Garman (1989) to represent the optimal time to exercise an American option. In the context of retirement modelling, Van Appel et al. (2021) defines the fugit as the expected life of the portfolio, or the expected time until ruin.

To define the fugit, we make use of information from the indicator matrix defined in (1). We determine the position of the first occurrence of a 0 value across each row (time grid). The time until ruin for each simulated path is then the first occurrence of $\Pi_{n,m} < 0$ across all simulations. The fugit can then be determined as the average time until the portfolio value becomes 0.

We provide a simple example to aid in the understanding of the success rate and fugit. Assume that we simulate three paths of the portfolio over a one-year period, i.e. the portfolio has a maturity of one year, with quarterly time steps. Then the value of the portfolio for each time step and simulation is given by

Table 1: Simulation example

	t = 0	t = 0.25	t = 0.5	t = 0.75	t = 1
Simulation 1	100	90	85	60	43
Simulation 2	100	45	0	0	0
Simulation 3	100	61	28	0	0

The indicator matrix $I_{3\times 5}$ is then determined to be

$$\begin{bmatrix} 1 & 1 & 1 & 1 & 1 \\ 1 & 1 & 0 & 0 & 0 \\ 1 & 1 & 1 & 0 & 0 \end{bmatrix}.$$

Therefore, SR is calculated as

$$SR = \frac{1}{3} \cdot (1 + 0 + 0) = 33.33\%.$$

The fugit of our simple example is then determined as

$$\text{Fugit} = \frac{1}{3} \cdot (1 + 0.5 + 0.75) = 0.75 \,\text{years}.$$

If the portfolio value were greater than zero across all simulated paths and time steps, then the success rate would be 100% and the fugit would just be the maturity of the portfolio, or one year in the case of the simple example.

In retirement modelling, the success rate of a portfolio offers a clear, intuitive measure of performance by indicating the likelihood that a retiree's assets will sustain their financial needs throughout retirement. Unlike traditional utility functions, which rely on abstract mathematical representations of risk aversion and consumption preferences, the success rate provides a straightforward, outcome-driven assessment. By directly evaluating the probability of outliving one's savings, the success rate aligns closely with real-world concerns, offering a practical benchmark for assessing the viability of different investment strategies.

While utility functions excel at capturing complex trade-offs between consumption and risk, they often introduce subjective parameters that can complicate the analysis. In contrast, success rate analysis is grounded in empirical simulations and historical data, emphasising tangible outcomes over theoretical constructs. This approach reflects the realities retirees face, namely prioritising the probability of maintaining income over time rather than optimising abstract satisfaction. Furthermore, integrating success rates with other metrics like fugit (the expected time until portfolio failure) pro-

vides a holistic view of portfolio health, ensuring that retirement plans are both resilient and easy to communicate.

Asset Allocation

Asset allocation is a critical component in optimising the performance and sustainability of living annuities in South Africa. Living annuities offer retirees flexibility in investment choices, but this freedom comes with the responsibility of making informed decisions to ensure long-term income sustainability. Allocating assets effectively across different classes, such as equities, bonds, property, and cash, can balance the dual objectives of capital growth and income preservation (Bodie et al., 2004; Swart, 2012). Equities, for example, often provide higher returns over the long term but are accompanied by significant volatility, while bonds and cash typically offer stability and predictable income, albeit at lower returns. A balanced approach to asset allocation is essential to mitigate risks and avoid the depletion of retirement funds prematurely.

The trade-off between risk and reward in asset classes becomes even more apparent when considering the specific needs (i.e.,withdrawal rates) of retirees. Equities, with their potential for high returns, can outpace inflation but expose the retiree to market downturns, which can be detrimental if withdrawals are made during a market slump. Bonds and fixed-income instruments provide steadier returns, offering a safer harbour during economic instability but often fail to keep up with inflation over the long term. Property investments, meanwhile, offer a mix of growth and income through rental yields, but they lack liquidity and carry risks such as valuation volatility and management costs. Striking the right balance among these asset classes requires a thorough understanding of market conditions, personal risk tolerance, and retirement goals (Dybvig and Liu, 1999; Van Heerden and Koekemoer, 2008).

Diversification is a cornerstone of a robust retirement strategy, and incorporating foreign exposure can further enhance portfolio resilience (Blake et al., 2006; Swart, 2012). By investing in global markets, retirees can access opportunities not available locally, such as industries or sectors that

are underrepresented in South Africa. Foreign exposure serves as a hedge against local economic and currency fluctuations, providing stability to the portfolio. However, it is crucial to manage the currency risk associated with foreign investments, as significant exchange rate movements can erode returns. A prudent allocation to foreign assets, alongside domestic investments, can provide retirees with the benefits of geographic and economic diversification.

When considering the growth potential of emerging markets versus developed economies, retirees must weigh the higher growth prospects of emerging markets against their inherent volatility. South Africa, as part of the emerging market category, often presents opportunities for rapid growth but remains subject to political and economic instability. Developed markets, on the other hand, typically offer steadier but slower growth rates, underpinned by mature economies and stable institutions. For retirees, blending exposure to both emerging and developed markets can create a balanced portfolio that leverages growth opportunities while managing downside risks. By thoughtfully combining asset allocation, diversification, and market selection, retirees can navigate the complexities of living annuities and secure their financial future (Merton, 1969).

Chapter 1

Introduction[1]

1.1 Navigating Retirement in South Africa

Living annuities are a prevalent retirement income solution in South Africa, offering retirees the flexibility to select their income levels and investment portfolios. Unlike guaranteed annuities, living annuities do not provide a fixed income for life; instead, the income depends on the performance of the underlying investments and the chosen drawdown rate. This structure places the investment and longevity risks squarely on the retiree, necessitating careful financial planning to ensure that retirement savings are not depleted prematurely.

However, the sustainability of living annuities is closely tied to the chosen drawdown rates and investment returns. Numerous studies, locally and abroad (e.g., Cooley et al. (1998), Finke et al. (2012), Maré (2016), Van Appel et al. (2021), and Daraei and Sendova (2024)) suggest that annual drawdown rates of between 4% and 5% are generally considered prudent. Exceeding these rates can lead to the rapid eroding of retirement capital, especially if investment returns are lower than expected.

The Association for Savings and Investment South Africa (ASISA) reported

[1] We assume that upon retirement, the retiree has access to savings or a pension and must make investment decisions to allocate these funds to income-generating portfolios, ensuring their financial needs are met throughout the retirement period.

that by the end of 2022, South African retirees had R625.9 billion invested in living annuities, marking a 47.3% increase from R424.8 billion in 2018. The number of living annuity policies also grew by 13.5% over the same period, reaching 527,038 by the end of 2022. Despite the economic volatility during these years, the average drawdown rate remained relatively stable, with a slight decrease to 6.66% in 2022 from 6.88% in 2021 (ASISA, 2022).

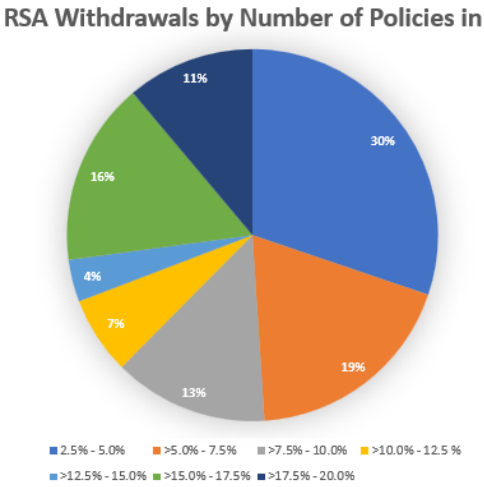

Figure 1.1: Withdrawal Rates from Living Annuities in 2022.

The National Treasury's technical discussion paper, 'Enabling a Better Income in Retirement', emphasises the low income replacement rates experienced by many retirees. According to the report, a significant portion of the population is unable to maintain their pre-retirement standard of living, with income replacement ratios often falling below the recommended 75% threshold. The study points to the uneven savings patterns, where a majority of individuals either delay starting their retirement savings or withdraw from retirement funds prematurely, which often leaves insufficient funds for retirement (National Treasury, 2012).

The National Treasury's technical discussion paper, 'Charges in South African Retirement Funds', delves into the impact of high fees on retirement savings. It reveals that administrative and investment charges, which can average 2% or more annually, significantly erode retirement savings over time. This is particularly concerning in a market where consistent, high returns are

not guaranteed. The compounded effect of these charges can result in retirees losing a substantial portion of their potential retirement wealth. The Treasury highlights the urgent need for cost-effective solutions, such as standardised low-cost products, to ensure that fees do not further undermine the already precarious financial situation of South African retirees (National Treasury, 2013).

As mentioned above, South African retirees face a plethora of risks when retiring. Some other retirement risks include, but are not limited to:

1. Lack of adequate savings: the risk that an individual's accumulated retirement savings are insufficient to generate the required income to sustain their desired lifestyle throughout retirement (National Treasury, 2012).
2. Volatility risk: This relates to investment risk assumed when investing in equities or other risky assets. A retiree that has sleepless nights over concerns about market volatility may derive increased utility from a life annuity that provides a guaranteed income until death (Blanchett, 2014).
3. Inflation risk: The risk that inflation will erode a retiree's purchasing power throughout retirement. This risk can be hedged by purchasing a life annuity with an inflation protection feature (Blanchett, 2014).
4. Longevity risk: The risk that a retiree will experience financial ruin (run out of money). One way to hedge against longevity risk is to purchase a life annuity that will provide a guaranteed income until death (Blanchett, 2014).
5. Bequest risk: The risk associated with the implications that life annuities have on retirement decision making. To a risk-averse retiree, a life annuity provides insurance against financial ruin. However, retirees who seek to maximise their wealth and leave an inheritance for their heirs may experience less utility from trading upside potential for safety (Blanchett, 2014).
6. High levels of debt: A significant portion of the population is burdened by debt in the form of credit cards, personal loans, and home loans.

7. Lack of financial literacy: The importance of retirement planning is not well understood by many South Africans, which results in poor investment decisions and inadequate savings.

8. Economic challenges: High inflation, unemployment, and slow economic growth exacerbate the financial stress that many South Africans face.

1.2 Thesis Scope

While numerous studies (Cooley et al., 1998; Maré, 2016; Van Appel et al., 2021) have explored the success rates and dynamics of living annuities, the majority of this work has been conducted in the United States, leaving a notable gap in the analysis specific to the South African context. There has been limited discussion on the success rates of living annuities tailored to South African retirees, despite the unique market and economic conditions they face. Recently, financial advisors have begun introducing hybrid retirement strategies into the South African retirement landscape, marketing them as less risky alternatives to traditional living annuities. However, much of the research conducted in South Africa has assumed that living annuities are solely invested in local equities, with modelling frameworks relying on constant correlation structures, which may not accurately reflect the complexities of dynamic markets.

Cooley et al. (1998) conducted a pivotal study examining the impact of various withdrawal rates on the sustainability of living annuities for United States(U.S.) retirees. They also explored the optimal asset allocation required to support these withdrawal rates. The framework proposed by Cooley et al. (1998) introduced a success rate criterion for retirement portfolios, defined as the probability of the portfolio outliving the retiree over a specified time horison, given a set withdrawal rate and asset allocation. Their analysis, often referred to as the 'Trinity Study', became a cornerstone for retirement planning, providing clear guidelines on the relationship between withdrawal rates and asset longevity. It highlighted the critical role of equities in ensuring portfolio success, emphasising that portfolios with higher equity allocations tended to have a higher likelihood of lasting

through extended retirement periods.

There are two popular methodologies in simulating retirement portfolios, namely Bootstrap and Monte Carlo simulation. Bootstrap (Efron, 1979) simulation with replacement is a non-parametric technique used to estimate the distribution of portfolio returns by resampling historical data. In the context of South African retirement portfolios, this method is particularly valuable due to the country's volatile market dynamics. By repeatedly drawing samples from observed returns, with replacement, bootstrap simulation generates numerous potential portfolio outcomes while preserving the statistical properties of the original dataset, such as the associated correlation structure. This approach avoids reliance on strict distributional assumptions and allows us to assess the variability of retirement outcomes under historical market scenarios, including periods of extreme economic shocks or high inflation, which are common in emerging markets.

Monte Carlo simulation (Metropolis and Ulam, 1949), introduced by Stanislaw Ulam and John von Neumann, employs stochastic processes to model the uncertainty of portfolio returns over time. Unlike bootstrap methods, Monte Carlo assumes specific probabilistic models, such as Geometric Brownian Motion, to simulate a wide range of future scenarios. A key advantage of Monte Carlo simulation is the rapid convergence of the sample mean, enabling efficient approximation of expected portfolio outcomes with fewer iterations compared to simpler resampling methods. However, when simulating portfolio scenarios using Monte Carlo, we work under the assumption of a constant correlation structure throughout the simulation period.

Monte Carlo simulations often assume a constant correlation structure, such as a Gaussian copula, when modelling retirement portfolio scenarios. While this simplifies computations and provides a baseline for understanding asset dependencies, it fails to capture the dynamic nature of correlations observed in real markets. In volatile environments like South Africa, correlations between asset classes can shift dramatically during economic downturns, financial crises, or periods of heightened uncertainty. A constant correlation structure risks underestimating the impact of such shifts, leading to overly optimistic or misleading portfolio outcomes. In contrast, stochastic correlation models, such as the Hyperbolic Tangent Ornstein-Uhlenbeck model

(Buraschi and Porchia, 2009), allow correlations to evolve over time based on market conditions. This provides a more realistic representation of inter-asset relationships, particularly during stress scenarios, and improves the accuracy of risk assessment and portfolio resilience analysis.

The scope of this thesis is to develop and implement a retirement simulation model, consistent with the framework proposed by Cooley et al. (1998), within a South African context. This includes evaluating two key performance metrics, namely success rates and fugits, relevant to South African retirees. The thesis evaluates the effectiveness of the hybrid retirement strategy, which combines living and life annuities, within the local context. Market consensus suggests that a hybrid strategy minimises longevity risk, and this research assesses its success rates using the success rate criteria defined by Cooley et al. (1998). Another critical focus of this thesis is the impact of foreign equity exposure on success rates and fugits, addressing an increasingly relevant factor in retirement portfolio management.

The research challenges conventional modelling techniques that assume constant correlation structures by incorporating stochastic correlation modelling to analyse its effect on the success rates and fugits of South African living annuities.

1.3 Thesis Aims

This thesis has several key objectives.

1. To adapt and apply a simulation framework, similar to that proposed by Cooley et al. (1998), within a South African context. We utilise an elementary gBm model to show consistency between previous bootstrapping work performed and simulation modelling.

2. To provide a scientific foundation for evaluating the success rate of a hybrid retirement strategy, where retirees allocate a portion of their savings to a life annuity and the remainder to a living annuity, thereby improving retirement outcomes for South African retirees.

3. To examine the impact of incorporating fees on hybrid strategies in

South Africa. Specifically, we analyse how advisor fees, fund management fees, and platform fees (including those related to life annuities) influence success rates and fugits in these strategies.

4. To examine the impact of foreign equity exposure on the success rates of living annuities, addressing the widely held view among asset managers that foreign exposure plays a critical role in the long-term success of retirement portfolios. We investigate a possible diversification benefit by incorporating the S&P 500 in our portfolio construction.

5. To explore the effect of stochastic correlation modelling on retirement portfolio success rates, given the dynamic nature of market risk factor correlations, which tend to fluctuate with market cycles. This is particularly relevant as retirement portfolio modelling typically spans extended time horizons, necessitating robust approaches to capture such complexities.

The foundation of this thesis is built upon four journal articles, three of which have undergone peer review, while the fourth is currently(January 2025) under review. These articles focus on the retirement landscape, highlighting the critical importance of effective retirement planning and the careful consideration of 'optimal' retirement strategies. A summary of these articles is presented in Table 1.1.

Table 1.1: Published doctoral research: Journal articles.

Peer-reviewed publications
1. **Van Niekerk, A. J.**, & Maré, E. (2020). Optimale ontrekkingskoerse vir aftreebeleggings in Suid-Afrika. *Suid-Afrikaanse Tydskrif vir Natuurwetenskap en Tegnologie, 139*(1).
2. Van Appel, V., & Maré, E., & **van Niekerk, A. J.** (2021). Quantitative guidelines for retiring (more safely) in South Africa. *South African Actuarial Journal, 21*(1), 75-91.
3. **Van Niekerk, A. J.**, Moutzouris, V., & Maré, E. (2024). Hybrid retirement strategy in South Africa. *South African Journal of Economic and Management Sciences, 27*(1).
4. **Van Niekerk, A. J.**, Moutzouris, V., & Maré, E. (2025). A Multivariate Stochastic Approach to Determine Long-term Success of SA Living Annuity Portfolios. **Accepted for publication at SAAJ - 8 March 2025**.

1.4 Thesis Structure

Chapter 2 lays the groundwork by presenting a preliminary retirement study that applies simulation modelling within a South African context, consistent with the framework proposed by Cooley et al. (1998). This chapter introduces the concepts of success rates and fugits, providing the analytical foundation for evaluating retirement strategies. The simulation model is elementary but provides a basis for our analysis performed in the rest of the chapters. The chapter visually presents how setting certain withdrawal rates influence portfolio success rates and fugits.

In Chapter 3, the focus shifts to the Hybrid retirement strategy, where Bootstrap sampling of historical asset returns is used to simulate 10,000 random scenarios. These simulations investigate the success rates of various compositions of the Hybrid strategy. The analysis aims to provide a scientific basis for enhancing the success rates observed in traditional living annuities, investigating the potential advantages of integrating a Hybrid approach in retirement. The chapter investigates how various levels of life annuity exposures influence respective success rates and fugits. It analyses the sustainability of setting certain withdrawal rates in retirement.

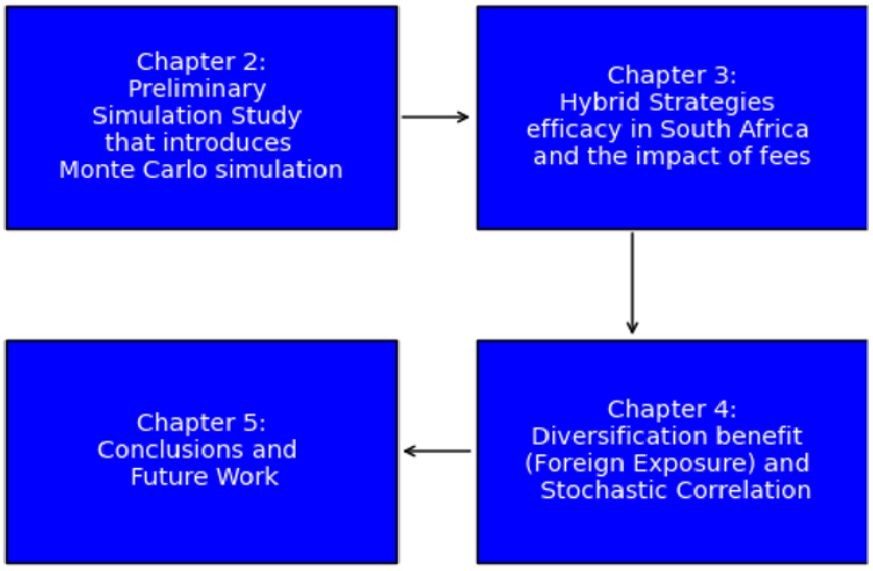

Figure 1.2: Flowchart of the Thesis.

Chapter 4 provides a scientific basis for the influence of foreign equity exposure on living annuity success rates and to determine the impact of stochastic correlation modelling on retirement portfolio success rates given that market risk factor correlations tend to change with market cycles, and retirement portfolio modelling is typically performed over long time horizons.

Chapter 5 summarises the thesis and the research questions that were addressed. The Appendices are split into three sections. Firstly, Appendix A discusses the possibility of construting an optimal portfolio for sustaining certain withdrawal rates over prolonged periods of time. Appendix B notes some general supplementary theory. Appendix C contains Python code that was used throughout the thesis.

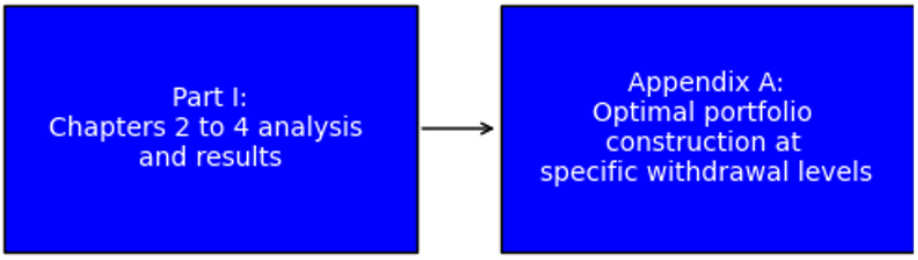

Figure 1.3: Flowchart of chapters and Appendix.

1.5 Data and Methodology

The data and methodology used in this thesis vary across chapters, reflecting the specific requirements of each analysis. Each chapter includes a dedicated methodology section that explains the intricacies of the modelling approach applied to the respective analyses. While the data used in Chapters 2 and 3 primarily focus on long-term historical data for South African equities and bonds, Chapter 4 shifts its emphasis to the most recent 20 years of data, incorporating both local and foreign equities. These differing datasets and modelling techniques have been carefully chosen to suit the objectives of each chapter and are clearly documented and defined throughout the thesis to ensure transparency and consistency.

The data in Chapters 2 and 3 were chosen with the aim to align with worked performed by Maré (2016) and Van Appel et al. (2021). Chapter 3 uses long term Dimson et al. (2014) data and Chapter 4 incorporates data from Firer and Staunton (2002) and Van Appel et al. (2021) These are long-term South African datasets that span over the course of a 100 years. The data used in Chapter 4 hlwere selected to represent the most recent 20 years of historical return data (Levendis and Maré, 2023). This selection was crucial to preserve the integrity of the correlations among the relevant asset classes.

The 20-year data encompass two major stress events, namely the Global Financial Crisis (GFC) and COVID-19, whereas the long-term data, though they also includes stress events, hlreflect a smoother trajectory due to the extended time horizon.

Important excerpts from the Python code used to perform the analysis in this thesis are provided in hlAppendix B

1.6 Research Questions

While the discussion has touched on various aims in this thesis, the main research question of this thesis is:

How does a retiree construct an 'optimal' portfolio according to his/her needs, which provides the retiree with a consistent standard of living in retirement?

This is a very broad question, as Cooley et al. (1998) emphasise that 'every retiree's situation is unique, requiring a tailored approach to retirement planning to address individual needs and circumstances.' Since every retiree has unique needs and specific assets or funds available at retirement, it is clear that retirement planning must be tailored to individual circumstances. This thesis provides an evaluation framework of various retirement strategies, providing retirees with guidance to arrive at a customised retirement solution that meets their specific needs.

We aim to address this central research question by exploring a series of sub-research questions, namely:

1. What are the success rates of living annuities that are exposed to local bond and equity markets?

   In this thesis, we assess the efficacy of each strategy by examining its performance using the success rate as the primary metric. This analysis is thoroughly explored in Chapters 2, 3, and 4. Chapters 2 and 3 focus on strategies within the local equities and bond markets,

while Chapter 4 expands the scope to include international assets, such as the S&P 500.

2. What is the 'optimal' ratio of equity to bond exposure for a living annuity?

   There are various portfolio compositions that contribute to a successful living annuity. However, each retiree is unique and requires a bespoke solution to his/her retirement solution. An 'optimal' solution would be found for a retiree's requirements and needs.

3. Does a hybrid retirement strategy pose less risk to a retiree?

   In Chapter 3, hybrid retirement strategies secure income from a third party provider and relieve the living annuity from any excessive withdrawal pressure.

4. What is the 'optimal' portion of life annuity that needs to be purchased in order to create a 'safe' hybrid strategy?

   We discuss the optimality of combining living and life annuities in Appendix A. The combination of living and life annuities are heavily dependent on the chosen withdrawal rate.

5. What is the overall impact on success rates when incorporating fees into a hybrid retirement strategy?

   In Chapter 3, we incorporate fees (management fees, platform fees, and financial adviser fees) and evaluate the overall impact these have on hybrid strategies.

6. What are the success rates of living annuities that are exposed to foreign equity/assets?

   We consider incorporating the S&P 500, with the aim to obtain a diversification benefit. In Chapter 4, we evaluate the effect of diversification on living annuities.

7. Does the assumption of modelling constant correlation influence living annuity success rates and fugits?

   In Chapter 4, we modelled correlation stochastically using the Hyperbolic Tangent of the Ornstein-Uhlenbeck process. While correlation is often assumed to remain constant over time, this assumption restricts the modelling process by limiting the ability to account for correlation risk.

8. Do modelling techniques yield different results for success rates and fugits(Bootstrap vs Monte Carlo)?

   In Chapter 2 and 4, we make use of Monte Carlo modelling and Chapter 3 uses Bootstrap modelling.

Chapter 2

Optimal Withdrawal Rates for Retirement Annuities in South Africa[1]

Keywords: Geometric Brownian motion · Monte Carlo simulation · Success Rate · Fugit · Bonds · Equities

2.1 Introduction

Retirees face a challenging financial dilemma: determining an appropriate withdrawal amount from their retirement investments. They must carefully balance the risk of outliving their savings with the possibility of underspending and living below their means. In the United States, financial advisors often recommend a "safe" withdrawal rate of 4%. This paper examines withdrawal rates for retirees within the South African context.

Maré (2016) highlights two primary types of annuities available to retirees in South Africa: guaranteed life annuities and living annuities.

[1]This chapter is based on conference proceedings and a paper (Van Niekerk and Maré, 2020) published in the *Suid-Afrikaanse Tydskrif vir Natuurwetenskap en Tegnologie*.

1. Life annuities provide a guaranteed, lifelong income to retirees in exchange for a lump-sum investment with an insurance company. This product offers financial security by ensuring a steady income regardless of the retiree's lifespan (Milevsky, 2013).

2. Living annuities, in contrast, allow retirees to invest their funds in a range of portfolios and withdraw income regularly. While these annuities offer flexibility and growth potential, they also expose retirees to market risks and require careful management to avoid depleting their savings (Beinash (2008); National Treasury (2012)). Living annuities are generally preferred by retirees who are comfortable with investment risks and seek more control over their retirement assets.

Living annuities in South Africa are a popular retirement income product due to their flexibility in investment and withdrawal options. The regulation governing living annuities allows retirees to withdraw an annual income of between 2.5% and 17.5% of the total investment value (*Long-Term Insurance Act, 1998: Regulation 39*, 1998). This percentage is chosen by the retiree and can be adjusted once a year. The purpose of this regulatory range is to provide retirees with sufficient flexibility to tailor their withdrawals to their financial needs while maintaining the sustainability of their investment. By setting a minimum withdrawal rate of 2.5%, the regulation ensures that retirees maintain access to their funds, while the 17.5% cap aims to prevent rapid depletion of retirement savings.

The World Health Organization (2019) reported that the average life expectancy at birth in South Africa was approximately 61.5 years for males and 67.7 years for females. For individuals reaching the age of 60, the conditional life expectancy, which indicates the additional years a person is expected to live after turning 60, was estimated at 15.9 years for males and 19.0 years for females in 2019. These figures suggest that, on average, a 60-year-old male could expect to live until approximately 75.9 years, while a female of the same age could anticipate living until about 79.0 years. These estimates are crucial for retirement planning and healthcare provisioning, as they provide insights into the expected longevity of the aging population.

The challenge for retirees is determining how much they can regularly with-

draw from their retirement investment portfolio without depleting their funds, given that they might live 20 years into retirement.

2.2 Simulation Methodology

Monte Carlo simulation, paired with geometric Brownian motion (gBm) model (Samuelson, 1965), is used for modelling retirement portfolios in South Africa. We initially model living annuities using a gBm framework to simulate portfolio performance and evaluate the success rates and fugits (the time until a portfolio fails to meet its objectives). The gBm model relies on key assumptions such as constant drift and volatility, as well as a constant correlation between asset classes. These simplifying assumptions allow for tractable modelling but may not fully capture the complexities of financial markets, especially under volatile conditions. While the gBm model provides a useful baseline for understanding portfolio behaviour under 'normal' market conditions, its limitations become apparent when market dynamics deviate significantly from historical norms.

We extend the modelling approach, later in the thesis, by incorporating the Heston model, which accounts for stochastic volatility, and further enhance the framework by integrating the Hyperbolic Tangent Ornstein-Uhlenbeck process. This advanced modelling addresses some of the shortcomings of the gBm by allowing for mean-reverting volatility and capturing more realistic market dynamics. Stress events such as the Global Financial Crisis (GFC) and COVID-19, which induce sudden and severe market shocks, challenge traditional continuous models like gBm and Heston. These events can often be better represented by incorporating jump processes, which introduce discontinuities to reflect sudden price drops or volatility spikes. By integrating jump processes into the framework, the models can more accurately reflect the fat-tailed nature of real-world asset returns and the outsized impact of rare but extreme market events on annuity portfolios.

In line with Maré (2016), we evaluate an investment portfolio with a fixed asset allocation between South African bonds and equities. However, instead of employing bootstrapping techniques, we use Monte Carlo-based simula-

tions that rely on distributional characteristics of asset classes, similar to that used by Cooley et al. (1998), that simulate a monthly inflation-adjusted income (i.e., focusing on real spending rates). This approach calculates end-of-period portfolio values based on historical JSE Top 40 and South African bond return information.

We model the portfolio over monthly time-steps and work under the assumption that the retiree receives their withdrawal from the portfolio on a monthly basis. The long-term correlation between the JSE All Share index and Local South African bonds is 0.265, as determined by Auret and Vivian (2014).

The South African asset return information, as determined by Dimson et al. (2014)[2], spans 114-years from 1900 to 2014 and a summary of the local equities and bonds returns can be seen in Table 2.1. For consistency with Maré (2016), the data were not updated and simulations were based on the Dimson et al. (2014) data.

Table 2.1: Real Returns and Standard Deviation for South Africa

Asset Class	**Real Return (%)**	**Std Dev (%)**
Equities	9.4	23.2
Bonds	2.4	10.1

A two-asset portfolio provides a simple yet effective framework for analysing the impact of diversification on returns and the associated risk of depleting a living annuity early. The expected return of a two-asset portfolio is the weighted average of the expected returns of the individual assets, adjusted for their weights in the portfolio. If w_E and w_B represent the weights of Equities E and Bonds B, respectively, and r_E and r_B are their expected returns, then the portfolio's expected return, r_p, is calculated as:

$$r_p = w_E \cdot r_E + w_B \cdot r_B, \tag{2.1}$$

where:

[2]The Dimson data were used in this study to closely align to work performed by Maré (2016).

1. $w_E + w_B = 1$,
2. r_E and r_B are the expected returns of equities E and bonds B.

The standard deviation of a portfolio measures the variability of its returns and serves as an indicator of risk. For a two-asset portfolio, the standard deviation (σ_p) is given by:

$$\sigma_p = \sqrt{w_E^2 \cdot \sigma_E^2 + w_B^2 \cdot \sigma_B^2 + 2 \cdot w_E \cdot w_B \cdot \rho_{E,B} \cdot \sigma_E \cdot \sigma_B} \tag{2.2}$$

where:

1. σ_E and σ_B are the standard deviations (risks) of equities E and Asset B,
2. $\rho_{E,B}$ is the correlation coefficient between the two assets,
3. The third term, $2 \cdot w_E \cdot w_B \cdot \rho_{E,B} \cdot \sigma_E \cdot \sigma_B$, with lower correlation reducing portfolio risk.

The study uses the assumption that the portfolio is modelled with the gBm process. The gBm process is a widely used stochastic process in finance to model the dynamics of asset prices, as presented in Hull (2018) and Bjork (2009). The SDE for gBm is given by:

$$dS_t = \mu S_t \, dt + \sigma S_t \, dW_t, \tag{2.3}$$

where:

1. S_t is the price of the portfolio at time, t,
2. μ is the drift term (representing the return of the portfolio),
3. σ is the volatility (representing the standard deviation of the portfolio), and
4. W_t is a Wiener process (standard Brownian motion).

The solution to the gBm SDE is given by:

$$S_t = (S_0 - k) \exp\left(\left(\mu - \frac{\sigma^2}{2}\right) t + \sigma W_t\right), \tag{2.4}$$

where

1. S_0 is the initial price of the asset at $t = 0$, and
2. k represents the proportional monthly withdrawal.

Following the approach of Cooley et al. (1998), we define a portfolio as successful if it retains a positive balance at the end of the specified investment period (e.g., 15, 20, 25, or 30 years). The success rates, representing the proportion of portfolios that meet this criterion under the simulation method, are then reported.

Another metric we use to evaluate a retirement strategy is the expected life of the portfolio, or the fugit. For example, if we simulate over a 50-year period with a certain portfolio composition and withdrawal rate, we might observe that the portfolio's average expected life might only be 35 years. This indicates that the average portfolio failed to sustain any additional withdrawals above 35 years and the portfolio reached a state of ruin. For the analysis of the expected life of a portfolio, we work under the assumption of 50-year simulated portfolios.

2.3 Simulation Results

Figure 2.1 presents simulated paths for 10,000 living annuities under varying allocations to equities (JSE All Share) and bonds, as well as differing withdrawal rates. The top row reflects a conservative investment strategy with 0% exposure to equities and 100% exposure to South African bonds. The middle row represents a balanced allocation of 50% equities and 50% bonds, while the bottom row is an aggressive strategy with 100% equities. The columns demonstrate increasing withdrawal rates of 3%, 6%, 9%, and

12%, respectively. The withdrawal occurs monthly at the end of each month, impacting the overall portfolio sustainability.

In the top row (100% bonds), the portfolios are notably less volatile across all withdrawal rates, with smoother trajectories. At a 3% withdrawal rate (first column), the portfolios show minimal risk of depletion over 20 years. However, as the withdrawal rate increases to 6% or higher, the likelihood of depletion increases significantly, with many paths depleting entirely before the end of the 20-year period. The limited volatility of bonds results in a narrower spread of outcomes, with most paths tightly clustered around similar gradients. This highlights the reduced growth potential of bonds, particularly considering higher withdrawal rates.

The middle row (50% equities and 50% bonds) introduces moderate volatility into the portfolio outcomes. At a 3% withdrawal rate, the inclusion of equities enables some paths to achieve substantial growth, although the increased volatility results in a wider spread of outcomes. As the withdrawal rate increases to 6%, 9%, and 12%, the impact of volatility becomes more pronounced, with a growing proportion of portfolios depleting prematurely. The balanced allocation provides a trade-off between growth and stability, but at higher withdrawal rates, the equity exposure appears insufficient to consistently counteract the depletion caused by aggressive withdrawals.

The bottom row (100% equities) demonstrates the highest levels of volatility and the widest spread of outcomes. At a 3% withdrawal rate, many portfolios experience significant growth, with some paths reaching very high portfolio values. This illustrates the potential for equities to sustain longer periods before depletion due to their higher returns. However, the volatility also results in steeper declines for certain paths, particularly at higher withdrawal rates. For withdrawal rates of 9% and 12%, the depletion of portfolios occurs faster for many paths, but the extended sustainability of some portfolios due to high equity returns is evident. This highlights the trade-off between volatility and potential growth when equities dominate the portfolio.

Overall, the inclusion of equities increases portfolio volatility, leading to a wider spread of outcomes and gradients in the simulated paths. While

higher equity exposure can prolong portfolio sustainability and enhance growth potential, especially at lower withdrawal rates, it also introduces significant risk, particularly for higher withdrawal rates. In contrast, bond-heavy portfolios provide more stability but are prone to earlier depletion under aggressive withdrawal strategies due to their lower growth potential. The choice of allocation and withdrawal rate must balance the retiree's risk tolerance and income requirements to ensure sustainable outcomes.

Table 2.2 illustrates the portfolio success rates, defined as the percentage of portfolios that maintain a positive balance at the end of a specified time horizon, under different withdrawal rates and asset allocations. We interpret the table by identifying the time horizon of interest (e.g., 20 years). Then, we examine how the success rate changes across withdrawal rates (columns) and asset allocations (sections). For example, the 20-year time horizon under a 0% equities (100% bonds) allocation, at a 3% withdrawal rate, yields a 100% success rate, meaning all portfolios end with a positive value. However, as the withdrawal rate increases to 6%, the success rate drops to 49%, indicating that only 49% of portfolios avoid depletion. In contrast, a more aggressive allocation with 100% equities for the same time period maintains a higher success rate of 81% at a 6% withdrawal rate. This demonstrates that portfolios with higher equity exposure have greater potential to sustain higher withdrawal rates but come with increased volatility.

Portfolios with lower withdrawal rates (3%–5%) show high success rates across all time periods and allocations, with almost all maintaining 100% success for 15 and 20 years, regardless of the equity-to-bond mix. However, as withdrawal rates increase to 6% and beyond, the success rates decline significantly, particularly for longer time horizons and conservative (bond-heavy) portfolios. Bond-only portfolios experience the steepest declines, reflecting their lower growth potential. Conversely, portfolios with higher equity exposure (75%–100% equities) display better sustainability at higher withdrawal rates. However, even these aggressive allocations struggle with 9%–12% withdrawal rates over 25 and 30 years, underscoring the challenges of sustaining high withdrawal levels regardless of asset allocation. Table 2.2 highlights the importance of balancing withdrawal rates with an appropriate asset allocation to ensure portfolio longevity.

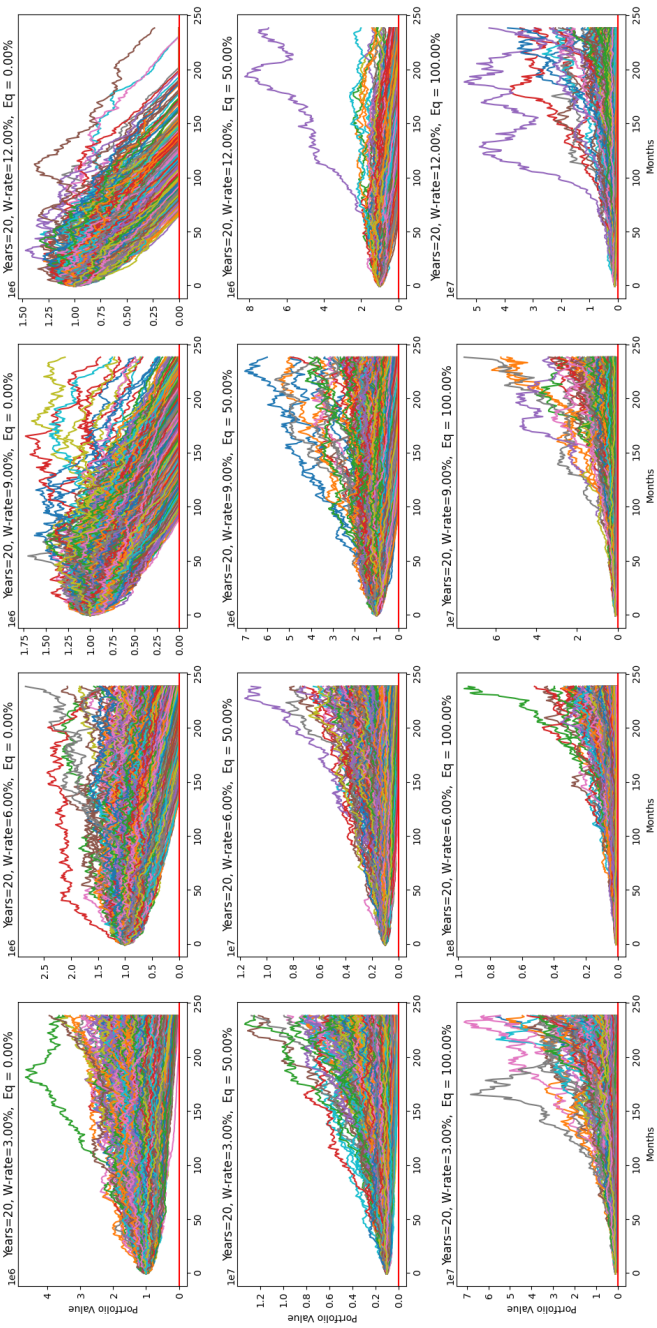

Figure 2.1: Retirement Portfolio Simulations at Various Withdrawal Rates and Equity Exposures over a 20-year period.

Table 2.2: Portfolio Success Rates Based on Withdrawal Rates and Asset Allocations

	Withdrawal rates p.a. (%) of the initial portfolio value									
Allocation	**3%**	**4%**	**5%**	**6%**	**7%**	**8%**	**9%**	**10%**	**11%**	**12%**
0% Stocks / 100% Bonds										
15 Year	100%	100%	97%	87%	66%	41%	22%	9%	4%	1%
20 Year	100%	94%	76%	49%	26%	11%	4%	0%	0%	0%
25 Year	96%	78%	49%	23%	9%	3%	1%	0%	0%	0%
30 Year	88%	60%	31%	11%	4%	1%	0%	0%	0%	0%
25% Stocks / 75% Bonds										
15 Year	100%	100%	100%	97%	87%	68%	44%	24%	11%	4%
20 Year	100%	96%	79%	53%	30%	13%	5%	1%	1%	0%
25 Year	100%	96%	81%	55%	30%	13%	5%	1%	0%	0%
30 Year	99%	80%	67%	39%	18%	7%	1%	0%	0%	0%
50% Stocks / 50% Bonds										
15 Year	100%	100%	99%	97%	90%	78%	62%	44%	29%	18%
20 Year	100%	99%	95%	86%	70%	51%	35%	22%	12%	6%
25 Year	100%	98%	90%	74%	54%	36%	22%	12%	6%	3%
30 Year	99%	94%	81%	63%	43%	27%	15%	8%	4%	2%
75% Stocks / 25% Bonds										
15 Year	100%	100%	98%	94%	88%	78%	66%	55%	41%	32%
20 Year	100%	98%	93%	85%	74%	60%	48%	37%	27%	18%
25 Year	98%	92%	82%	70%	57%	44%	31%	22%	16%	10%
30 Year	100%	98%	90%	74%	55%	38%	28%	16%	9%	6%
100% Stocks / 0% Bonds										
15 Year	100%	99%	95%	89%	84%	75%	67%	57%	48%	39%
20 Year	98%	95%	89%	81%	72%	63%	54%	44%	37%	28%
25 Year	97%	92%	84%	74%	65%	54%	44%	37%	28%	23%
30 Year	95%	89%	80%	70%	60%	49%	41%	32%	25%	20%

Table 2.3 presents the expected time to ruin (i.e., when the portfolio is depleted) for a living annuity simulated over a 50-year period, across varying

Table 2.3: Expected Time to Ruin for Various Withdrawal Rates and Equity Allocations (Time in Years)

Equity	**Withdrawal Rate (%)**									
	3%	4%	5%	6%	7%	8%	9%	10%	11%	12%
0%	43.2	34.8	27.4	21.6	17.9	15.1	13.0	11.6	10.4	9.4
10%	46.6	39.1	31.1	24.3	19.4	16.1	13.9	12.2	10.8	9.8
20%	48.4	43.1	35.4	27.5	21.9	17.8	15.0	13.0	11.3	10.2
30%	49.1	45.4	38.8	31.5	24.7	19.9	16.3	13.9	12.0	10.7
40%	49.4	46.6	41.5	34.6	28.0	22.3	18.2	15.2	13.2	11.5
50%	49.4	47.3	43.0	36.9	30.7	25.2	20.5	17.1	14.3	12.4
60%	49.3	47.4	43.3	39.0	33.3	27.0	22.2	18.2	15.7	13.7
70%	49.2	47.2	44.1	39.7	34.6	29.4	24.9	21.2	17.5	15.5
80%	48.5	46.5	43.3	39.4	35.7	31.5	27.4	22.6	20.7	17.9
90%	48.1	46.0	43.0	39.0	35.5	31.5	28.4	24.6	21.8	19.2

withdrawal rates and equity exposures. At lower withdrawal rates (e.g., 3%), the time to ruin is generally longer regardless of equity allocation, indicating the sustainability of smaller withdrawals. Conversely, as withdrawal rates increase, the expected time to ruin decreases significantly, highlighting the compounding pressure of larger withdrawals on portfolio longevity.

For example, with a low equity allocation of 10% and a 5% withdrawal rate, the expected fugit is 31.1 years. In contrast, a higher equity allocation of 70% at the same withdrawal rate results in a longer expected time to ruin of 44.1 years. This difference underscores the advantage of higher equity exposure in achieving portfolio growth, although it comes with greater volatility. However, at very high withdrawal rates (e.g., 12%), even portfolios with high equity exposure experience rapid depletion, emphasising the importance of moderating withdrawal rates.

2.4 Conclusion

This chapter introduced a simulation-based methodology to evaluate withdrawal rates for retirement portfolios in the South African context. The analysis focuses on the distribution of end-of-period account balances and estimates the likelihood of capital depletion. The findings reveal a significant

decline in portfolio success rates as retirement spending increases, measured as an annual, inflation-adjusted percentage.

The results illustrate the impact of asset allocation on portfolio success. For instance, a 30-year portfolio composed entirely of bonds achieves only a 1% success rate with an annual withdrawal rate of 8%. In contrast, a portfolio consisting solely of equities significantly improves the success rate to 54% under the same conditions. This indicates that sustaining higher withdrawal rates over prolonged periods requires sufficient equity exposure.

The analysis demonstrates that lower withdrawal rates significantly extend the expected time to ruin for living annuities, regardless of equity exposure. Portfolios with higher equity allocations tend to last longer due to the potential for greater growth, as illustrated by the 44.1-year ruin time for a 70% equity allocation compared to 31.1 years for a 10% allocation at a 5% withdrawal rate. However, at high withdrawal rates, even portfolios with substantial equity exposure face rapid depletion, reinforcing the need for careful balance between withdrawal rates and asset allocation.

In the South African context and in agreement with Maré (2016), a 5% withdrawal rate appears sustainable for shorter investment horizons of 20 years or less. However, for longer-term periods, the outcomes align closely with those observed in the Cooley et al. (1998) and Maré (2016) studies, highlighting similar patterns in withdrawal rate sustainability. At higher withdrawal rates, it is vital that living annuities are exposed to more high return risky assets in the attempt to expend the expected life of the portfolio.

In this chapter, we have addressed research questions 1 and 2. For the first research question, we developed a benchmark simulation model to evaluate success rates and fugit outcomes within the South African context. The second research question explores the optimal ratio of bond and equity exposure, which is influenced by the retiree's individual risk profile and chosen withdrawal rate. By refining these models, we provide a foundation for tailoring retirement strategies that align with varying financial needs and market conditions.

Chapter 3

Hybrid retirement strategy in South Africa[1]

Keywords: Retirement · Living annuity · Life annuity · Bootstrap simulation · Portfolio management

3.1 Introduction

'The question is not at what age I want to retire, it's at what income.' George Foreman

The quote above, from George Foreman, is a great reminder that retirement ages are not fixed; they are unique to everyone. Some people can retire earlier than others. Hence, a retiree faces the following problem at retirement. They must decide on an appropriate amount to withdraw from their retirement investment, and 'optimise' between outliving their money and living below their means, wrote Maré (2016).

A recent study by Allianz (2023) revealed that 61% of respondents fear running out of savings during retirement more than they fear death. Conducted among U.S. adults aged 44 to 75, the study highlights the growing anxiety

[1]This chapter is based on a paper (Van Niekerk et al., 2024) published in the *South African Journal of Economic and Management Sciences*.

retirees feel about financial insecurity. Around 46% of participants reported having to reduce or stop saving for retirement due to inflation, market volatility, and recurring financial crises. Additionally, 40% acknowledged flaws in their retirement strategies, admitting uncertainty about when or how they would be able to realign their plans.

In South Africa, retirees are faced with emerging market conditions that presents unique challenges for retirees, as these conditions often introduce volatility, uncertainty, and financial strain. A study conducted by the Association for Saving and Investments in South Africa (ASISA) suggests that only 6% of economically active South Africans will be able to retire comfortably, and many are at risk of living below their pre-retirement standard of living (ASISA, 2022). Several factors contribute to the financial stress for those seeking to retire comfortably, as mentioned in the introduction. Addressing these challenges requires proactive policy interventions, improved financial literacy programmes, and a broader cultural shift toward long-term financial planning. For retirees in South Africa, adapting to these conditions means staying informed, seeking professional advice, and exploring diversified income streams to navigate the complexities of an emerging market economy.

Retirees in South Africa can choose from various retirement strategies, but they risk selecting an option that may not effectively meet their specific needs. According to Visser (2024), South African retirees typically choose between two main types of annuities: guaranteed life annuities and living annuities. Guaranteed life annuities, also known as life annuities, are insurance contracts that provide a predetermined income for the rest of the retiree's life. In contrast, living annuities offer greater flexibility, allowing retirees to select from a wide range of investment options.

A life annuity is a financial product that guarantees the holder a stream of income for the rest of their life (Milevsky, 2013). It is typically purchased from an insurance company using a lump-sum investment. The main feature of a life annuity is its ability to provide financial security by ensuring that the annuitant (the person who receives the payments) will receive a steady income, regardless of how long they live.

3.1. Introduction

A living annuity is a type of retirement income product that allows retirees to invest their retirement funds in various investment portfolios and draw a regular income from it (Beinash, 2008). Living annuities are popular for their flexibility and potential for growth, but they also carry more risk compared to life annuities, particularly due to market fluctuations and the responsibility placed on retirees to manage their investment choices wisely so that they do not outlive their assets (National Treasury, 2012). As such, living annuities are often chosen by retirees who are more comfortable with investment risk and who desire greater control over their retirement funds (National Treasury, 2012).

A typical retirement strategy requires a multifaceted approach, considering various products like annuities and a well-structured investment portfolio. Balancing risks such as mortality and longevity, alongside factors like healthcare costs, inflation, and tax implications, are essential for a secure retirement. Regularly reviewing and adjusting a retirement plan in response to life changes and to the current economic climate will help ensure that a retiree's retirement years are not only financially secure but also fulfilling.

The National Treasury (2012) conducted a study that indicated a sharp decline in the purchase of life annuities in South Africa. In 2003, 50% of retirement funds were used to buy life annuities and in 2011 this value had significantly decreased to only 14%. The study concluded that the decrease in the purchasing of life annuities can be attributed to sales incentives, particularly the higher commission earned by brokers for selling a living annuity compared to a life annuity (National Treasury, 2012).

Blanchett (2014) conducted a study to identify the various risks that annuitants might face when investing their retirement savings in either a living annuity or life annuity.

Given the risks identified by Blanchett (2014) and mentioned in the introduction, we investigate the merit of investing in a 'hybrid' retirement strategy, which consists of a combination of a life annuity and a living annuity, to increase the success rate of a retiree attaining their required withdrawal rate without outliving their retirement savings. The rationale for investing in a 'hybrid' strategy is that the life annuity will provide a

guaranteed income until death (partially reducing the longevity, volatility, and bequest risk). On the other hand, the living annuity provides flexibility, allows retirees to maximise their upside potential from investment returns, and provides benefits for a retiree's heir, but is still subject to volatility risk and longevity risk. The aim of the 'hybrid' retirement strategy is to increase the success rate of retirement portfolios overall.

The rest of this chapter is structured as follows: we provide a detailed literature review as well as a problem statement and proposed extension of previous work with reference to the retirement landscape in South Africa. An overview of the data used to simulate portfolios is provided. The methodology and assumptions describe the general methodology followed, which is based on sampling with replacement. This is followed by the results, which add to the existing literature by detailing the portfolio success rates for various 'hybrid' portfolio compositions. Lastly, we provide the conclusion and highlight other related areas for further research.

3.2 Literature Review

Bengen (1994) introduced the '4% rule', by demonstrating that an inflation-adjusted withdrawal rate of 4% of the initial portfolio amount is most likely sustainable over a 30-year period. This formed the foundation upon which other researchers have built, by investigating various strategies and asset allocations under different economic conditions.

Cooley et al. (1998) conducted a study to determine the impact of various withdrawal rates for US retirees investing in living annuities, as well as the necessary asset allocation to support the withdrawal rates. The framework proposed by Cooley et al. (1998) introduced a criterion for assessing the success rate of a retirement portfolio, which is defined by the probability of a portfolio 'outliving' the retiree over a predetermined period, withdrawal rate and asset allocation (for example, 30 years, 6% withdrawal rate and a portfolio consists of 75% equity and 25% bonds).

The success rate metric was used to evaluate the performance of living annuities for a variety of portfolios, and Cooley et al. (1998) found that an

inflation-adjusted withdrawal rate of between 4% to 5% is 'safe' for portfolios consisting of at least 75% equity and 25% bonds over a 30-year period. By adjusting withdrawals for inflation, all withdrawals in the near term are substantially reduced to allow for larger withdrawals in the long term to protect a retiree from inflation.

Pfau (2011) examined over 100-years of historical stock, bond, and inflation data from 17 developed countries and found that the 4% withdrawal rate was deemed to be too risky in 13 of the 17 countries. A fixed asset allocation throughout the investment period was shown to fail in all countries.

Finke et al. (2012) considered the impact of risk tolerance on retirement decisions by investigating the relationship between risk tolerance and asset allocation (stock, bonds, and bills) and withdrawal rates. They found that the 4% 'safe' withdrawal rate was appropriate for risk-averse retirees over a 30-year period. However, risk tolerant retirees may prefer higher withdrawal rates from riskier retirement portfolios, albeit with a greater probability of ruin.

Maré (2016) conducted a study to investigate safe withdrawal rates for South African retirees investing in living annuities. The analysis is based on historical inflation-adjusted equity and bond returns from 1950 to 2014; similarly, as in Cooley et al. (1999), portfolio success rates were used to infer a safe withdrawal rate. Various fixed investment periods were considered, ranging between 15 years and 30 years, assuming no mortality or transaction fees.

Maré (2016) notes that spending patterns, mortality rates, and asset returns tend to differ in South Africa, with which we concur. Remarkably, Maré (2016) results suggest that a 5% withdrawal rate is sustainable over a relatively short period of 15 years or less in South Africa. For longer investment horizons, the results are comparable to those of Cooley et al. (1998).

Van Appel et al. (2021) extended the research by investigating the effect of transactional fees and longevity using a dataset that spans from 1900 to 2020 for South African equities, bonds, cash and inflation. An analysis was performed to investigate the time until a living annuity depletes for

various withdrawal rates, termed 'fugit'. Van Appel et al. (2021) suggested a strategy to hedge some of the equity risk in the portfolio by taking long positions in put options and short positions in call options on a rolling one-month basis.

Van Appel et al. (2021) concluded that the portfolio success rate decreases rapidly when the withdrawal rate increases. For low withdrawal rates, the asset allocation does not have a significant impact on the portfolio success rate, and by making use of derivative instruments, retirees are able to hedge some of their risk and increase the success rate of the portfolio.

Anarkulova et al. (2023) examined retirement spending rules using historical stock and bond returns from 38 countries. Their findings suggest that a 65-year-old couple can withdraw only 2.26% of their retirement savings annually with a 5% probability of ruin over a 30-year period. This is significantly lower than the previously considered 4% 'safe' withdrawal rate.

Daraei and Sendova (2024) used a ruin-theory approach to analyse the inflows and outflows of a Canadian retiree's portfolio based on age, gender, initial wealth, and transaction data. By employing a sophisticated ruin model, they determined the average and median time until the portfolio is depleted, assessed the likelihood of the funds being exhausted within the retiree's remaining lifetime, and evaluated the deficit at the point of ruin.

Daraei and Sendova (2024) concluded that a withdrawal rate of approximately 4.5% is 'safe' over a 20-year period, but may not be enough to provide a sufficient income to ensure that a retiree can still live comfortably.

Structuring a 'safe' retirement and evaluating the relevant success rate of a certain retirement strategy is critically important. The consensus among the research done by Cooley et al. (1998), Finke et al. (2012), Maré (2016), Van Appel et al. (2021), and Daraei and Sendova (2024) is that staying within the 4% to 5% spending band will significantly increase the probability of the success of a retiree's retirement portfolio. Additional research done by, for example, Bengen (1994), Milevsky and Haung (2011), Butler and Van Zyl (2012), Warring and Siegel (2015), Maré (2016), Rusconi (2020), Klein and Sapra (2020), and Visser (2024) also highlights the fact that each retiree is unique and will require a distinct retirement solution to their retirement

situation (e.g., some may require medical care from the start of retirement, others may seek to maximise their heirs' inheritance, etc.).

From our literature review, the research above has considered the success rate of investing in a living annuity as a retirement strategy by looking at different compositions of bonds, bills, and equities while taking inflation into account for different withdrawal rates. However, the novelty of our research looks at the success rate of a 'hybrid' strategy that entails investing in both a life annuity and a living annuity for different portfolio compositions in the living annuity while still attaining the required withdrawal rate.

3.3 Problem Statement and Assumptions

Bengen (1994), Cooley et al. (1998), Finke et al. (2012), Maré (2016), Van Appel et al. (2021), and Daraei and Sendova (2024) all suggest that a 4% withdrawal rate is deemed 'safe' over a 30-year period. Using a 30-year period to model the success rate of a living annuity aligns with the period used by Cooley et al. (1998) as it assumes death at age 90, which sits on the tail end of the conditional life expectancy for South African retirees derived in the data section.

The research conducted by Maré (2016) and Van Appel et al. (2021) is specific to the South African retirement landscape, where they found that withdrawal rates greater than 5% are not sustainable over a 30-year period. It is alarming that a study conducted by ASISA (2022) suggests that approximately 69% of annuatised retirees have income drawdown rates greater than 5%.

Figure 3.1 suggests that approximately 50% of retirees in South Africa have an annual income drawdown rate of between 2.5% to 7.5%, where the average fund size-weighted annual drawdown rate is 6.66% (ASISA, 2022). Given that the 'safe' withdrawal rates, determined by Bengen (1994), Cooley et al. (1998), Finke et al. (2012), Maré (2016), Van Appel et al. (2021), and Daraei and Sendova (2024) are lower than the average fund size-weighted annual drawdown rate determined by ASISA (2022), further research is required to determine whether a 'hybrid' retirement strategy may yield higher success

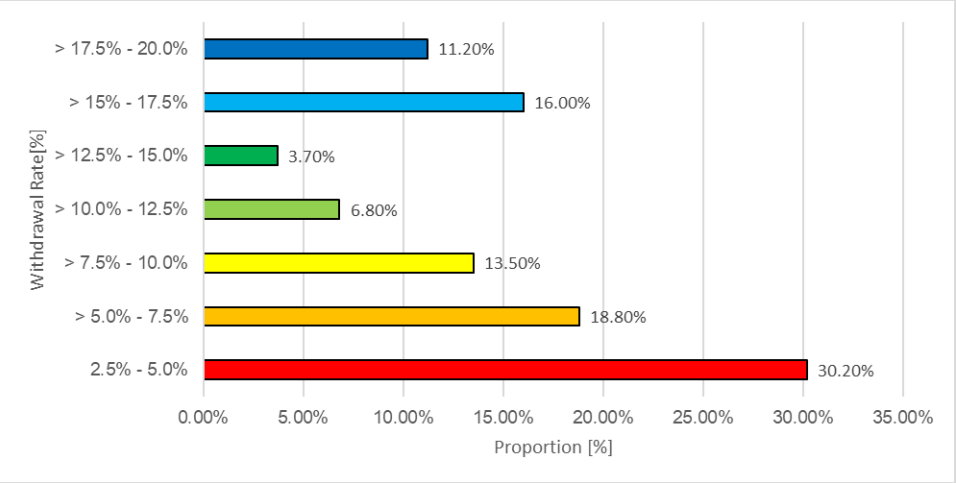

Figure 3.1: Proportion of Withdrawal Rate by Number of Policies in South Africa for 2022 (ASISA, 2022)

rates for higher withdrawal rates.

In managing a retirement portfolio, it is common for institutions to charge various fees, including advisor fees, fund management fees, and platform fees, which can significantly affect the portfolio's success rate; it is thus a crucial consideration for retirement planning. We consider the following fee structure for the living annuity by Van Appel et al. (2021):

Table 3.1: Fund Management Fees

Variable	**Fee Per Annum (%)**
Bonds	0.5
Equities	0.75
Platform fee	0.5
Financial advisor fee	1

The fees associated with a life annuity are typically lower than those associated with a living annuity, largely because once the investment is made in the life annuity, insurers are free to invest the money as they see fit. The insurance company will calculate the annuity rate by factoring in the costs of commission and investment charges that the insurance company will have to fund over the life of the product (National Treasury, 2013). We assume that the initial costs associated with a life annuity amount to 1% of the initial investment.

To evaluate the effectiveness of a 'hybrid' retirement strategy, we consider different portfolio compositions with respect to the allocations in a life annuity and a living annuity. Our analysis of the success rate assumes that the retirement age is 60 and spans a 30-year period, which is conservative given the conditional median life expectancy in Table 3.3. It is crucial to acknowledge that our analysis does not include considerations for taxes; however, these could, in theory, be incorporated into our analysis.

We make the following assumptions to determine the success rate of our 'hybrid' retirement strategy:

1. An initial investment of R1 million, where a portion of the initial investment is invested in a life annuity and the remaining portion is invested in a living annuity.
2. The asset allocation between bonds and equities in the living annuity remains fixed over the life of the investment.
3. Asset returns have been adjusted for inflation and are thus real returns.
4. The mortality rates used for the life annuity calculation are for assured lives (Dorrington and Tootla, 2007), with a 10% mortality adjustment factor.
5. The interest rate curve used for the life annuity calculation is an inflation adjusted curve, i.e., real interest rates as of 29 December 2023 (Bank, 2024).
6. The life annuity includes a five-year guarantee period, which means that if death occurs between age 60 to 65, the remaining balance of the life annuity will be paid to the retiree's heirs.
7. Withdrawals from both the life annuity and living annuity are monthly.
8. A static withdrawal rate over the 30-year period.

In this study, we extend the research of Maré (2016) by investigating the success rate of a 'hybrid' strategy, whereby a portion of a retiree's portfolio is invested in a life annuity and the remaining portion is invested in a living annuity. The rationale behind this 'hybrid' approach is twofold. The life

annuity diminishes longevity risk but provides no flexibility. On the other hand, the living annuity provides flexibility and benefits for a retiree's heir but has significant longevity risk. By investing in a combination of the two products, a retiree may find a suitable risk-adjusted hybrid strategy to meet their specific needs.

3.4 Data

The value of a living annuity is dependent on asset class returns, where a typical living annuity portfolio consists of a risky asset (equity) and a 'safe' asset (bonds). We highlight summary statistics for South African bonds and equities for the period from 1900 to 2020 in Table 3.2[2], which is based on data sourced from Firer and Staunton (2002), Dimson et al. (2014), and Van Appel et al. (2021).

Table 3.2: Asset Class Statistics for South Africa Over the Period 1900 to 2020

Variable	Nominal Return (%)	Real Return (%)	Standard Deviation (%)	Skewness	Kurtosis
Equity	13.7	8.4	15.7	-0.15	4.19
Bonds	7.0	2.1	5.7	-0.05	12.05

Throughout our research, we only consider real returns for equities and bonds, which means that the returns used in modelling the 'hybrid' retirement strategy have been adjusted for future inflation.

The value of a life annuity is dependent on the age of the insured, mortality rates, and interest rates. We assume that the average retirement age in South Africa is 60 and derive conditional survival probabilities from the South African life tables for assured lives (Dorrington and Tootla, 2007).

Given that these life tables are based on data from 1996 to 2000, a mortality adjustment factor of 10% is applied. The rationale for applying a mortality

[2]The long-term data that were used in this study, were used to closely align to align to work performed by Maré (2016) and Van Appel et al. (2021).

adjustment factor is because an analysis conducted by the World Health Organization (WHO) suggests that the life expectancy for both males and females has increased by 10.2% from the year 2000 to 2021 (World Health Organization, 2021).

In South Africa, the World Health Organization (2019) suggests that the average life expectancy from birth is approximately 62 years of age for both males and females. However, using the South African life tables for assured lives (Dorrington and Tootla, 2007), the expected lifespan extends to approximately 79 years for males and 84 years for females, provided that they have already reached the age of 60.

The conditional survival probabilities, with and without a mortality adjustment, are presented in Table 3.2.

Table 3.3: Conditional Survival Probabilities for South African Retirees Given Age 60

Conditional survival probability age 60 to:	**Unadj. Mortality (%)**			**Adj. Mortality (%)**		
	Male	**Female**	**Both**	**Male**	**Female**	**Both**
65	89	95	92	90	95	93
70	77	88	82	79	89	84
75	62	78	70	65	80	72
80	46	64	54	49	67	58
85	28	45	35	32	49	39
90	12	24	17	15	28	21
95	3	8	5	5	11	7
100	0	2	1	1	2	1
Conditional median life expectancy given age 60	**78.7**	**83.3**	**81.1**	**79.8**	**84.7**	**82.2**

Source: Dorrington and Tootla (2007).

After applying the mortality improvement factor of 10% to the South African life tables for assured lives, the conditional survival probabilities increase for both males and females. Further, the conditional median life expectancy increases to approximately 80 years for males and 85 years for females.

3.5 Modelling Methodology

The methodology used to simulate our portfolios is based on random sampling with replacement, also known as bootstrapping. The technique was first introduced by Efron (1979). This resampling technique is used to estimate the distribution of a statistic by resampling, with replacement from a dataset. It allows for estimating the precision of sample statistics by using subsets of accessible data or repeatedly drawing samples from the original dataset with replacement.

We created our bootstrapped samples by repeatedly resampling with replacement from our monthly return dataset for equities, bonds, and inflation from January 1900 to April 2020. Let $Y_1^j, Y_2^j, Y_3^j, \ldots, Y_{1444}^j$ denote the historical return for the i^{th} month and j^{th} asset class. Based on the historical returns, we posit that each $Y_i^j, \forall i$ is equally likely to be chosen. Moreover, the i^{th} return sample is then consistently applied across all asset classes to maintain the integrity of the correlation structure.

This produces a 30-year bootstrap sample that is composed of randomly selected observations, where each observation can be chosen more than once. This process is repeated many times (in our case 10 000 samples) to build the distributional characteristics of our returns path process. Each individual path constitutes a random scenario based on the monthly bootstrapped returns. The process uses simulation by random sampling.

A typical retirement strategy is to invest in either a living annuity, where the living annuity portfolio typically consists of bonds and equities, or a life annuity. Retirees who opt for the aforementioned are required to choose the composition of bonds and equities according to their risk appetite.

The 'hybrid' retirement strategy is multidimensional in the sense that a retiree needs to decide how much of their investment to invest in:

1. A living annuity, which typically comprises holdings of equities, bonds, and money market assets, or
2. A life annuity.

Furthermore, a retiree is also required to decide on an income drawdown rate to suit their specific spending requirements.

The value of the hybrid retirement strategy, denoted by Π, at inception is given by (Equation 3.1):

$$\Pi(0) = \Pi_{\text{life}}(0) + \Pi_{\text{living}}(0) \tag{3.1}$$

$$\Pi(0) = N \cdot \omega_{\text{life}} + N \cdot \omega_{\text{living}}; \tag{3.2}$$

where:

1. N denotes the initial investment;
2. ω_{life} denotes the weight invested in the life annuity;
3. ω_{living} denotes the weight invested in the living annuity; and
4. $\omega_{\text{life}} + \omega_{\text{living}} = 1$.

If $\omega_{\text{life}} = 1$, then the portfolio defaults to a living annuity; similarly, if $\omega_{\text{living}} = 1$, then the portfolio defaults to a life annuity.

The life annuity provides a predetermined income for the rest of the assured life and is known at inception of the policy. The value of the living annuity fluctuates with respect to asset class returns and withdrawals. We consider the life annuity and living annuity in the 'hybrid' retirement strategy separately.

We denote the total annual withdrawal rate required by a retiree as $r_{\text{portfolio}}$, and the fixed withdrawal rate obtained from the life annuity as r_{life}, then the withdrawal rate required from the living annuity, r_{living}, is determined subject to the following condition: $r_{\text{portfolio}} = r_{\text{life}} + r_{\text{living}}$.

The total withdrawal is based on the initial investment amount, i.e., $\Pi(0)$. For example, if $\Pi(0) = R1,000,000$ and a retiree requires a total annual withdrawal of 5%, then an annual income of R50 000, paid monthly, is required for the remainder of the insured life.

$$\Pi_{\text{living}}(t) = \Pi_{\text{living}}(t-1)\left[\omega_{\text{equity}}\left(1 + r_{\text{equity}}(t)\right) + \omega_{\text{bond}}\left(1 + r_{\text{bond}}(t)\right) - r_{\text{living}}\right] \tag{3.3}$$

where

1. ω_{equity} denotes the weight invested in *equities*;
2. ω_{bond} denotes the weight invested in *bonds*;
3. r_{equity} denotes the monthly real return from *equities*;
4. r_{bond} denotes the monthly real return from *bonds*; and
5. r_{living} denotes the monthly withdrawal required by a retiree from the living annuity.

The Gompertz Annuity Pricing Model (GAPM) is used to determine the price of a life annuity. This price – or the amount of income you can expect for a given premium deposit – is influenced by the competitive market interactions among insurance companies. Although market forces partly determine the actual price, a strict mathematical relationship links mortality expectations and interest rates to observed prices in direct similarity to the concept of arbitrage in securities markets. Milevsky (2013) provides the following formula to price a life annuity:

$$a(x, g, R) = \sum_{i=1}^{g} \frac{1}{(1+R)^i} + \sum_{i=g+1}^{\varphi - x} \frac{p(x,i)}{(1+R)^i}, \tag{3.4}$$

where

1. $a(x, g, R)$ is the upfront cost of R1 per year for life, starting at age x, guaranteed for g periods, given annual nominal interest rate R;
2. $p(x, i)$ is the survival probability from age x to age $x + i$;
3. R is the interest rate; and
4. φ denotes the oldest possible age attainable.

This formula3.4 includes two components: the guaranteed portion and the life-contingent portion. The guaranteed portion is the sum of the present values of payments for the guaranteed period, while the life-contingent portion considers survival probabilities.

Table 3.4 illustrates the contribution of the life annuity and living annuity to the total withdrawal rate for different proportions invested in the life annuity and living annuity. The life annuity withdrawal contribution is determined at inception, which is assumed to be at age 60. The required contribution from the living annuity is determined by subtracting the life annuity withdrawal contribution from the required annual withdrawal rate.

Table 3.4: Life Annuity Withdrawal Contribution

Invested in life annuity (%)	Life annuity withdrawal contribution (%)	4%	6%	10%
0	0.00	4.00	6.00	10.00
10	0.71	3.29	5.29	9.29
20	1.42	2.58	4.58	8.58
30	2.13	1.87	3.87	7.87
40	2.85	1.15	3.15	7.15
50	3.58	0.42	2.42	6.42
60	4.31	0.00	1.69	5.69
70	5.04	0.00	0.96	4.96
80	5.78	0.00	0.22	4.22
90	6.52	0.00	0.00	3.48
95	6.89	0.00	0.00	3.11

To interpret the results in Table 3.4, we consider when the required withdrawal rate is 10%, which is illustrated in Figure 3.2. The required withdrawal rate is split into two components, the life annuity will contribute a percentage, depending on the % invested in a living annuity, and the rest of the withdrawal composition will then be drwan from the living annuity.

When the initial investment in a life annuity is 0%, then the 'hybrid' retirement strategy defaults to a living annuity and the total annual income drawdown required from the living annuity is 10%. As the initial investment in the life annuity increases, the contribution from the life annuity to the total required withdrawal rate increases. As a result, the contribution

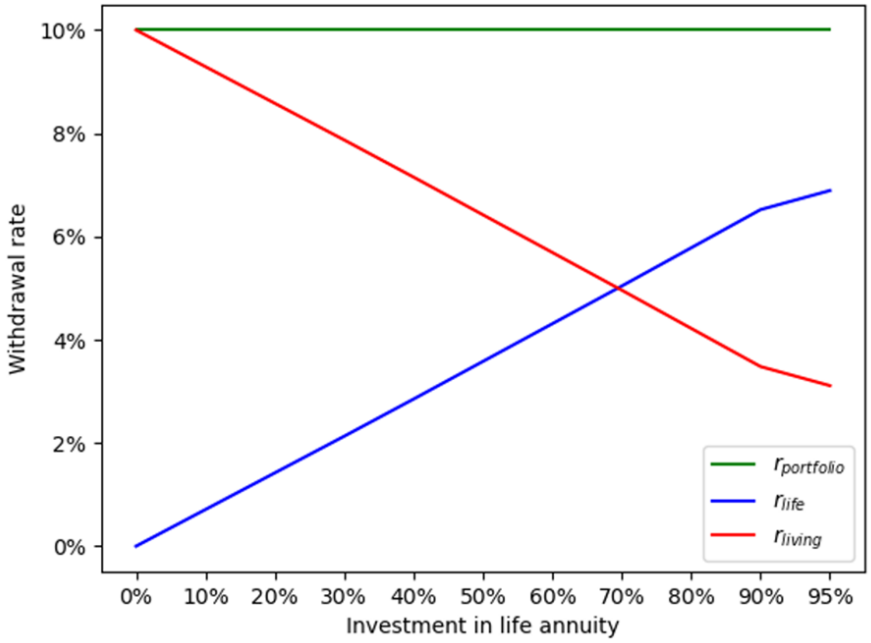

Figure 3.2: Withdrawal Contributions from Annuity Products to the Required Withdrawal Rate.

required from the living annuity decreases – but the total withdrawal rate from the two annuities is always equal to the required withdrawal rate.

If a portion of retirement savings is invested in a life annuity, even if the living annuity depletes, the retiree will still be partially secured for the rest of their life from the predetermined income from the life annuity. This allows retirees to assume some level of safety from the life annuity, while allowing for flexibility from the riskier living annuity.

3.6 Results

As a preliminary analysis, we illustrate what the value of a living annuity may look like for two different random paths over 30 years, assuming an annual withdrawal rate of 6%, an initial investment amount of R1 million, and equal weights invested in bonds and equities. We perform the analysis over a period of 30 years given that the conditional median life expectancy, starting from age 60, is 82 years.

From Figure 3.3, the value of the portfolio along path 2 reaches 0 at approximately 25 years. However, the value of the portfolio along path 1 does not reach 0. Therefore, we consider path 1 to be successful since a retiree will not run out of money. The success rate of this simple example is 50%.

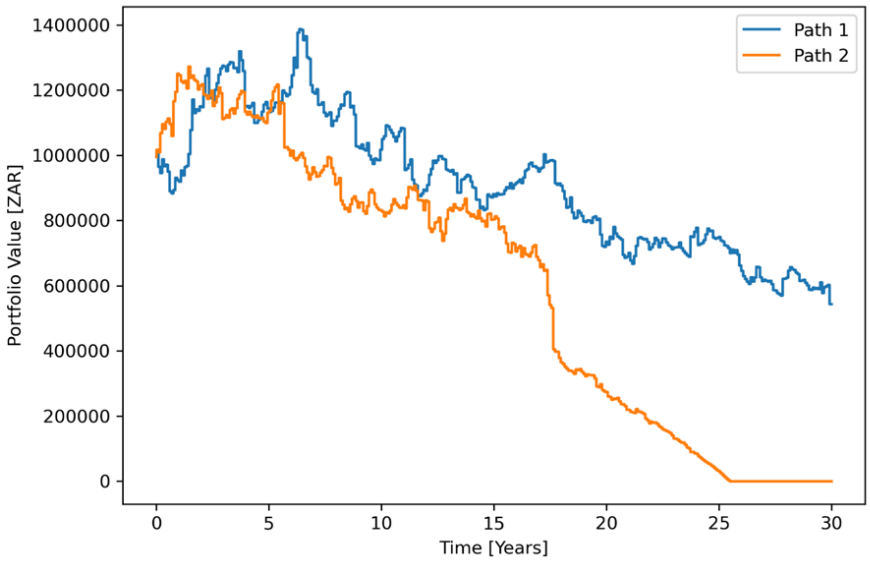

Figure 3.3: Two Simulated Paths of a Living Annuity.

Portfolio 1: 100% investment in living annuity

To aid in analysing the results, we first consider a retirement strategy where 100% of a retiree's portfolio is invested in a living annuity, thus reducing the dimension of the 'hybrid' retirement strategy, i.e. $\omega_{\text{life}} = 0$ and $\omega_{\text{living}} = 1$.

The success rate of the portfolio is determined using 10 000 simulations, where the annual withdrawal rates range from 3% to 12% and the asset allocation in bonds and equities vary.

Figure 3.4 illustrates the success rate for varying asset allocations and withdrawal rates for Portfolio 1.

Two important observations can be inferred from Figure 3.4:

1. The success rate increases as the withdrawal rate decreases; and

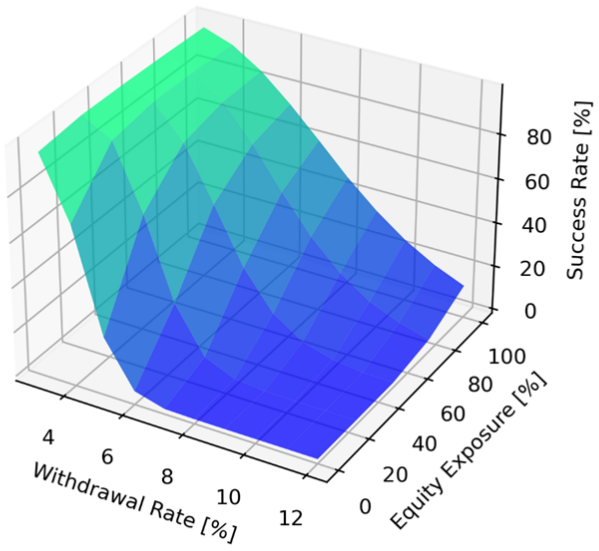

Figure 3.4: Success Rates for Portfolio 1 ($\omega_{\text{living}} = 1$, $\omega_{\text{life}} = 0$)

2. The success rate increases as the equity exposure in the living annuity increases.

Our results indicate that increased withdrawal rates result in dramatically reduced success rates, regardless of the asset allocation. The greater the asset allocation to equity, the greater the success rate. This is expected since equities typically have higher returns compared to bonds, although they are more volatile.

Portfolio 2: 50% investment in living annuity and 50% investment in life annuity

Our 'hybrid' retirement strategy introduces another dimension, an initial allocation in a life annuity. We consider the case when 50% of a retiree's initial investment is invested in a life annuity and the remaining 50% is invested in a living annuity, i.e. $\omega_{\text{life}} = 0.5$ and $\omega_{\text{living}} = 0.5$.

The annual withdrawal rate from the life annuity is 3.58% of the original

investment amount. Therefore, for example, if a retiree requires a withdrawal rate of 6% annually, the remaining 2.42% will be withdrawn from the living annuity. As a result, the withdrawal from the living annuity is significantly reduced in comparison to Portfolio 1. This ensures that the retiree will always receive their required withdrawal rate, albeit from two different retirement products.

We superimpose a surface of the success rates using a 'hybrid' strategy over the surface of success rates for a pure living annuity in Figure 3.5.

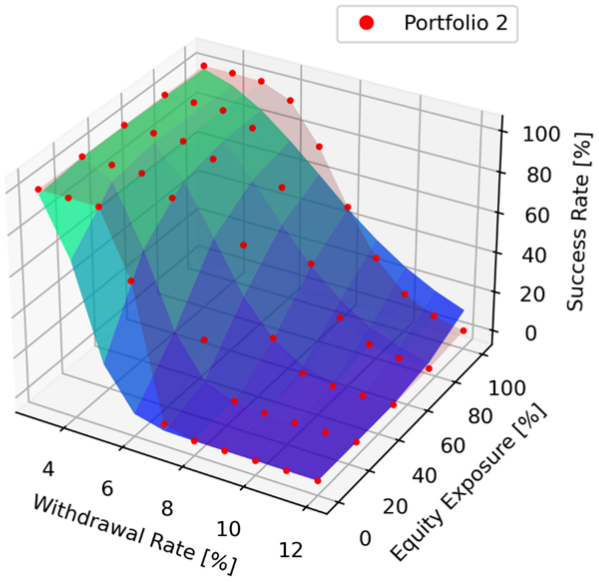

Figure 3.5: Success Rates for Portfolio 1 ($\omega_{\text{living}} = 1$, $\omega_{\text{life}} = 0$) vs Portfolio 2 ($\omega_{\text{living}} = 0.5$, $\omega_{\text{life}} = 0.5$).

There is a notable increase in the success rate of Portfolio 2 in comparison to Portfolio 1 when the withdrawal rate is less than, or equal to, 8% across all portfolio compositions for the living annuity. However, for higher withdrawal rates, the success rate of Portfolio 1 dominates that of Portfolio 2, specifically when the equity exposure is high.

The results from Portfolio 2 indicate that an initial investment in a life annuity increases the likelihood of success compared to retirement portfolios

that consist of pure living annuities for withdrawal rates of 8% or less. This is a significant result because the study conducted by ASISA suggests that approximately 50% of South African retirees withdraw between 2.5% and 7.5% of their portfolios annually.

The success of approximately 50% of South Africans with living annuities can be increased by investing in a combination of a living annuity and a life annuity. Furthermore, retirees who have invested a portion of their portfolio in a life annuity will still receive an income drawdown until death, even if their living annuity depletes.

Until this point, we have only considered the 'hybrid' retirement strategy without fees. However, fees can have a large impact on the longevity and success of a retiree's portfolio. For example, if a retiree invested in a pure living annuity, where the asset allocation to bonds is 100%, a retiree may experience significant capital erosion as the average real return on bonds is approximately 2.1% and the fund management fees amount to approximately 2.25%. This results in an average negative real return of -0.15%.

To illustrate the impact of fees on a living annuity, we consider a pure living annuity with an annual drawdown rate of 6% and equal weights in bonds and equities. We plot the average portfolio value over 10 000 simulations, including and excluding fees. Figure 3.6 shows that the impact of fees cannot be ignored as the portfolio value erodes significantly faster. The average value of the portfolio without fees is approximately R680 000 with a success rate of 57%. Once fees are introduced, the portfolio value decreases to approximately R120 000 after 30 years, with a success rate of just 20%.

We illustrate the effect of fees on the success rate of Portfolio 1 for different asset allocations and withdrawal rates in Figure 3.6. We superimpose the success rate surface of Portfolio 1 with fees on the success rate surface of Portfolio 1 without fees.

It is evident from Figure 3.7 that fees drastically reduce the success rate of a living annuity, especially when the equity exposure is low as the returns from bonds are not sufficient to offset the fees.

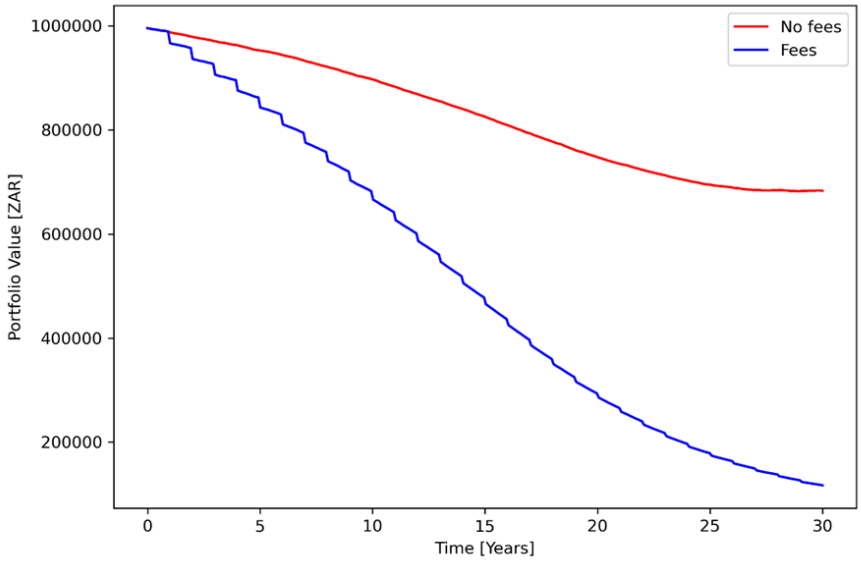

Figure 3.6: Impact of Fees on Portfolio Value ($\omega_{\text{living}} = 1$, $\omega_{\text{life}} = 0$,$\omega_{\text{equity}} = 0.5$,$\omega_{\text{bond}} = 0.5$,$r_{\text{portfolio}} = 6\%$).

We now consider the effect of fees on the 'hybrid' retirement strategy, where equal portions are invested in a life annuity and a living annuity, i.e., Portfolio 3. Figure 3.8 illustrates the success rate of Portfolio 1 (blue surface) and the success rate of Portfolio 2 (red surface), with fees taken into consideration for both portfolios.

The success rate of Portfolio 2 is still significantly higher than the success rate of Portfolio 1 when accounting for fees in both portfolios for withdrawal rates less than 8% per annum. This is expected as the fees typically associated with a life annuity are less than those associated with a living annuity.

We note that although the success rates may be lower for Portfolio 2 compared to Portfolio 1 when the withdrawal rates are greater than 7% and fees are accounted for, a retiree will still receive an income until death from the life annuity.

The success rates for different portfolio compositions in life and living annuities, asset allocations, and withdrawal rates including fees is provided in

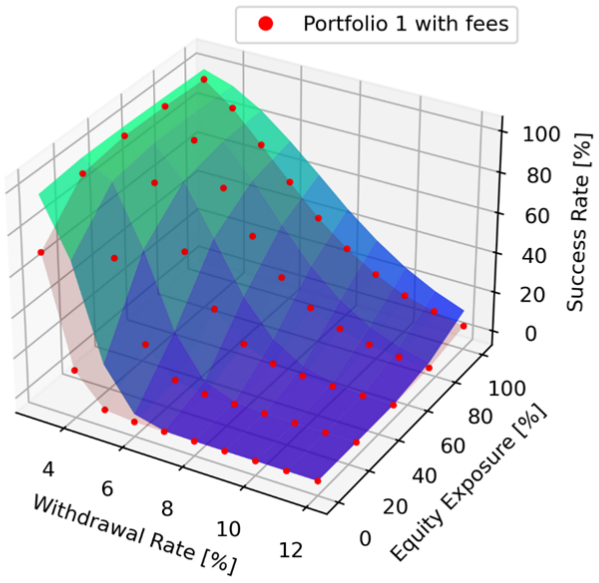

Figure 3.7: Impact of Fees on the Success Rate of Portfolio 1 ($\omega_{\text{living}} = 1$, $\omega_{\text{life}} = 0$).

Table 5. Similarly, as noted previously, as the investment in a life annuity at inception increases, so does the success rate when the withdrawal rate is less than or equal to 7%.

Table 3.5 provides the portfolio success rates for different portfolio compositions in life and living annuities, asset allocations, and withdrawal rates. The success rates for portfolios, excluding fees, are provided along with the success rates for portfolios with the associated portfolio management fees in square brackets.

From Table 3.5, we observe that the fee structure of a retirement portfolio significantly decreases the success rate for all portfolio compositions. For example, the success rate of Portfolio 1 with equal weights in bonds and equities, and a 6% withdrawal rate is 57% without fees compared to a success rate of just 20% when fees are included.

With respect to Portfolio 2, with equal weights in bonds and equities,

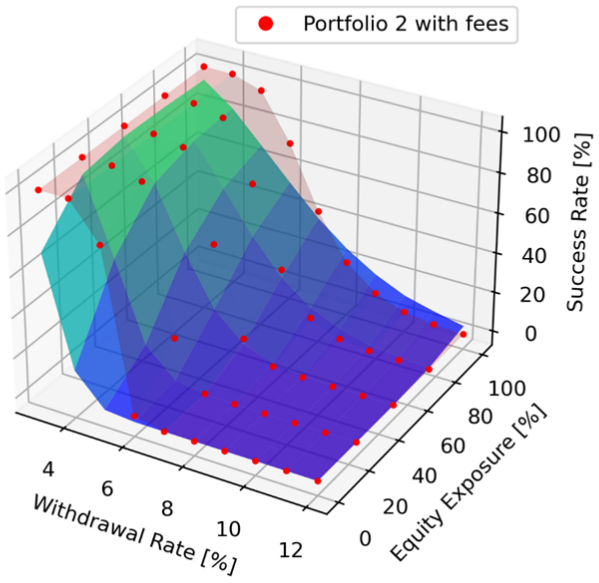

Figure 3.8: Impact of Fees on the Success Rate of Portfolio 1 ($\omega_{\text{living}} = 1$, $\omega_{\text{life}} = 0$) vs Portfolio 2 ($\omega_{\text{living}} = 0.5$, $\omega_{\text{life}} = 0.5$).

and a 6% withdrawal rate, we obtain a success rate of 95% without fees. This success rate declines to 53% when taking fees into account, but it is still significantly higher than the success rate of the pure living annuity (Portfolio 1).

For all different compositions of the 'hybrid' retirement strategy considered, we observe that the success rates of the 'hybrid' strategy dominate those of the pure living annuity for withdrawals less than 8%. Portfolio management fees impact the success rate of all strategies but are more pronounced for portfolios that have a larger weight invested in a living annuity.

Table 3.5: Portfolio Success Rates for Different Asset Allocations, Withdrawal Rates and Life Annuity Proportions Over 30 Years (excluding fees)

	Withdrawal rate as a percentage of initial investment									
Equity Exposure	**3%**	**4%**	**5%**	**6%**	**7%**	**8%**	**9%**	**10%**	**11%**	**12%**
0% Life Annuity / 100% Living Annuity										
0%	98%	70%	24%	4%	0%	0%	0%	0%	0%	0%
25%	100%	93%	64%	28%	8%	1%	0%	0%	0%	0%
50%	100%	95%	81%	57%	32%	16%	7%	2%	1%	0%
75%	99%	95%	86%	69%	52%	35%	23%	13%	8%	4%
100%	98%	94%	86%	74%	61%	48%	36%	26%	19%	13%
25% Life Annuity / 75% Living Annuity										
0%	100%	100%	70%	14%	1%	0%	0%	0%	0%	0%
25%	100%	100%	93%	52%	12%	1%	0%	0%	0%	0%
50%	100%	100%	95%	74%	41%	16%	4%	1%	0%	0%
75%	100%	100%	95%	80%	59%	36%	19%	9%	4%	1%
100%	100%	99%	93%	82%	66%	49%	33%	21%	13%	8%
50% Life Annuity / 50% Living Annuity										
0%	100%	100%	100%	68%	3%	0%	0%	0%	0%	0%
25%	100%	100%	100%	92%	27%	1%	0%	0%	0%	0%
50%	100%	100%	100%	95%	57%	16%	2%	0%	0%	0%
75%	100%	100%	100%	95%	70%	36%	13%	4%	1%	0%
100%	100%	100%	100%	94%	75%	49%	27%	13%	5%	2%
75% Life Annuity / 25% Living Annuity										
0%	100%	100%	100%	100%	66%	0%	0%	0%	0%	0%
25%	100%	100%	100%	100%	91%	1%	0%	0%	0%	0%
50%	100%	100%	100%	100%	94%	15%	0%	0%	0%	0%
75%	100%	100%	100%	100%	94%	35%	4%	0%	0%	0%
100%	100%	100%	100%	100%	93%	48%	12%	2%	0%	0%
90% Life Annuity / 10% Living Annuity										
0%	100%	100%	100%	100%	100%	0%	0%	0%	0%	0%
25%	100%	100%	100%	100%	100%	1%	0%	0%	0%	0%
50%	100%	100%	100%	100%	100%	14%	0%	0%	0%	0%
75%	100%	100%	100%	100%	100%	34%	0%	0%	0%	0%
100%	100%	100%	100%	100%	100%	46%	1%	0%	0%	0%

Table 3.6: Portfolio Success Rates for Different Asset Allocations, Withdrawal Rates and Life Annuity Proportions Over 30 Years (including fees)

	Withdrawal rate as a percentage of initial investment									
Equity Exposure	**3%**	**4%**	**5%**	**6%**	**7%**	**8%**	**9%**	**10%**	**11%**	**12%**
0% Life Annuity / 100% Living Annuity										
0%	70%	16%	1%	0%	0%	0%	0%	0%	0%	0%
25%	92%	54%	16%	2%	0%	0%	0%	0%	0%	0%
50%	95%	76%	46%	20%	7%	2%	1%	0%	0%	0%
75%	95%	82%	62%	41%	24%	13%	7%	3%	1%	1%
100%	93%	83%	69%	53%	38%	27%	17%	11%	7%	4%
25% Life Annuity / 75% Living Annuity										
0%	100%	74%	10%	0%	0%	0%	0%	0%	0%	0%
25%	100%	94%	43%	6%	0%	0%	0%	0%	0%	0%
50%	100%	96%	69%	30%	8%	2%	0%	0%	0%	0%
75%	100%	95%	77%	50%	26%	11%	4%	2%	1%	0%
100%	99%	94%	79%	60%	39%	25%	14%	7%	4%	2%
50% Life Annuity / 50% Living Annuity										
0%	100%	100%	82%	3%	0%	0%	0%	0%	0%	0%
25%	100%	100%	96%	23%	0%	0%	0%	0%	0%	0%
50%	100%	100%	97%	53%	10%	1%	0%	0%	0%	0%
75%	100%	100%	96%	67%	28%	8%	2%	0%	0%	0%
100%	100%	100%	95%	72%	41%	20%	8%	3%	1%	0%
75% Life Annuity / 25% Living Annuity										
0%	100%	100%	100%	97%	0%	0%	0%	0%	0%	0%
25%	100%	100%	100%	100%	2%	0%	0%	0%	0%	0%
50%	100%	100%	100%	99%	18%	0%	0%	0%	0%	0%
75%	100%	100%	100%	99%	38%	3%	0%	0%	0%	0%
100%	100%	100%	100%	98%	49%	11%	1%	0%	0%	0%
90% Life Annuity / 10% Living Annuity										
0%	100%	100%	100%	100%	4%	0%	0%	0%	0%	0%
25%	100%	100%	100%	100%	29%	0%	0%	0%	0%	0%
50%	100%	100%	100%	100%	58%	0%	0%	0%	0%	0%
75%	100%	100%	100%	100%	71%	0%	0%	0%	0%	0%
100%	100%	100%	100%	100%	75%	1%	0%	0%	0%	0%

From Table 3.5 and Table 3.6, we observe that a larger investment in a life annuity at inception generally results in increasing success rates for withdrawal rates less than 8%. However, each retiree is unique, and some

may prefer the flexibility offered by investing a smaller portion in a life annuity.

Overall, an average decrease of 11% in the success rate is observed over the different portfolio compositions considered from Table 3.5 to Table 3.6.

Table 3.7 indicates that the success rates of retirement portfolios, which have a high percentage invested in a living annuity, are, on average, affected more by portfolio management costs. This is mainly due to the nature of the retirement products, where living annuities have annual management costs and life annuities only have once-off costs at inception.

Table 3.7: The Average Impact of Portfolio Management Costs on Success Rates

Portfolio Scenarios	**Average Success Rate Impact (%)**
0% Life Annuity / 100% Living Annuity	-14
25% Life Annuity / 75% Living Annuity	-12
50% Life Annuity / 50% Living Annuity	-11
75% Life Annuity / 25% Living Annuity	-9
90% Life Annuity / 10% Living Annuity	-7

The goal of the 'hybrid' strategy is twofold:

1. To increase the success rate of a retirement strategy for a given withdrawal rate.
2. To increase the inheritance of a retiree's heir.

Figure 3.9 illustrates the average value of a retiree's living annuity for different weights invested in a life annuity and a living annuity, assuming a 6% drawdown rate, portfolio management fees, and equal weights invested in bonds and equities.

When investing purely in a living annuity, the value of the portfolio decreases rapidly, which is consistent with the low success rate of 20% observed for this portfolio. Although the value of the pure living annuity portfolio is the greatest at inception, it has the lowest average value after 30 years. The portfolio composition that maximises both the success rate and the living

annuity value after 30 years is where there is an initial investment of 75% in a life annuity and 25% investment in a living annuity. The success rate for this portfolio composition is 99%, and the average living annuity value increases over time, allowing a retiree to leave an inheritance to their heir, while still achieving the required withdrawal rate of 6%.

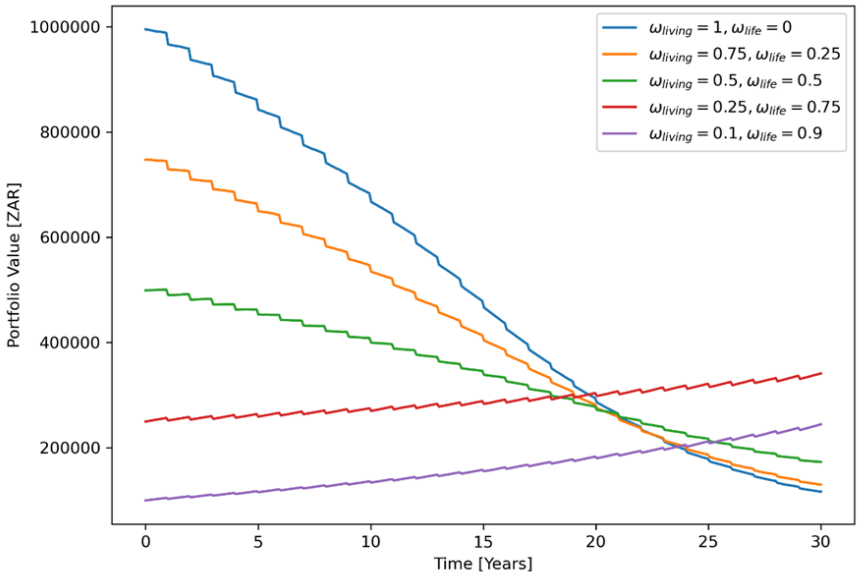

Figure 3.9: Average Portfolio Values for a Pure Living Annuity versus Various Hybrid Strategy Exposures.

In Figure 3.9 we compare the Average Portfolio Values for a Pure Living Annuity versus Various Hybrid Strategy Exposures, we have only considered a 6% withdrawal rate with an equal composition in bonds and equities. Our analysis can be extended to different withdrawal rates and living annuity compositions as each retiree is unique and some may require higher withdrawal rates than others, or some may seek to maximise their heir's inheritance. A 'hybrid' strategy increases both the success rate and the value of a retiree's living annuity when the withdrawal rate is less than 8%, which has the potential to increase the success rate of approximately 50% of annuatised South Africans.

3.7 Conclusion

'The choice of a withdrawal rate involves individual preference for current consumption, uncertainty of life expectancy, and variable financial needs, there is no single globally optimal withdrawal rate.' (Cooley et al., 1999)

The quote by Cooley et al. (1999) is significant because every retiree has different needs and will have to adopt a strategy that meets their needs. In a South African context, we have shown that a 'hybridised' retirement portfolio increases the probability of success for retirees withdrawing less than 8% of their portfolio annually, which is approximately 50% of the annuatised population. We observed that portfolio management fees influence the success rate of our results significantly and cannot be ignored. However, the 'hybrid' strategy still has a higher success rate when portfolio management costs are accounted for. We have shown that a 'hybrid' retirement strategy not only has an increased success rate but, on average, the living annuity portion has a higher value after 30 years (depending on the portfolio composition), providing a larger inheritance for a retiree's heir.

There are optimal thresholds of holding a certain level of life annuity, depending on the set withdrawal rates. Portfolios that have to sustain higher levels of withdrawals will have to hold a significant holdings in life annuity as well as expose the living annuity to a higher level of equity exposure to improve the probability of success. Lower withdrawal rates, like 3%, do not necessarily necessitate the purchasing of a life annuity as the probability of having a successful portfolio is quite high. Refer to Appendix A for more analyses on the success rates at set withdrawal rates

A 'hybrid' retirement strategy could provide 'safe' withdrawal rates of up to 6% when accounting for fees, which is a significant increase from the 4% 'safe' withdrawal rate without fees recommended by Maré (2016) for South African retirees.

In this chapter, we have addressed research questions 3, 4, and 5, each contributing to a deeper understanding of retirement strategy optimisation. The third research question highlights how a hybrid retirement strategy

secures income from a third-party provider, alleviating pressure on the living annuity by reducing excessive withdrawals and mitigating longevity risk. This approach enhances portfolio sustainability by balancing guaranteed income with market exposure.

The fourth research question focuses on determining the 'optimal' ratio between life annuities and living annuities. However, this ratio is inherently dependent on the retiree's individual withdrawal needs and risk tolerance. Addressing the fifth research question, the results section of this chapter demonstrates that fees play a critical role in shaping withdrawal rates and influencing fugit calculations. This underscores the importance of cost efficiency in retirement planning, as even modest fee adjustments can significantly impact long-term outcomes.

In the following chapter, we discuss the effect that stochastic correlation has on the modeling process. By incorporating stochastic correlation, we aim to enhance the consistency and accuracy of the modeling approach, ensuring a more robust representation of real-world dynamics. This inclusion allows for a more comprehensive understanding of the inherent uncertainties.

Chapter 4

A Multivariate Stochastic Approach to Determine Long-term Success of SA Living Annuity Portfolios[1,2]

Keywords: Stochastic correlation · Withdrawal Rates · Living annuities · Diversification · Heston model · Hyperbolic Tangent Ornstein-Uhlenbeck · Efficient Method of Moments · Foreign Exposure

4.1 Introduction

Proactive retirement planning is essential for ensuring financial security in the latter stages of life, as it helps retirees manage their assets to support a sustainable income stream over, potentially decades of retirement. By carefully planning withdrawal rates and asset allocations, retirees can significantly increase the success rates of their portfolios, reducing the risk

[1]This chapter is based on a paper that has been submitted to *South African Actuarial Journal*.

[2]This chapter builds a general scenario for evaluating the impact of stochastic correlation and foreign exposure.

of outliving their savings and maintaining their desired standard of living. Several research papers have contributed to the literature on retirement planning and the associated success rates of a retiree's portfolio. They include, but are not limited to, Cooley et al. (1998), Pfau (2011), Finke et al. (2012), Butler and Van Zyl (2012), Maré (2016), Rusconi (2020), Klein and Sapra (2020), Van Appel et al. (2021), Anarkulova et al. (2023), and Daraei and Sendova (2024).

Several other factors, as mentioned in the introduction of this document, exacerbate the financial strain on individuals striving to retire comfortably.

Regulation 28 of the Pension Funds Act(1956), as set out by the South African government, indicates that a retiree may invest a maximum of 45% of their retirement savings in foreign assets, 25% in property, 15% in private equity, 10% in commodities, 10% in hedge funds, and 2.5% in other excluded assets. Regulation 28 also has a limit on the total equity exposure a retiree may have in their portfolio, which is capped at 75%. The current South African regulation allows retirees to withdraw between 2.5% and 17.5% of their retirement savings annually – which can be paid out monthly or annually.

Living annuities provide retirees with autonomy, allowing them to select a variety of different investment options and withdrawal rates to sustain their required lifestyle. This flexibility makes living annuities attractive for retirees who are comfortable with investment risk and those who desire more control over their retirement savings. However, these annuities also involve higher risks due to market volatility and the onus is on the retiree to manage their investments prudently. Living annuities are preferred by retirees who are more investment-savvy, gain utility from potential growth in their retirement savings (albeit with increased risk), and wish to leave an inheritance for their heirs.

The success rate metric was employed to assess the performance of living annuities across various portfolio compositions and periods by Cooley et al. (1998). They concluded that an inflation-adjusted withdrawal rate of 4% to 5% is considered 'safe' for portfolios comprising at least 75% equities and 25% bonds over a 30-year period. By adjusting withdrawals for inflation,

initial withdrawals are significantly reduced, allowing for larger nominal withdrawals in the future to safeguard retirees from the effects of inflation – ensuring that a retiree's drawdown rate has the same purchasing power over time.

Maré (2016) observed that spending patterns, mortality rates, and asset returns in South Africa differ from those in other markets, which is a view we share. The findings by Maré (2016) indicate that a 5% withdrawal rate is sustainable over a relatively short period of 15 years or less in South Africa when investing in local bonds and local equities. For longer investment horizons, the results align with those of Cooley et al. (1998).

Van Appel et al. (2021) investigated the effect of fees and longevity on success rates using a dataset that spans from 1900 to 2020 for South African equities, bonds, cash, and inflation. They determined the average time until a living annuity depletes for various withdrawal rates, termed the 'fugit' of the portfolio. Van Appel et al. (2021) concluded that the asset allocation has an insignificant impact on portfolio success rates for low withdrawal rates and the risk inherent in living annuities may be hedged by taking short positions in call options and long positions in put options on a rolling 1-month basis to increase success rates.

The '4% safe withdrawal rate' is frequently used by financial advisors as a general guideline for determining 'safe' inflation-adjusted spending for retirees. The consensus among the research done by Cooley et al. (1998), Finke et al. (2012), Maré (2016), Van Appel et al. (2021), and Daraei and Sendova (2024) is that staying within the 4%–5% spending band will significantly increase the probability of success of a retiree's retirement portfolio.

Portfolio success rates can be determined by employing either bootstrap sampling of historical returns or Monte Carlo methods. For example, Cooley et al. (1999) determined 'safe' withdrawal rates in the US using Monte Carlo simulation, and Maré (2016) determined 'safe' withdrawal rates for South African retirees using random sampling with replacement.

When performing a Monte Carlo simulation for different market risk factors, it is important to consider the correlation between risk factors. The con-

vention is to assume a constant correlation structure when using a Monte Carlo simulation model, as seen in Cooley et al. (1998). Maré (2016) and Van Appel et al. (2021) used bootstrap modelling with replacement, which assumed constant point in time correlation structures when sampling from asset return populations. However, the financial markets move in cycles, and these correlation structures tend to differ significantly through the cycle as evidenced in Figure 4.1 below.

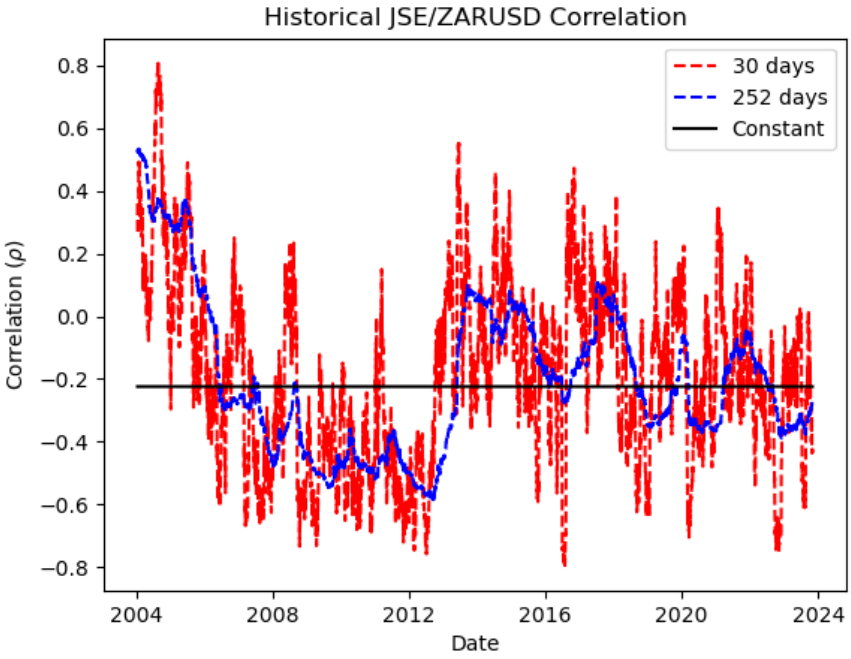

Figure 4.1: Historical JSE/ZARUSD Correlation Plots.

The 30-day correlation is obtained by applying a 30-day sliding window to historical JSE Top 40 and ZAR/USD FX returns. Similarly, the 252-day correlation is obtained by applying a 252-day sliding window to historical JSE Top 40 and ZAR/USD FX returns. We observe that when the sliding window is small (30-days), then the historical correlations exhibit substantial volatility with large swings between positive and negative correlations. However, when the sliding window is approximately 1 year (252-business days), then the historical correlations are considerably more stable and do not exhibit large swings, but better captures cycles within the financial markets.

Research by Markus and Kumar (2020) investigates the relationship between two stock prices, using stochastic correlation to model their interdependence through Wiener processes and the Heston model. After comparing a constant correlation model and two stochastic correlation models (Jacobi model and Hyperbolic Tangent Ornstein-Uhlenbeck model), Markus and Kumar (2020) conclude that both stochastic correlation models are better suited for capturing tail dependence and correlation risk, as they can describe potentially riskier scenarios compared to the constant correlation model, which lacks tail dependence. Teng et al. (2016) found that the correlation risk inherent when pricing a Quanto Put option with stochastic correlation cannot be neglected, for example.

Normally, correlations are assumed to be constant when modelling market risk factors. However, from Figure 4.1, it is evident that the correlation is dynamic and may better be captured by a stochastic correlation process. To understand what a density function for a stochastic correlation process may look like, we plot the historical density of the 30-day correlation in Figure 4.2 below.

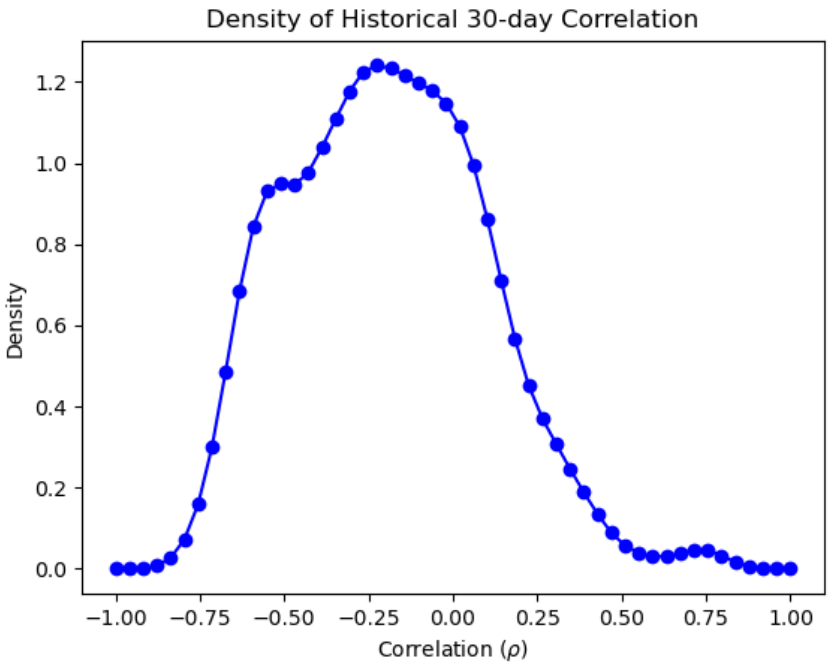

Figure 4.2: Historical 30-day Correlation Plot.

We make similar observations as Van Emmerich (2006), where we want to model correlation such that:

1. The correlations are bounded between [-1,1];
2. The stochastic correlation process is mean-reverting; and
3. The probability mass function approaches zero at the boundaries.

Stochastic correlation is desired to be mean-reverting because it reflects the realistic behaviour of correlations in financial markets, which tend to fluctuate around a long-term average rather than drifting indefinitely. This mean-reverting property helps ensure stability and consistency in pricing and risk management models, aligning them with observed market dynamics (Van Emmerich, 2006).

While numerous studies have contributed to the work that investigates 'safe' withdrawal rates across various asset allocations, the purpose of this chapter is to investigate the impact of foreign equity exposure on success rates and the effect of stochastic correlation modelling. Therefore, the aim of our research is to:

1. Provide a scientific basis for the influence of foreign equity exposure on living annuity success rates – given that the consensus among asset managers is that foreign exposure is a key factor in the long-term success of retirement portfolios.
2. Determine the impact of stochastic correlation modelling on retirement portfolio success rates given that market risk factor correlations tend to change with market cycles, and retirement portfolio modelling is typically performed over long time horizons.

An outline of the rest of the chapter is as follows: in the following section, we provide details of our data used to calibrate our simulation models as well as quantitative framework of the various stochastic models with the results of the calibration of each model. The results section provides both the portfolio success rates and fugits, which is followed by our concluding comments.

4.2 Methodology

We model living annuity success rates using a Monte Carlo simulation approach, which requires both calibration and simulation of various risk factors that affect the value of a living annuity. We consider the following risk factors in our portfolio modelling, which is made up of riskier assets (equities) and assets that are fairly risk-free (cash). We model local equities based on the JSE Top 40 Index, foreign equities based on the S&P 500, and the cash-component is modelled using 90-day ZAR T-bills. Given the exposure to both local and foreign equities, we also model ZAR CPI, US CPI, and the ZAR/USD FX rate.

4.2.1 Data

Details of the associated historical data used in the risk factor calibration procedure are provided in Table 1 below.

Table 4.1: Historical Data Description

Description	**Data Period**	**Freq.**
S&P 500 Index[1]	14-Jan-2003 to 01-Nov-2023	Daily
JSE Top 40 Index[2]	14-Jan-2003 to 01-Nov-2023	Daily
USD/ZAR FX rate[3]	14-Jan-2003 to 01-Nov-2023	Monthly
RSA 3-month T-bills[4]	14-Jan-2003 to 01-Nov-2023	Monthly
RSA inflation[5]	Jan 2003 to Nov 2023	Monthly
USA inflation[6]	Jan 2003 to Nov 2023	Monthly

We plot the daily returns[7]associated with the S&P 500 and JSE Top 40, and the monthly returns associated with the USD/ZAR FX rate, 3-month T-bills, RSA CPI and USA CPI in Figure 4.3. Our calibration period includes two stress events, the Global Financial Crisis (GFC) of 2008 and the Covid-

[1] https://za.investing.com/indices/us-spx-500-historical-data
[2] https://za.investing.com/indices/ftse-jse-top-40-historical-data
[3] https://za.investing.com/currencies/usd-zar-historical-data
[4] https://www.resbank.co.za/en/home/what-we-do/statistics/key-statistics/selected-historical-rates
[5] https://fred.stlouisfed.org/tags/series?t=cpi%3Bsouth+africa
[6] https://fred.stlouisfed.org/series/CPIAUCSL

19 crisis. Large swings in the returns are observable during both these stress periods.

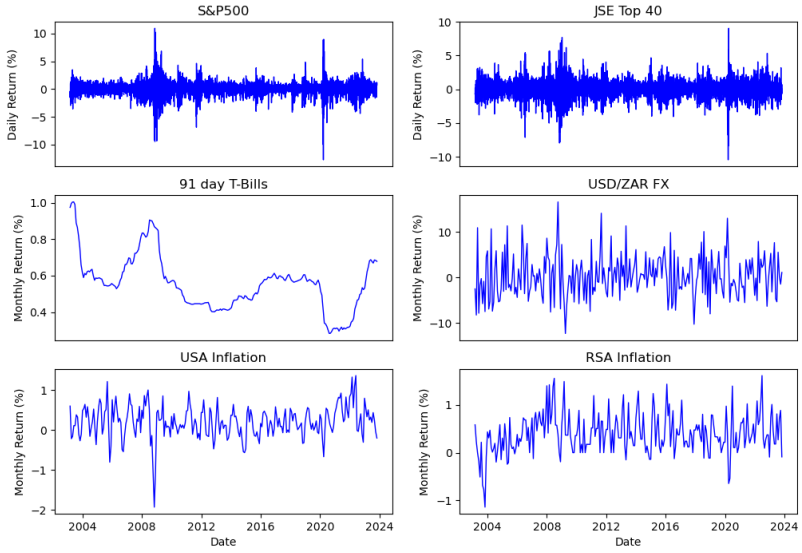

Figure 4.3: Historical Risk Factor Returns.

A summary of the annualised mean and standard deviation for each risk factor is provided in Table 4.2 below. We note that the average annualised returns from the JSE Top 40 are greater than that of the S&P 500, which is expected due to the well-known 'risk vs return' dilemma, where the JSE Top 40 has a higher return. It is also important to observe that inflation in South Africa is typically higher than that in the USA, meaning that the real returns obtained from investing in the S&P 500 are higher than those obtained from investing in the JSE Top 40.

The Pearson correlation coefficient is used to determine the historical correlation between the various assets considered in our analysis. The Pearson correlation coefficient is

[7]The data used in this study were chosen to ensure the integrity of the correlation structure.

Table 4.2: Annualised Data Statistics

	Mean	Standard deviation	Skewness	Kurtosis
S&P 500 Index	0.08	0.19	-0.51	15.82
JSE Top 40 Index	0.10	0.20	-0.20	8.10
USD/ZAR foreign exchange	0.04	0.16	0.42	4.02
RSA 3-month T-bills	0.07	0.07	0.01	11.34
RSA inflation	0.05	0.01	0.19	4.06
USA inflation	0.03	0.01	-0.60	6.26

$$\rho_{xy} = \frac{\sum(x_i - \bar{x})(y_i - \bar{y})}{\sqrt{\sum(x_i - \bar{x})^2 \sum(y_i - \bar{y})^2}}.$$

The historical correlations between asset class returns are presented in Table 4.3 below. We observe a fairly strong positive correlation between the S&P500 and JSE Top 40 (0.63), which is expected.

Table 4.3: Historical Asset Class Correlations

	S&P 500	JSE Top 40	T-bills	RSA CPI	US CPI	USD/ ZAR	S&P vol	JSE vol
S&P 500	1.00	0.63	-0.06	-0.04	0.02	-0.46	-0.75	0.00
JSE Top 40	0.63	1.00	-0.06	-0.15	-0.03	-0.16	0.00	-0.87
T-bills	-0.06	-0.06	1.00	0.31	0.07	0.08	0.00	0.00
RSA CPI	-0.04	-0.15	0.31	1.00	0.38	-0.01	0.00	0.00
US CPI	0.02	-0.03	0.07	0.38	1.00	-0.07	0.00	0.00
USD/ZAR	-0.46	-0.16	0.08	-0.01	-0.07	1.00	0.00	0.00
S&P vol	-0.75	0.00	0.00	0.00	0.00	0.00	1.00	0.00
JSE vol	0.00	-0.87	0.00	0.00	0.00	0.00	0.00	1.00

4.3 Interest Rate Modelling

The Cox-Ingersoll-Ross (CIR) model, introduced by Cox, Ingersoll, and Ross (Cox et al., 1985), is a stochastic differential equation used in finance for modelling the dynamics of interest rates. Its formulation encapsulates the essential characteristic of mean reversion - a phenomenon frequently

observed in real-world interest rates, where rates tend to revert to a long-term average over time. The CIR model is mathematically represented by the Stochastic Differential Equation (SDE):

$$dr_t = \kappa(\theta - r_t)dt + \sigma\sqrt{r_t}dW_t, \tag{4.1}$$

where r_t denotes the instantaneous interest rate at time, t, κ represents the speed of mean reversion, θ indicates the long-term mean level of interest rates, σ signifies the volatility of the process, and dW_t is the increment of a Wiener process.

The square root term, $\sqrt{r_t}$, in the discretisation ensures that the simulated rates remain positive as long as the Feller condition is met. This feature renders it particularly well-suited for applications in interest rate modelling in economies where interest rates remain positive (Cox et al., 1985). Specifically, the Feller condition stipulates that (Cox et al., 1985)

$$2\kappa\theta \geq \sigma^2, \tag{4.2}$$

which guarantees that the process will not hit zero with positive probability (Feller, 1951).

4.3.1 Interest Rate Calibration

To calibrate the CIR model, we first discretise the SDE in (1) by applying the Euler -Maruyama scheme

$$r_{t+\Delta} - r_t = \kappa(\theta - r_t)\Delta + \sigma\sqrt{r_t} \cdot N(0, \Delta), \tag{4.3}$$

where Δ represents the time-step and $N(0, \Delta)$ is a normal random variable with mean 0 and variance Δ.

We can re-write the discretisation in Equation (4.3) as

$$\frac{r_{t+\Delta} - r_t}{\sqrt{r_t}} = \frac{\kappa\theta\Delta}{\sqrt{r_t}} - \kappa\Delta\sqrt{r_t} + \sigma\sqrt{\Delta} \cdot N(0,1), \tag{4.4}$$

where $N(0,1)$ is a standard normal random variable.

Equation (4.4) can be expressed as

$$y_i = \beta_1 x_{i1} + \beta_2 x_{i2} + \epsilon_i, \tag{4.5}$$

where

1. $y_i = \frac{r_{t+\Delta} - r_t}{\sqrt{r_t}}$
2. $x_{1,i} = \frac{\Delta}{\sqrt{r_t}}$
3. $x_{2,i} = \sqrt{r_t}\Delta$
4. $\epsilon_i = \sigma\sqrt{\Delta} \cdot N(0,1)$
5. $\beta_1 = \kappa\theta$
6. $\beta_2 = -\kappa$.

We can solve the estimates of the parameters $\hat{\beta}_1$ and $\hat{\beta}_2$ by employing ordinary least-squares regression.

The calibrated parameters are then determined as

$$\hat{\kappa} = -\hat{\beta}_2, \hat{\theta} = \frac{\hat{\beta}_1}{\hat{\kappa}}, \text{and} \hat{\sigma}^2 = \frac{\text{var}(\epsilon)}{\Delta}. \tag{4.6}$$

The parameters obtained from fitting the CIR process to historical T-bill data are provided in Table 4.4 below.

Table 4.4: Calibrated T-Bill parameters for the CIR model

T-bill Parameters	**Estimate**
κ	0.24
θ	0.06
σ	0.03

4.3.2 Interest Rate Simulation

After calibrating the parameters of the CIR model, we make use of the Euler-Maruyama scheme to discretise the SDE in Equation (4.3) as

$$r_{t+\Delta} = r_t + \kappa(\theta - r_t)\Delta + \sigma\sqrt{\Delta}Z_t, \tag{4.7}$$

where $Z_t \sim \mathcal{N}(0,1)$ is a sequence of independent and identically distributed standard normal random variables, representing the discretised increments of the Wiener process.

We illustrate the percentiles of the simulated interest rate (using the calibrated parameters) and the historical T-bill data in Figure 4.4. We observe that the simulated percentiles fit the historical data well and revert to a long-term mean of approximately 6%. We do, however, note that the calibration period includes two stress periods, namely the Global Financial Crisis (GFC) that saw high interest rates and the Covid-19 pandemic that gave rise to very low interest rates and then a sharp increase in interest rates to tame inflationary pressure. The red shaded area in the graph below, indicates the 5th and 95th percentile plots of the interest rate process.

4.4 FX and Inflation Modelling

The gBm model is one of the fundamental models in finance for forecasting stock price trajectories. Its appeal stems from its ability to capture asset prices' multiplicative growth and inherent randomness in a mathematically tractable way.

The gBm model describes asset price dynamics through an SDE that assumes asset prices follow a continuous path with proportional growth and volatility. The gBm model is:

$$dS(t) = \mu S(t)dt + \sigma S(t)dW(t), \tag{4.8}$$

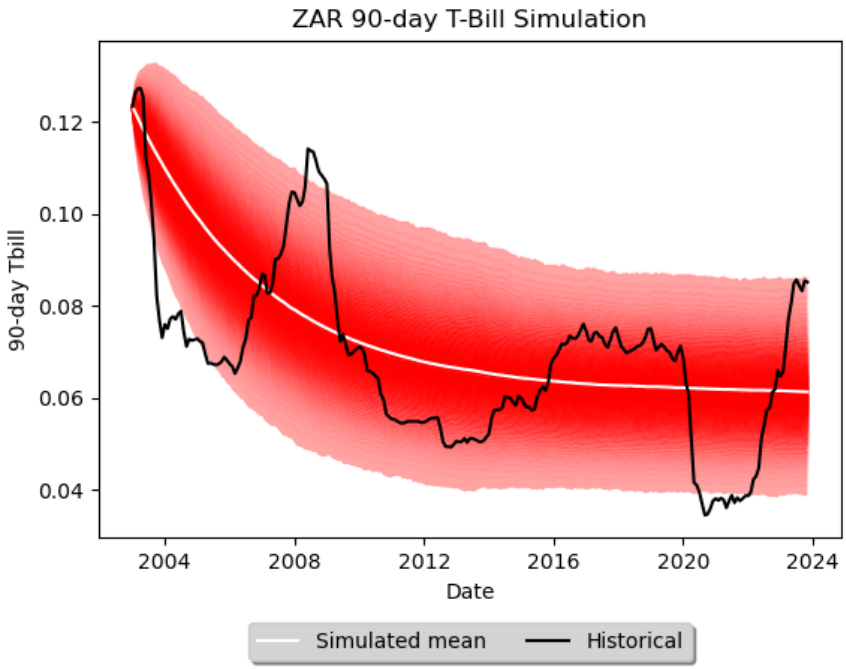

Figure 4.4: ZAR 90-day T-Bill Simulated Percentile Fit.

where $S(t)$ is the asset price at time, t, μ is the drift of the process, σ represents the volatility of the standard deviation of the returns, and $W(t)$ is a standard Brownian motion.

The well-known analytical solution of this SDE provides the asset price at time, t, as:

$$S(t) = S(0) \exp\left(\left(\mu - \frac{1}{2}\sigma^2\right) t + \sigma W(t)\right), \tag{4.9}$$

where $(\mu - \frac{1}{2}\sigma^2)t$ is the deterministic component of the exponential function and $\sigma W(t)$ represents the stochastic component within the exponential function. This expression(4.9) implies that asset prices follow a lognormal distribution, making the logarithm of the price, $\log S_t$, normally distributed (Black and Scholes, 1973).

Although commonly used to model stock prices, the gBm model ensures

that asset prices cannot become negative, which is also a desirable feature when modelling the Consumer Price Index (CPI) and Foreign Exchange (FX) rates.

4.4.1 FX and Inflation Calibration

To calibrate the gBm model to historical asset price data, Maximum Likelihood Estimation (MLE) is used. Assume that we have historical asset prices, $S_1, S_2, \ldots, S_n$, sampled at regular intervals, δ. The log-returns of the asset prices are defined as

$$X_i = \log\left(\frac{S_t}{S_{t-1}}\right). \tag{4.10}$$

The likelihood function of the observed log-returns is (Hull, 2018)

$$L(\mu, \sigma \mid X_1, \ldots, X_n) = \prod_{i=1}^{n} \frac{1}{\sqrt{2\pi\sigma^2\Delta}} \exp\left(-\frac{\left(X_i - \left(\mu - \frac{\sigma^2}{2}\right)\Delta\right)^2}{2\sigma^2\Delta}\right). \tag{4.11}$$

By maximising the likelihood function in Equation (4.8), μ and σ can be estimated as

$$\hat{\sigma}^2 = \frac{1}{n\Delta}\sum_{i=1}^{n}\left(X_i - \frac{1}{n}\sum_{j=1}^{n} X_j\right)^2, \tag{4.12}$$

$$\hat{\mu} = \frac{1}{n\Delta}\sum_{i=1}^{n} X_i + \frac{\hat{\sigma}^2}{2}. \tag{4.13}$$

The results from calibrating the gBm model to historical USD/ZAR FX rates, ZAR CPI and US CPI are provided in Table 4.5 below.

We observe that the calibrated drift and volatility of the ZAR CPI is higher

Table 4.5: Calibrated parameters for the USD/ZAR FX rate, ZAR CPI, and US CPI

Description	$\hat{\mu}$	$\hat{\sigma}$
USD/ZAR FX rate	0.05	0.16
ZAR CPI	0.05	0.01
US CPI	0.03	0.01

than its US counterpart. This is expected as inflation is typically higher in South Africa than it is in the U.S..

4.4.2 FX and Inflation Simulation

We make use of Euler scheme to discretise the gBm SDE in Equation (4.8) as

$$S_{t+\Delta} = S_t e^{\left(\mu - \frac{1}{2}\sigma^2\right)\Delta + \sigma\sqrt{\Delta}Z_t}, \tag{4.14}$$

where $Z_t \sim N(0,1)$.

We illustrate the percentiles of the simulated FX rate, RSA CPI, and US CPI (using the calibrated parameters) and the historical prices in Figure 4.5, Figure 4.6, and Figure 4.7, respectively.

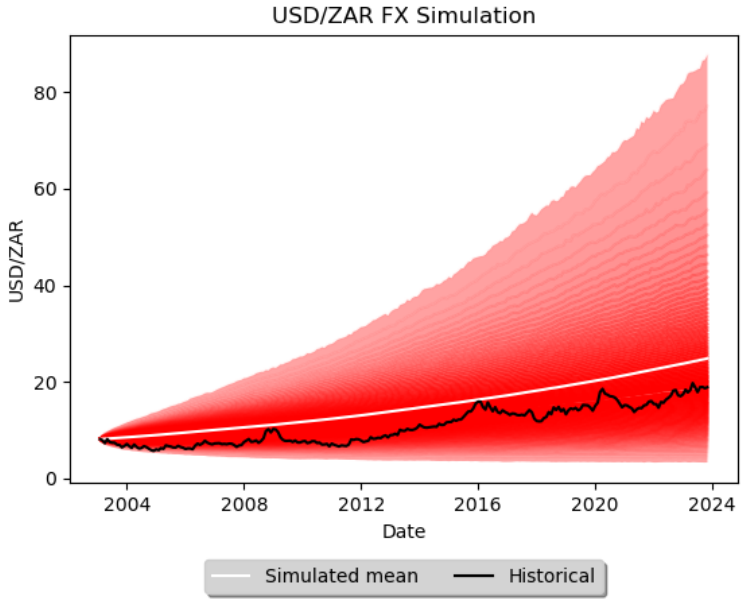

Figure 4.5: ZAR/USD Simulated Percentile Fit.

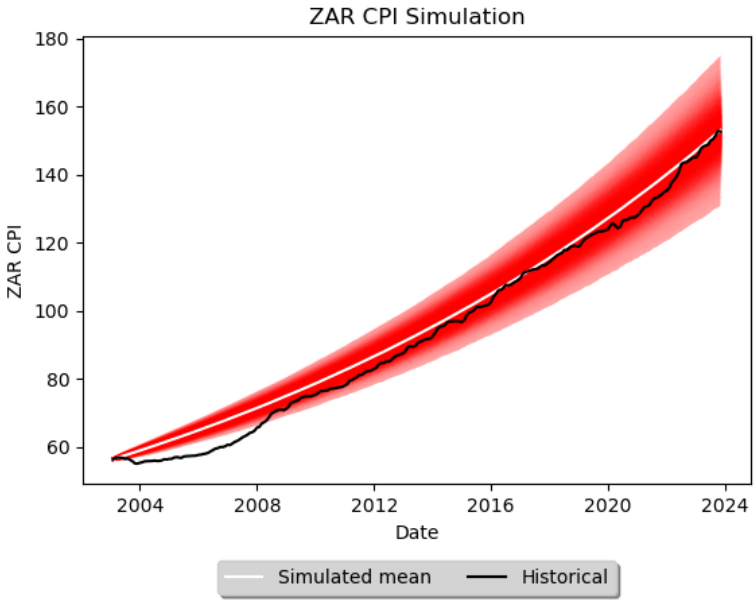

Figure 4.6: ZAR CPI Simulated Percentile Fit.

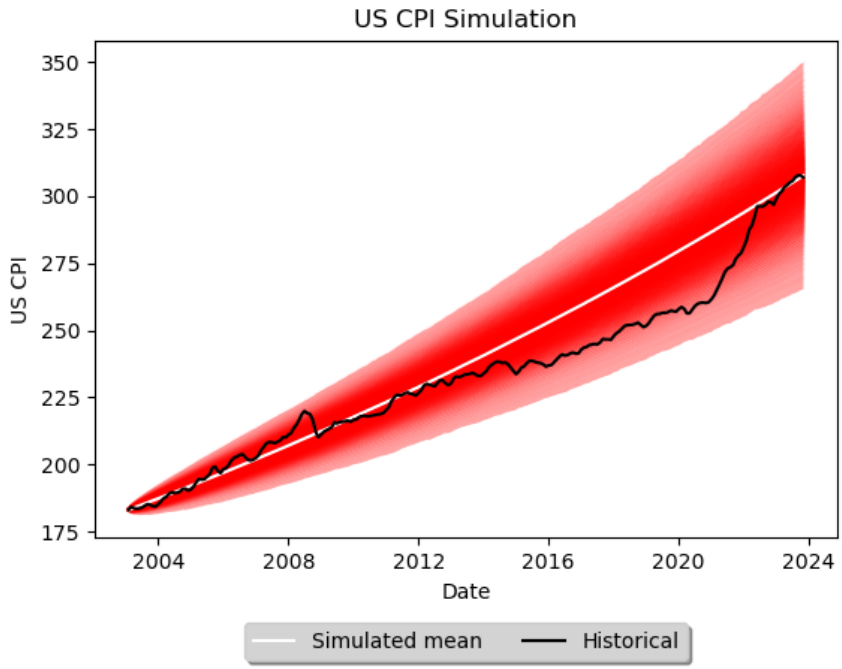

Figure 4.7: US CPI Simulated Percentile Fit.

The simulated percentile plots (5th and 95th percentiles) illustrate that the calibrated parameters are adequate in capturing the historical time series across all risk factors where the gBm model is used. We do, however, note that the simulated percentiles of the RSA CPI process do not capture the lower CPI growth observed from 2004 to 2008. However, the mean of the simulations follows the historical data closely, indicating an adequate fit.

4.5 Equity Modelling

The Heston model is a widely used stochastic volatility model in financial mathematics, specifically developed to describe the evolution of stock prices with volatility that varies over time. This model allows the volatility itself to follow a random process, which helps capture features of market prices, such as the volatility smile often observed in options markets (Heston, 1993).

The Heston model assumes that stock prices and their volatility are driven by two coupled SDEs:

$$dS(t) = \mu S(t)dt + \sqrt{v(t)}S(t)dW_s(t), \tag{4.15}$$

$$dv(t) = (\alpha - \beta v(t))dt + \sigma_v\sqrt{v(t)}dW_v(t), \tag{4.16}$$

$$dW_s(t)dW_v(t) = \rho_{sv}dt, \tag{4.17}$$

where the ratio of α/β is the long run mean of the observed variance, μ denotes the expected rate of return, β is the speed of mean reversion of the variance, σ_v is the volatility of the variance, and ρ_{sv} denotes the correlation between the stock and the variance processes.

4.5.1 Equity Calibration

The Efficient Method of Moments (EMM) technique was introduced by Bansal et al. (1995) and Gallant and Tauchen (1996). The EMM method is a derivative of the work of Duffie and Singleton (1993), which investigated the Simulated Method of Moments (SMM), and combines two procedures, namely MLE and General Method of Moments (GMM).

Recently, Levendis and Maré (2023) used the EMM to calibrate the Heston and Bates model to historical South African stock price data. A detailed exposition of the EMM procedure is outlined in Andersen et al. (1999). Assume a time-series of historical stock prices $x_1, x_2, \ldots, x_k$, and that the parameters of the stochastic volatility model are given by the vector δ. The EMM technique is deployed in two stages.

The first stage involves choosing an auxiliary model $(x_k|X_{\text{k-1}};\varphi)$, which is parameterised by the pseudo parameter vector, φ. The purpose of the auxiliary model is to closely fit the original model such that maximum likelihood estimation is possible. The semi-nonparametric density of Gallant and Nychka (1987) is a popular choice as it is characterised by a leading parametric term that captures the majority of the dependency of the conditional mean and variance. Hermite polynomials are added to capture any residual non-Gaussian features. The density of the auxiliary model is given

by

$$f(x_k \mid X_{k-1}, \varphi) = \left(\nu + (1-\nu)\frac{P_T(z_k)^2}{\int_{\mathbb{R}} P_T(z_k)^2 \phi(u)du}\right)\frac{\phi(z_k)}{\sqrt{h_k}}. \tag{4.18}$$

where v is chosen to be a constant to avoid any instability in the EMM procedure when $P_T(z_k) = 0$. Therefore, $v = 0.01$ and $\varphi(.)$ is the standard normal density function, and z_k is defined as

$$z_k = \frac{x_k - \mu_k}{\sqrt{h_k}}, \tag{4.19}$$

with $\mu_k = 0$ and,

$$h_k = \omega + \gamma_0 x_{k-1}^2 + \gamma_1 h_{k-1}, \tag{4.20}$$

$$h_k \sim \text{GARCH}(1,1),$$

and where μ_k and h_k represent the conditional mean and variance, respectively.

The Hermite polynomials are defined as

$$P_T(z_k) = \sum_{i=0}^{U_z} a_i z_k^i, \tag{4.21}$$

where we define $a_0 = 1$ and U_z denotes the order of the Hermite polynomial.

The EMM technique requires the dimension of the pseudo parameter vector, ϕ to be at least as large as the vector of parameters required for the stochastic volatility model, δ. The pseudo parameter vector, ϕ can now be estimated by maximum likelihood estimation, where the score function of the auxiliary model is

$$s_f(X_k, \hat{\varphi}_k) = \frac{\partial}{\partial \hat{\varphi}} \log f(x_k \mid X_{k-1}; \hat{\varphi}_k), \tag{4.22}$$

which leads to the following first-order condition for $\hat{\varphi}$

$$\frac{1}{k} \sum_{i=1}^{k} s_f(X_i, \hat{\varphi}_k) = 0. \tag{4.23}$$

The second phase of the EMM procedure makes use of the SMM. For a fixed parameter vector, δ, and large K, simulate a series $\hat{x_1}(\delta), \hat{x_2}(\delta), \ldots, \hat{x_K}(\delta)$from the stochastic volatility model and determine the sample moments at the fixed MLE $\hat{\varphi_k}$:

$$m_K(\delta, \hat{\varphi}_k) = \frac{1}{K} \sum_{i=1}^{K} \frac{\partial}{\partial \varphi} \log f(\hat{x}_i(\delta) \mid \hat{X}_{i-1}(\delta), \hat{\varphi}_k). \tag{4.24}$$

The parameter vector, δ, that best represents the historical data for the chosen model is determined by minimising

$$\arg\min_{\delta} \left[m_K(\delta, \hat{\varphi}_k)' \hat{I}_K^{-1} m_K(\delta, \hat{\varphi}_k) \right], \tag{4.25}$$

where $\hat{I}_k$ is a consistent estimator of the asymptotic covariance matrix of the sample pseudo score vector and is calculated as the outer product of scores.

Equation 4.25 minimises a quadratic form involving $m_K(\delta, \hat{\varphi}_k)$, the score evaluated at the estimated parameters. The inverse of $\hat{I}_K$ is used to scale this minimisation, indicating its role in normalising the score based on its variability. This process ensures that the optimisation accounts for the covariance structure of the pseudo score vector.

$$\hat{I}_K = \frac{1}{K} \sum_{i=1}^{K} \frac{\partial}{\partial \varphi} \log f(x_i \mid X_{i-1}, \hat{\varphi}_k) \frac{\partial}{\partial \varphi} \log f(x_i \mid X_{i-1}, \hat{\varphi}_k)'. \tag{4.26}$$

Equation 4.25 shows how $\hat{I}_K$ is calculated as the outer product of score

functions. This expression sums over the squared gradients (score functions) of the log-likelihood, scaled by the sample size K. The idea is that $\hat{I}_K$ estimates the dispersion of the score vector, reflecting how much the estimated parameters, φ, deviate from their true values.

Andersen et al. (1999) note that the simulated series should be large enough to ensure that the Monte Carlo error can be ignored. Our observation is that values of K greater than 100 000 are sufficient to obtain convergence. The parameters obtained by performing the EMM to calibrate the Heston model to historical S&P 500 and JSE Top 40 data are provided in Table 4.6 below. We also provide the Kolmogorov-Smirnov (KS) goodness-of-fit test p-value at a 95% confidence level.

Table 4.6: S&P 500 Parameters Using the Heston Model

Parameter	S&P 500	JSE Top 40
μ	0.09	0.11
α	0.07	0.16
β	3.09	5.25
σ	0.33	0.27
KS p-value	0.45	0.22

4.5.2 Equity Simulation

By firstly applying the log-tansform $x(t) = \ln s(t)$ and the applying Itô's lemma to the set of equations in Equation (4.17), we get

$$\begin{aligned} dx(t) &= \left(\mu - \frac{1}{2}v(t)\right)dt + \sqrt{v(t)}dW_s(t), \\ dv(t) &= (\alpha - \beta v(t))dt + \sigma_v\sqrt{v(t)}dW_v(t), \\ dW_s(t)dW_v(t) &= \rho_{sv}dt. \end{aligned} \tag{4.27}$$

In order for $v(t) > 0$, the Feller condition must be satisfied:

$$2\alpha > \sigma_v^2. \tag{4.28}$$

Applying the Euler-Maruyama scheme to discretise the log-transformed Heston SDE yields the following discretisation for the evolution of the stock price and variance process, respectively.

$$\begin{aligned} x_{t+\Delta} &= x_t + \left(\mu - \frac{1}{2}v_t\right)\Delta + \sqrt{v_t\Delta}Z_s, \\ v_{t+\Delta} &= v_t + (\alpha - \beta v_t)\Delta + \sigma_v\sqrt{v_t\Delta}Z_v, \\ Z_v &= \rho_{s,v}Z_s + \sqrt{1-\rho_{s,v}^2}Z_x, \end{aligned} \tag{4.29}$$

where $Z_s, Z_v, Z_x \sim \mathcal{N}(0,1)$.

This correlation structure ensures that the correlation between the increments of Z_s and Z_v over any time step Δ is $\rho_{1,2}$. Throughout our analysis, we assume that the correlation between the stock price process and volatility process remains constant. We provide plots of the simulated percentiles(5th and 95th percentiles) and distributional fits below.

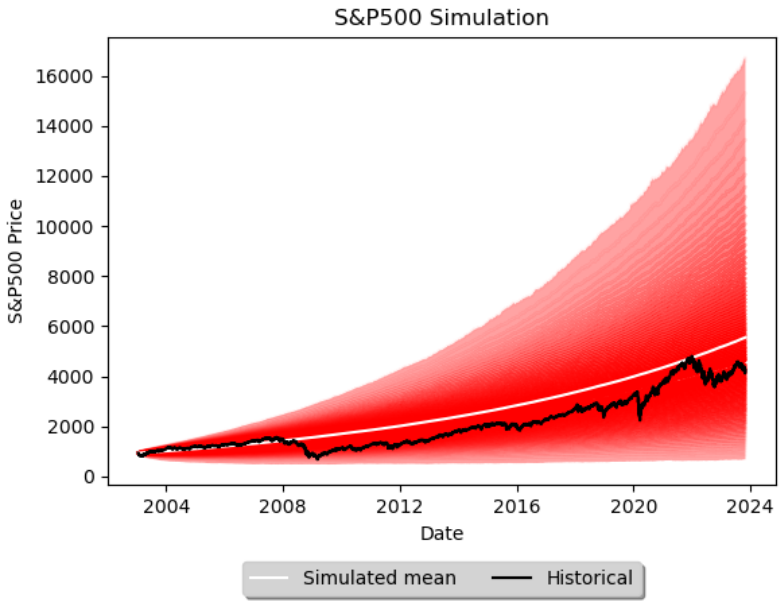

Figure 4.8: S&P 500 Simulated Distributional Percentile Plot versus Observed Market Data.

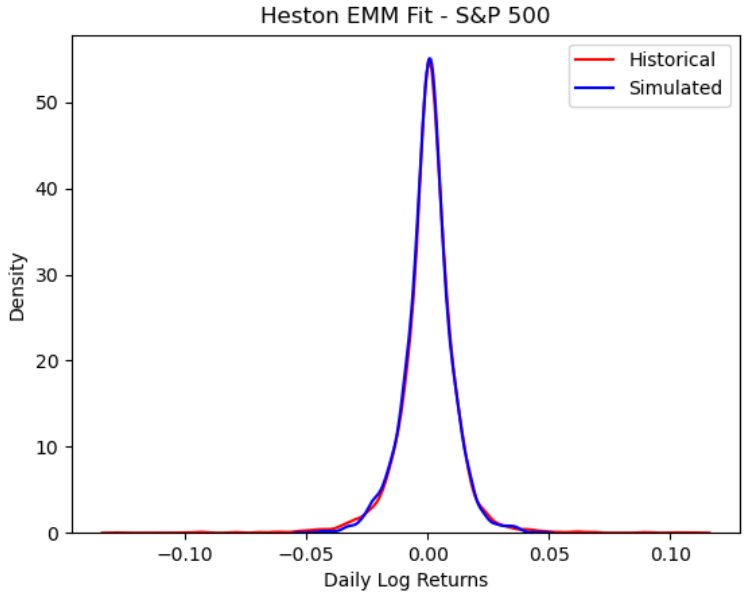

Figure 4.9: S&P 500 Simulated Distributional Fit versus Observed Market Data.

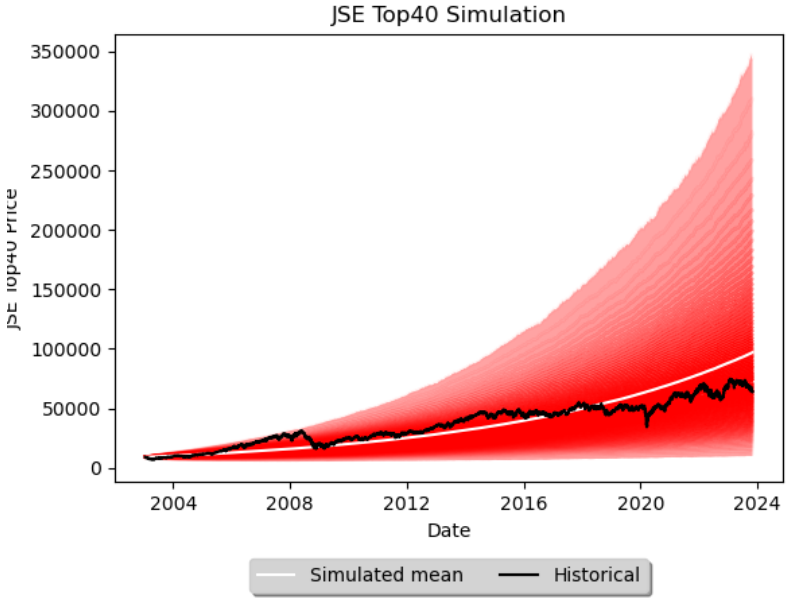

Figure 4.10: JSE Simulated Distributional Percentile Plot versus Observed Market Data.

The simulated percentile and distributional plots, for both the S&P 500 and JSE Top 40 demonstrate that the calibrated parameters effectively capture the historical time series across all risk factors where the Heston model is applied. However, we observe that there is a slight misalignment on the tail end of the distributional plots. These are explained by the two significant stress events that are included in our data calibration period. The KS goodness-of-fit test p-value indicates a good fit at a 95% confidence level.

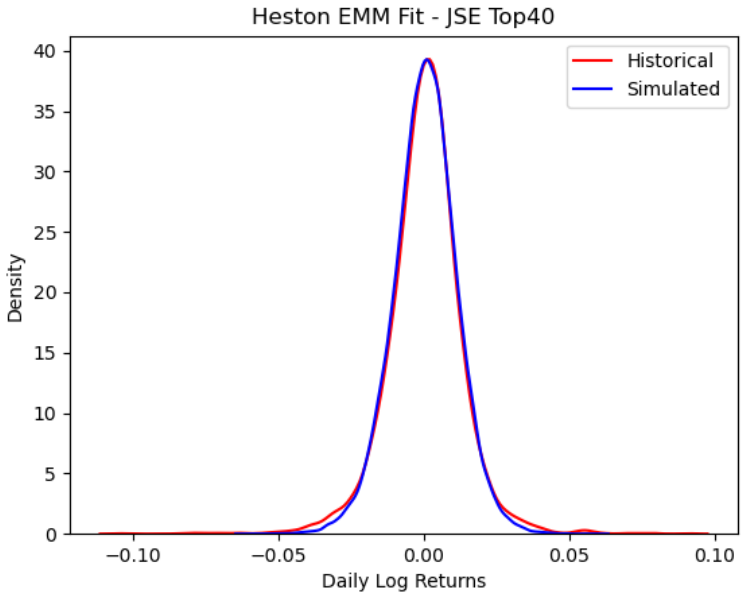

Figure 4.11: JSE Simulated Distributional Plot versus Observed Market Data.

4.6 Stochastic Correlation

It is common market practice to assume that correlations between risk factors remain constant. However, as illustrated in Figure 4.1, the correlation between risk factors changes over time. Recall that a stochastic correlation process should be bounded between $[-1, 1]$, mean-reverting and the probability mass function should approach zero at the boundaries. Keeping this in mind, Teng et al. (2016) propose using the Ornstein-Uhlenbeck (OU) process given by the following SDE

$$dY_t = \kappa(\mu - Y_t)dt + \sigma\ dW_t, \tag{4.30}$$

where κ represents the speed of mean reversion, μ represents the long-term mean, σ represents the volatility, and W_t is a Wiener process.

The O-U process defined above can take on any values between $(-\infty, \infty)$. Teng et al. (2016) propose the following modified OU process to restrict $\mu \in [-1, 1]$.

$$dY_t = \kappa(\mu - \tanh(Y_t))dt + \sigma\, dW_t, \tag{4.31}$$

where $\kappa, \sigma > 0$ and $\mu, Y_0 \in [-1, 1]$.

The hyperbolic tangent function proposed by Teng et al. (2016) is bounded between $[-1, 1]$ as illustrated in Figure 4.12 below. We note that the hyperbolic tangent function only approaches the extremities -1 and 1, representing perfect negative and positive correlation, respectively, which is very rarely seen in financial markets.

$$\begin{aligned}
d\rho_t &= \left(\frac{\partial \rho_t}{\partial t} + \kappa(\mu - \tanh(y))\frac{\partial \rho_t}{\partial y} + \frac{1}{2}\sigma^2\frac{\partial^2 \rho_t}{\partial y^2}\right)dt + \sigma\frac{\partial \rho_t}{\partial y}dW_t \\
&= \Big[\kappa(\mu - \tanh(y))(1 - \tanh^2(y)) \\
&\quad + \frac{1}{2}\sigma^2(-2(1 - \tanh^2(y))\tanh(y))\Big]dt + \sigma(1 - \tanh^2(y))dW_t \\
&= \Big[\kappa(\mu - \rho_t)(1 - \rho_t^2) - \sigma^2\rho_t(1 - \rho_t^2)\Big]dt + \sigma(1 - \rho_t^2)dW_t \\
&= (1 - \rho_t^2)\Big[\kappa\mu - \kappa\rho_t - \sigma^2\rho_t\Big]dt + \sigma(1 - \rho_t^2)dW_t. \\
&= (1 - \rho_t^2)\Big[(\kappa\mu - \rho_t(\kappa + \sigma^2))dt + \sigma dW_t\Big] \\
&= (1 - \rho_t^2)\Big[(\kappa + \sigma^2)\left(\frac{\kappa\mu}{\kappa + \sigma^2} - \rho_t\right)dt + \sigma dW_t\Big] \\
&= (1 - \rho_t^2)\Big[\kappa^*(\mu^* - \rho_t)dt + \sigma^* dW_t\Big],
\end{aligned} \tag{4.32}$$

where $\kappa^* = \kappa + \sigma^2, \mu^* = \kappa\mu/(\kappa + \sigma^2)$ and $\sigma^* = \sigma$.

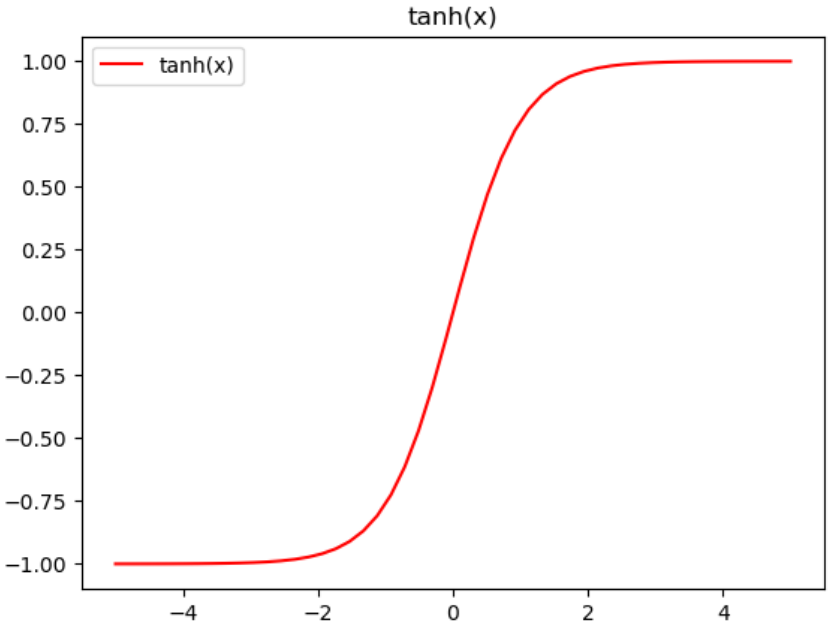

Figure 4.12: Plot of the Hyperbolic Tangent Function.

Applying the transformation $\rho_t = \tanh(Y_t) := \tanh(y)$ to Equation (4.31) and applying Ito's Lemma, we obtain the following

Rewriting Equation (4.32) so that the RHS resembles that of the OU process

$$\frac{d\rho_t}{1-\rho_t^2} = \kappa^*(\mu^* - \rho_t)dt + \sigma^* dW_t, \tag{4.33}$$

where $t \geq 0, \rho_0 \in [-1, 1], \kappa^*, \sigma^* > 0$ and $\mu^* \in [-1, 1]$.

The HtanOU model assumes mean reversion in correlation, which may not hold during market regime shifts, leading to potential misestimation of long-term correlation structures. Its non-linearity increases sensitivity to input choices, limiting robustness in real-world applications. The model fails to capture jumps and structural breaks, making it less effective in modeling sudden correlation shifts during financial crises or extreme events.

4.6.1 Stochastic Correlation Calibration

To calibrate the stochastic correlation model in Equation (4.31) to historical correlation data, Teng et al. (2016) first determine the transition density function by making use of the Fokker-Planck equation (Fokker, 1914). Assume that the transition density function $f(t, \tilde{\rho} \mid \rho_0)$ satisfies the following Fokker-Planck equation

$$\frac{\partial}{\partial t} f(t, \tilde{\rho}) + \frac{\partial}{\partial \tilde{\rho}} \left(\hat{a}(t, \tilde{\rho}) f(t, \tilde{\rho}) \right) - \frac{1}{2} \frac{\partial^2}{\partial \tilde{\rho}^2} \left(\hat{b}(t, \tilde{\rho})^2 f(t, \tilde{\rho}) \right) = 0, \tag{4.34}$$

where

$$\hat{a}(t, \tilde{\rho}) = \kappa^*(\mu^* - \tilde{\rho})(1 - \tilde{\rho}^2) \quad \text{and} \quad \hat{b}(t, \tilde{\rho}) = (1 - \tilde{\rho}^2)\sigma^*.$$

Teng et al. (2016) note that for the purpose of calibration, only the stationary density should be considered, i.e.

$$f(\tilde{\rho}) := \lim_{t \to \infty} f(t, \tilde{\rho} \mid \rho_0). \tag{4.35}$$

Since the stochastic correlation process in Equation (4.32) is mean-reverting, every two solutions of Equation (4.34) are the same as $t \to \infty$, i.e., a unique stationary solution exists.

The stationary density function $f(\tilde{\rho})$ satisfies

$$\frac{\partial}{\partial \tilde{\rho}} \Big((1 - \tilde{\rho}^2)(\kappa^*(\mu^* - \tilde{\rho})) f(\tilde{\rho}) \Big) = \frac{1}{2} \frac{\partial^2}{\partial \tilde{\rho}^2} \Big((1 - \tilde{\rho}^2)^2 \sigma^{*2} f(\tilde{\rho}) \Big). \tag{4.36}$$

which is an elliptic equation, for which Teng et al. (2016) provide the following solution:

$$f(\tilde{\rho}) = \frac{m}{2^{\frac{\kappa^*}{\sigma^{*2}}}}(1+\tilde{\rho})^{\frac{\kappa^*-2\sigma^{*2}}{\sigma^{*2}}+\frac{\kappa^*\mu^*}{\sigma^{*2}}}(1-\tilde{\rho})^{\frac{\kappa^*-2\sigma^{*2}}{\sigma^{*2}}-\frac{\kappa^*\mu^*}{\sigma^{*2}}} + \frac{n}{\tilde{\rho}^2-1}\left(\frac{1}{2}\right)^{\frac{2\sigma^{*2}-\kappa^*}{\sigma^{*2}}} F\left(1, \frac{2\sigma^{*2}-2\kappa^*}{\sigma^{*2}}, \frac{(-\mu^*-1)\kappa^*+2\sigma^{*2}}{\sigma^{*2}}, \frac{\tilde{\rho}}{2}+\frac{1}{2}\right), \tag{4.37}$$

where $m, n \in \mathbb{R}$, and the hypergeometric function F is defined by

$$F(a,b,c,x) = \sum_{k=0}^{\infty} \frac{x^k}{k!}\frac{(a)_k(b)_k}{(c)_k}, \quad |x|<1, \tag{4.38}$$

where $(.)_k$ denotes the Pochhammer symbol,

$$(a)_k = a(a+1)(a+2)\dots(a+k-1), \quad (a)_0 = 1.$$

Note that due to the mean-reversion property, the stationary density function, $f(\tilde{\rho})$, must satisfy

$$\int_{-1}^{1} \tilde{\rho} f(\tilde{\rho})\, d\tilde{\rho} = \mu^*. \tag{4.39}$$

For a stochastic process with a mean-reverting property, the stationary density function $f(\tilde{\rho})$ represents the long-term equilibrium distribution of the process. This condition holds because the mean-reverting property forces the process to oscillate around a central tendency μ^* over time, and the stationary density $f(\tilde{\rho})$ describes the likelihood of the process being at any particular value. This ensures that the process does not drift away indefinitely and stays bounded between $[-1, 1]$.

Choosing $\mu^* = 0$, Teng et al. (2016) observe that the first term in Equation (4.37) becomes

$$\frac{m}{2^{\frac{\kappa^*}{\sigma^{*2}}}}(1+\tilde{\rho})^{\frac{\kappa^*-2\sigma^{*2}}{\sigma^{*2}}}(1-\tilde{\rho})^{\frac{\kappa^*-2\sigma^{*2}}{\sigma^{*2}}}, \tag{4.40}$$

which is symmetric around $\tilde{\rho} = 0$. Therefore, condition Equation (4.40) will be fulfilled for $n = 0$ in Equation (4.37).

Now assuming $n \equiv 0$ for all general $\mu^* \in [-1, 1]$, the transition density function in Equation (4.37) can be written as (Teng et al., 2016)

$$f(\tilde{\rho}) = \frac{m}{2^{\frac{\kappa^*}{\sigma^{*2}}}}(1+\tilde{\rho})^{\frac{\kappa^*-2\sigma^{*2}}{\sigma^{*2}}+\frac{\kappa^*\mu^*}{\sigma^{*2}}}(1-\tilde{\rho})^{\frac{\kappa^*-2\sigma^{*2}}{\sigma^{*2}}-\frac{\kappa^*\mu^*}{\sigma^{*2}}}. \tag{4.41}$$

To solve the unknown, m, in Equation (4.41), we use the basic property of a density function

$$\int_{-1}^{1} f(\tilde{\rho})\, d\tilde{\rho} = 1. \tag{4.42}$$

To determine m, we require Equation (4.42) to hold. We set the following (Teng et al., 2016)

$$a = \frac{\kappa^* - 2\sigma^{*2}}{\sigma^{*2}} \quad \text{and} \quad b = \frac{\kappa^*\mu^*}{\sigma^{*2}},$$

and substitute into Equation (4.41)

$$f(\tilde{\rho}) = \frac{m}{2^{\frac{\kappa^*}{\sigma^{*2}}}}(1+\tilde{\rho})^{[a+b]}(1-\tilde{\rho})^{[a-b]}. \tag{4.43}$$

For any values of a and b such that $a \pm b > -1$, Teng et al. (2016) show that the integral

$$\int_{-1}^{1}(1+\tilde{\rho})^{[a+b]}(1-\tilde{\rho})^{[a-b]}\, d\tilde{\rho}. \tag{4.44}$$

has a solution

$$M := \frac{\Gamma(1+a-b)F(1,-a-b,2+a-b,-1)}{\Gamma(2+a-b)} + \frac{\Gamma(1+a+b)F(1,-a+b,2+a+b,-1)}{\Gamma(2+a+b)}. \tag{4.45}$$

where Γ and F define the gamma and hypergeometric functions, respectively. For the full derivation of the solution, refer to Section B.5.

The final step in the derivation involves ensuring that the condition $a \pm b > -1$ holds. Recall that $\mu \in [-1, 1]$, and a and b are defined as

$$a = \frac{\kappa^* - 2\sigma^{*2}}{\sigma^{*2}} = \frac{\kappa - \sigma^2}{\sigma^2}, \quad b = \frac{\kappa^*\mu^*}{\sigma^{*2}} = \frac{\kappa\mu}{\sigma^2}. \tag{4.46}$$

If we consider the following boundary conditions

$$\mu > -1 \implies \kappa(1+\mu) > 0 \implies \frac{\kappa - \sigma^2}{\sigma^2} + \frac{\kappa\mu}{\sigma^2} > -1 \implies a + b > -1,$$
$$\mu < -1 \implies \kappa(1-\mu) > 0 \implies \frac{\kappa - \sigma^2}{\sigma^2} - \frac{\kappa\mu}{\sigma^2} > -1 \implies a - b > -1.$$

Therefore, the required condition that $a \pm b > -1$ will always hold since $\mu \in [-1, 1]$. The constant m can now be determined as (Teng et al., 2016)

$$m = \frac{\frac{\kappa^*}{2\sigma^{*2}}}{M}. \tag{4.47}$$

The closed form solution of the transition density function is given by

$$f(\tilde{\rho}) = \frac{(1+\tilde{\rho})^{a+b}(1-\tilde{\rho})^{a-b}}{M}. \tag{4.48}$$

The stochastic correlation model can now be calibrated by minimising the squared error between the historically observed density for each correlation pair and the closed form solution to the transition density function. For the full derivation of the solution, refer to Section B.6.

To calibrate our stochastic correlation model, we make use of a 12-month sliding window to calculate historical correlations between risk factors, shifting the window one month at a time. Given that the data used to calibrate the stochastic correlation model are monthly, a sliding window shorter than 12 months yields correlations that jump too erratically due to less than 12 values being used to obtain the point in time correlation.

4.6.2 Stochastic Correlation Simulation

To simulate the stochastic correlation, recall that the hyperbolic tangent stochastic correlation model defined by Teng et al. (2016) is given by

$$d\rho_t = (1-\rho_t^2)\Big(\kappa^*(\mu^* - \rho_t)dt + \sigma^* dW_t\Big). \tag{4.49}$$

There is no solution for the SDE, thus we use the Euler-Maruyama method to approximate

$$\rho_{t+\Delta} = \rho_t + \kappa^*(\mu^* - \rho_t)(1-\rho_t^2)\Delta + (1-\rho_t^2)\sigma^*\sqrt{\Delta}Z, \tag{4.50}$$

where $Z \sim \mathcal{N}(0,1)$.

Caution should be applied when simulating SDEs with no solution due to the discretisation error that occurs when simulating the SDE directly. To ensure that in Equation (4.50) is simulated accurately, we set the time-step, Δ, to be infinitesimally small and we sample points that are congruent with the necessary simulation dates.

The simulated stochastic correlation percentiles (red) are plotted against the historical data (black) used to calibrate the models in Figure 4.13. We observe that the simulated percentiles capture the historical correlations well for all combinations of risk factors. The mean of the simulations (white line) appears to capture the 'average' correlation over the period for each risk factor couple.

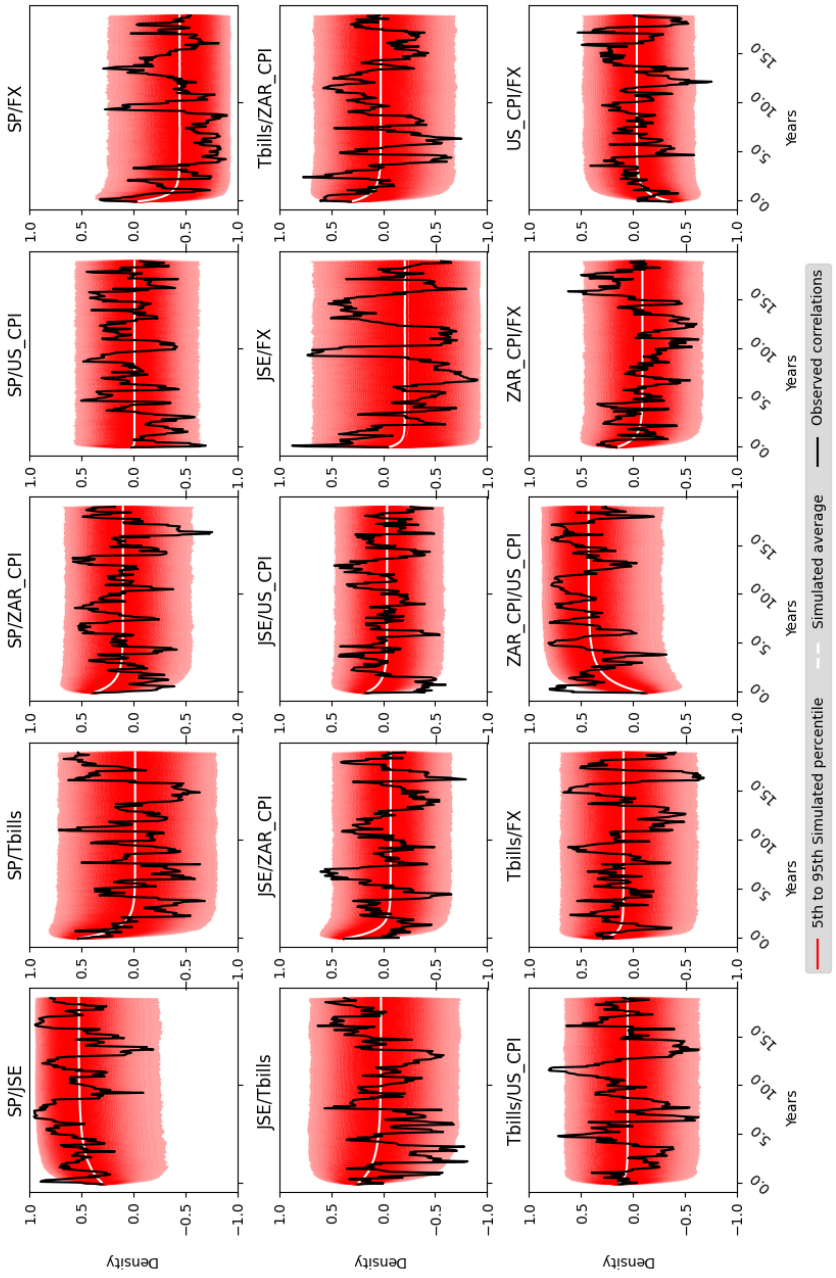

Figure 4.13: 5th and 95th Simulated Percentile Plots.

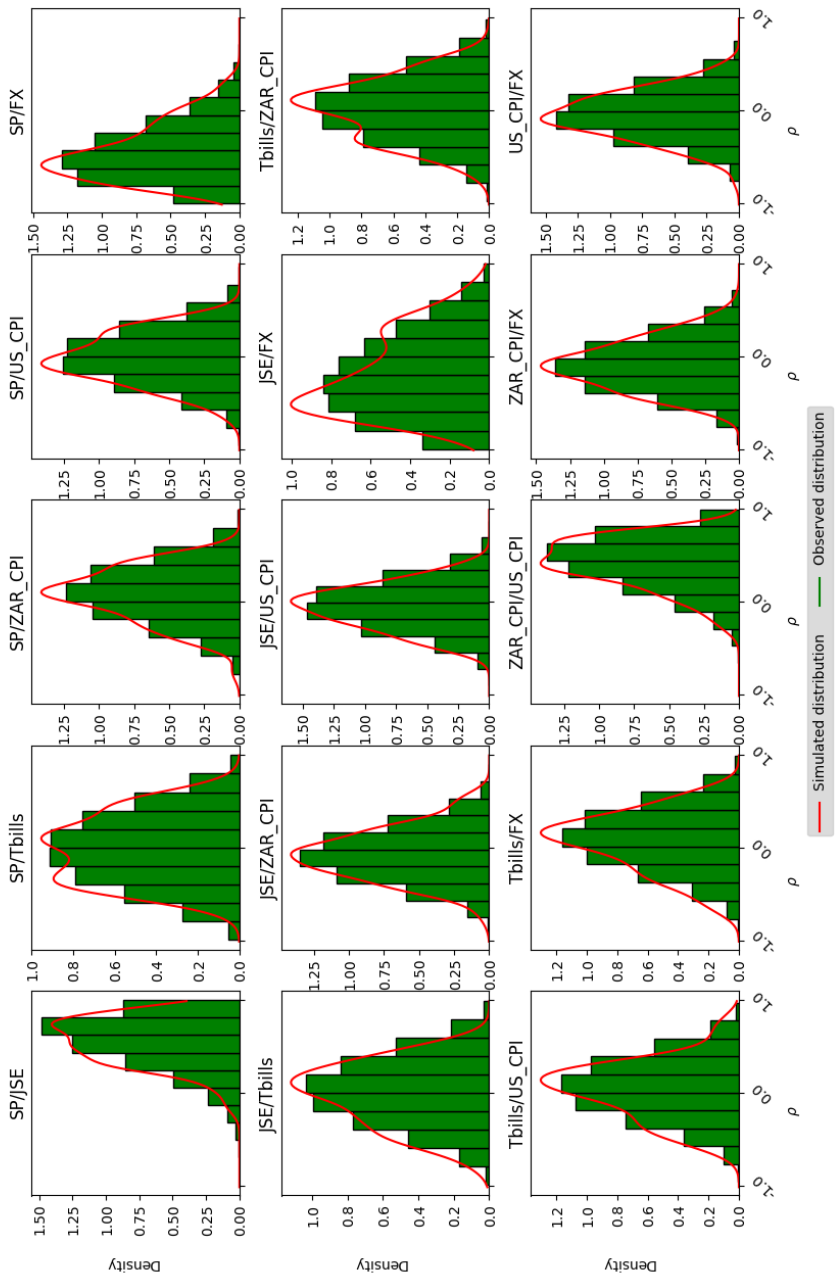

Figure 4.14: Simulated and Empirical Distributional Fits.

We illustrate the distributional fits of the simulated correlations and the empirical correlations in Figure 4.14. We observe that the distribution of simulated correlations fit the distribution of empirical correlations well.

It is important to note that when simulating portfolio values using stochastic correlation, a new correlation matrix needs to be constructed for each simulation and time-step. For example, performing a 30-year simulation with monthly time-steps and 10 000 simulations produces 3.6 million different correlation matrices. To ensure that each correlation matrix is valid (i.e., positive semi-definite), Higham (1989) eigenvalue raising is used for each correlation matrix.

4.7 Portfolio Construction

Monte Carlo methods are used to simulate future portfolio values to analyse the success rate for different portfolio compositions. The advantage of using a Monte Carlo simulation is that valuable insights into the range of possible outcomes can be obtained, and the distributional characteristics of our asset price process can be determined. The technique was first introduced by Metropolis and Ulam (1949). Monte Carlo simulation is a computational technique used to model the probability of different outcomes in processes that involve random variables.

A living annuity typically constitutes various compositions invested in T-bill/bonds and equities. A retiree that has opted for a living annuity is required to select the composition of bonds/T-bill and equities based on their risk tolerance, investment goals, and lifestyle requirements. Every retiree is unique and will need to decide on their required drawdown rate to match their specific needs. Further, a retiree will need to decide on how much of their savings they want to invest in risky assets (equities) and less risky assets (T-bill).

This technique produces a variable-year Monte Carlo sample and is repeated many times (in our case 10 000 samples) to build the distributional characteristics of our returns path process. Each individual path constitutes a random scenario based on the monthly simulated returns. A retiree is

also required to decide on an income drawdown rate [withdrawal rate] to suit their specific spending requirements. Each individual retiree would be unique in this case and have a desired income and investable assets available to support their lifestyle in retirement.

We first define a mathematical framework for the value of the portfolio, Π. At inception, the value of the portfolio is given by

$$\Pi(0) = N\omega_{\text{Tbills}} + N\omega_{\text{JSE}} + N\omega_{\text{S\&P}}, \tag{4.51}$$

where:

1. N denotes the initial investment;
2. ω_{Tbills} denotes the weight invested in T-bill;
3. ω_{JSE} denotes the weight invested in the JSE Top 40;
4. $\omega_{\text{S\&P}}$ denotes the weight invested in the S&P 500; and
5. $\omega_{\text{Tbills}} + \omega_{\text{JSE}} + \omega_{\text{S\&P}} = 1$.

The total withdrawal is based on the initial investment amount, i.e., $\Pi(0)$. For example, if $\Pi(0) =$ R1 000 000 and a retiree requires a total annual withdrawal of 4%, then an annual income of R40 000, paid monthly, is required for the remainder of the insured life. The value of the retiree's living annuity at any time, t,$\Pi(t)$, is given by

$$\begin{aligned}\Pi(t) = \Pi(t-1)\Bigg[&\omega_{\text{JSE}}\big(1 + r_{\text{JSE}}(t)\big) \\ &+ \omega_{\text{S\&P}}\big(1 + r_{\text{S\&P}}(t)\big) \cdot \frac{X(t)}{X(t-1)} \\ &+ \omega_{\text{Tbills}}\big(1 + r_{\text{t-bill}}(t)\big) - r_{\text{living}}\Bigg],\end{aligned} \tag{4.52}$$

where:

1. $\omega_{\text{JSE}}, \omega_{\text{S\&P}}$, and ω_{Tbills} denote the weight invested in the JSE Top 40, S&P 500, and T-bills respectively;
2. $r_{\text{JSE}}, r_{\text{S\&P}}$, and r_{Tbills} denote the monthly real return from the JSE Top 40, S&P 500, and T-bills respectively;
3. r_{living} denotes the monthly withdrawal rate required by a retiree from the living annuity; and
4. X denotes the USD/ZAR FX rate.

4.8 Results

In industry, 'safe' withdrawal rates are largely influenced by the retiree's life expectancy. To determine a realistic time-horizon over which to perform portfolio values and determine success rates, we make use of the South African life tables for assured lives (Dorrington and Tootla, 2007). We consider the 'mixed' life expectancy, i.e., both male and female, where the conditional median life expectancy given age 60 is approximately 81 years old. These life tables are based on data sourced from 1996 to 2000, which may not be indicative of current mortality rates. The WHO suggests that the life expectancy for both males and females has increased by approximately 10.2% from 2000 to 2021. Therefore, we derive a new conditional life expectancy given age 60, by applying a mortality adjustment factor of 10%. The new conditional life expectancy given age 60 is approximately 80 and 85 years old, for males and females, respectively. This yields a combined conditional life expectancy of approximately 82 years old (Van Niekerk et al., 2024).

Throughout our analysis, we perform portfolio simulations over a 30-year period, which we consider to be prudent, to determine portfolio success rates. Results are also provided in the Appendix A for portfolio success rates over 15, 20, 25, and 30-year periods. To ensure stability in the results from the Monte Carlo simulation, we employ 10 000 simulations and fix the random seed across all simulations. Further, we assume that withdrawals from the portfolio occur annually and are based on the initial amount invested in the portfolio. For example, if a retiree requires a 4% withdrawal rate, and

the initial amount invested is R1 million, then R40 000 will be withdrawn annually. All modelling is performed in the real space, i.e. all returns have been adjusted for inflation.

4.8.1 Portfolio Success Rates

Throughout our analysis, we perform portfolio simulations over a 30-year period, which we consider to be prudent, to determine portfolio success rates. Results are also provided in the Appendix A for portfolio success rates over 15, 20, 25 and 30-year periods. To ensure stability in the results from the Monte Carlo simulation, we employ 10 000 simulations and fix the random seed across all simulations. Further, we assume that withdrawals from the portfolio occur annually and are based on the initial amount invested in the portfolio. For example, if a retiree requires a 4% withdrawal rate, and the initial amount invested is R1 million, then R40 000 will be withdrawn annually. All modelling is performed in the real space, i.e., all returns have been adjusted for inflation.

We consider the following portfolio compositions when modelling success rates:

1. Portfolio 1 – investment in the JSE Top 40 and, RSA 90-day Tbill (cash),
2. Portfolio 2 – investment in the JSE Top 40, S&P 500 and, RSA 90-day Tbills.

Portfolios modelled with a constant correlation are denoted with a superscript 'CC' and portfolios modelled with a stochastic correlation are denoted with a superscript 'SC'. For example, Portfolio 1^{CC} refers to Portfolio 1 with a constant correlation.

To aid in interpreting the surface plots, Table 4.7 provides a breakdown of the weights applied to each portfolio. For example, when the equity exposure is 50%, then Portfolio 1 will have 50% invested in equity (100% of the allocation is in the JSE Top 40) and 50% invested in cash. However,

when the equity exposure is 50% for Portfolio 2, 50% is still invested in equities and 50% in cash, but the equity allocation is split as 50% in the JSE Top 40 and 50% in the S&P 500.

Table 4.7: Breakdown of Portfolio Weights

Equity Exposure	**Portfolio 1 weights**		**Portfolio 2 weights**		
	Tbills	**JSE Top 40**	**Tbills**	**JSE Top 40**	**S&P 500**
0%	100%	0%	100%	0%	0%
25%	75%	25%	75%	12.5%	12.5%
50%	50%	50%	50%	25%	25%
75%	25%	75%	25%	37.5%	37.5%
100%	0%	100%	0%	50%	50%

As mentioned in the data section of this article, we are cognisant of the fact that our data selection period includes not only one but two considerable stress events in a 20-year period. As a result, portfolio success rates may vary compared to those obtained by Maré (2016) and Van Appel et al. (2021), where both analyses were based on a data calibration period spanning from 1900 to 2020.

As a base case, we consider Portfolio 1^{CC}, which consists of only local equities and local Tbills, where the success rates are determined by assuming a constant correlation between all risk factors. Figure 4.15 below illustrates the success rates for Portfolio 1^{CC} for varying withdrawal rates and equity exposure. We observe that for low withdrawal rates, a portfolio that consists of only Tbills performs better than portfolios that are exposed to local equities. However, for withdrawal rates greater than 5%, equity exposure is necessary to achieve a higher success rate.

The success rates obtained appear muted compared to those obtained by both Maré (2016) and Van Appel et al. (2021). This is largely driven by the different calibration periods used and the two stress events included in our calibration period. A lacklustre local economy over the past 20 years has also contributed to the underperformance of the JSE Top 40. The results from Portfolio 1^{CC} indicate a similar conclusion to that obtained by both Maré (2016) and Van Appel et al. (2021), where 'safe' withdrawal rates over a 30-year period are between 3% to 5%.

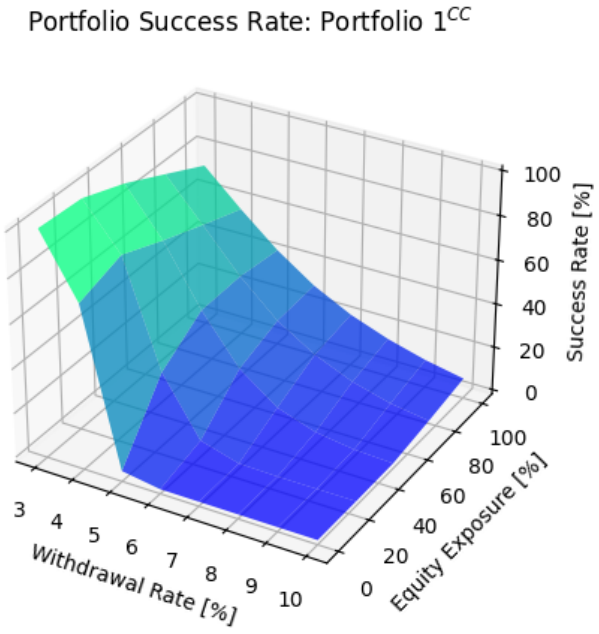

Figure 4.15: Portfolio Success Rates – Portfolio 1^{CC}.

To our knowledge, success rates specific to South Africa have not been investigated when a portfolio is exposed to both local and foreign equities. We now consider portfolio 2^{CC}, and superimpose the success rate surface in red over the base portfolio (Portfolio 1^{CC}) in Figure 4.16. We observe that including foreign equity exposure in a South African retiree's portfolio increases the success rate significantly – where the largest increase is observed for lower withdrawal rates and increasing equity exposure.

The portfolio success rates over a 30-year period increase by approximately 15% on average when including foreign equity exposure. As expected, the success rate decreases for higher withdrawal rates – although portfolios with higher withdrawal rates require increased equity exposure to obtain an increased success rate.

Having investigated the effect of foreign equity exposure on the success rate of a retirement portfolio, we now turn our focus to investigate the effect of stochastic correlation on portfolio success rates. As evidenced in Figure 4.1

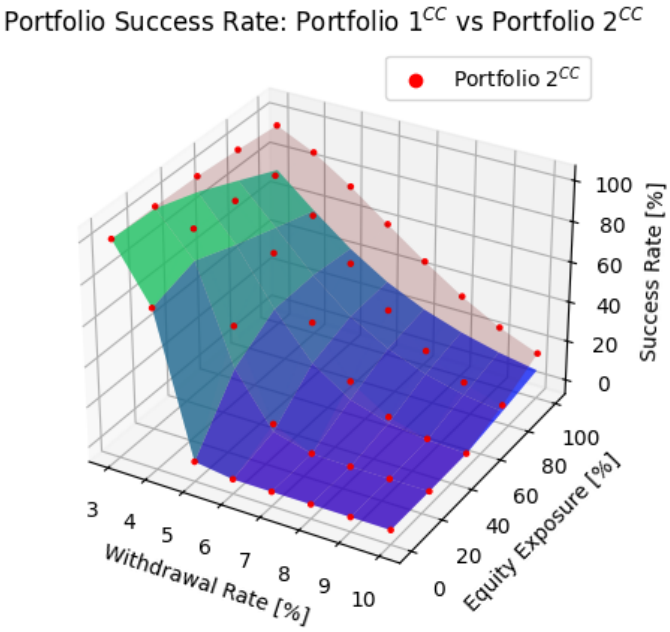

Figure 4.16: Portfolio Success Rates – Portfolio 1^{CC} vs Portfolio 2^{CC}.

and Figure 4.2, correlations between risk factors are not constant and vary through cycles. Making use of the stochastic correlation process defined in Equation (4.31), we model a more realistic representation of portfolio success rates – increasing a retiree's ability to make a more informed and accurate decision on their retirement portfolio allocation.

If we now assume Portfolio 2^{CC} to be the baseline, we again superimpose the success rates from the stochastic correlation portfolio (Portfolio 2^{SC}) in red over the success rate surface of Portfolio 2^{CC} in Figure 4.17. We observe that employing stochastic correlation in future portfolio value modelling increases the success rate over a 30-year period compared to the constant correlation portfolio. For example, at a 7% withdrawal rate and portfolio composition of 25% S&P 500, 25% JSE Top 40, and 50% T-bill, Portfolio 2^{CC}had a success rate of only 30.5% compared to Portfolio 2^{SC} which has a success rate of 78.5% – yielding an increase in the success rate of 48%. Overall, including stochastic correlation in portfolio modelling results in increased success rates for all portfolio compositions and withdrawal rates.

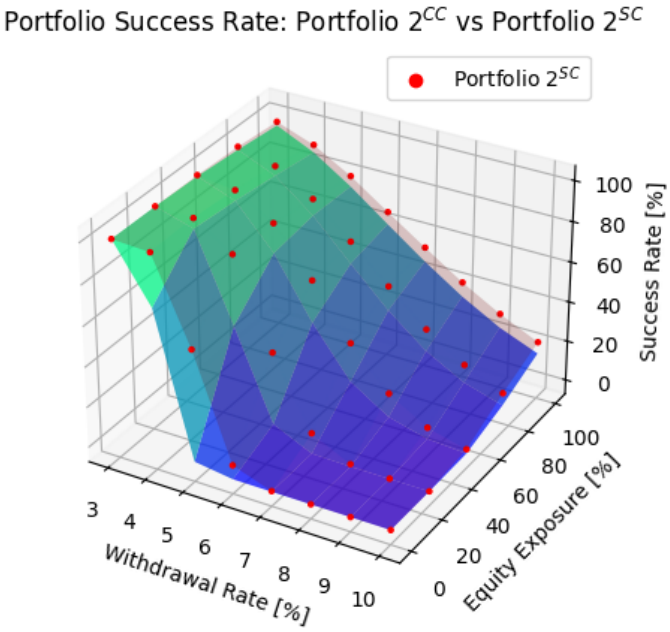

Figure 4.17: Portfolio Success Rates – 2^{CC} vs Portfolio 2^{SC}.

4.8.2 Fugit of the Portfolio

Recall from earlier comments that the fugit of a portfolio is defined as the average expected time for the portfolio to reach a state of ruin. We simulate portfolios over a 50-year period and calculate the average time that it would take for living annuities to reach a state of ruin. A summary of Portfolio 1^{CC}'s fugit (in years) is provided in Table 4.8 and Figure 4.18. As expected, retirees requiring higher withdrawal rates will reach a state of ruin much quicker than retirees requiring lower withdrawal rates. For example, consider the case when Portfolio 1^{CC} has 50% equity exposure. The fugit of a retiree requiring a 7% withdrawal rate is approximately 20 years compared to a retiree requiring a 12% withdrawal rate, which will reach a state of ruin in as little as nine years.

Table 4.8: Portfolio 1^{CC} Fugit (Years) at Varying Withdrawal Rates and Equity Exposures

Equity Exposure	**3%**	**4%**	**5%**	**6%**	**7%**	**8%**	**9%**	**10%**	**11%**	**12%**
0%	45.0	32.0	24.3	19.5	16.2	13.9	12.1	10.7	9.6	8.7
25%	47.0	37.3	27.7	21.5	17.5	14.8	12.7	11.2	10.0	9.0
50%	45.2	38.2	30.7	24.3	19.5	16.1	13.7	11.8	10.4	9.3
75%	42.6	36.7	30.8	25.6	21.2	17.7	14.9	12.8	11.2	9.9
100%	39.8	34.5	29.6	25.2	21.5	18.4	15.8	13.7	12.0	10.6
Average	43.9	35.7	28.6	23.2	19.2	16.2	13.9	12.1	10.6	9.5

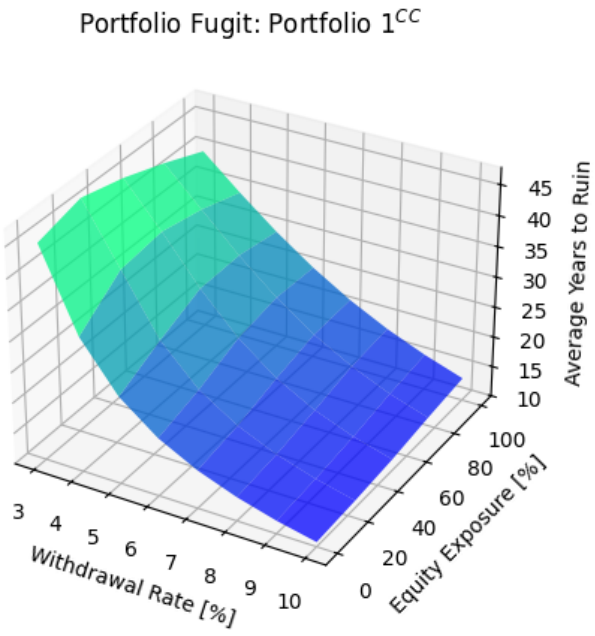

Figure 4.18: Portfolio Fugit - Portfolio 1^{CC}.

We now introduce foreign equity exposure into the portfolio, and superimpose the fugit surface of Portfolio 2^{CC} (red) on the fugit surface of Portfolio 1^{CC} (blue) in Figure 4.19. For ease of reference, the fugit results for Portfolio 2^{CC} are also provided in Table 4.9 below. We observe a distinct increase in the fugit of Portfolio 2^{CC} compared to Portfolio 1^{CC} across all portfolio compositions that have exposure to equity. This is expected given that we

observed increased success rates when exposing our portfolio to foreign equity. On average, the fugit of Portfolio 2^{CC} has increased by 8.5% compared to Portfolio 1^{CC}.

Table 4.9: Portfolio 2^{CC} Fugit (Years) at Varying Withdrawal Rates and Equity Exposures

Equity Exposure	**3%**	**4%**	**5%**	**6%**	**7%**	**8%**	**9%**	**10%**	**11%**	**12%**
0%	45.0	32.0	24.3	19.5	16.2	13.9	12.1	10.7	9.6	8.7
25%	49.4	42.6	31.3	23.5	18.7	15.6	13.3	11.7	10.3	9.3
50%	49.3	45.7	38.6	30.5	23.5	18.7	15.3	13.0	11.3	10.0
75%	48.8	45.7	40.8	34.7	28.6	23.2	18.8	15.6	13.1	11.3
100%	48.0	45.0	40.9	36.0	31.1	26.4	22.2	18.6	15.7	13.3
Average	48.1	42.2	35.2	28.8	23.7	19.6	16.4	13.9	12.0	10.5

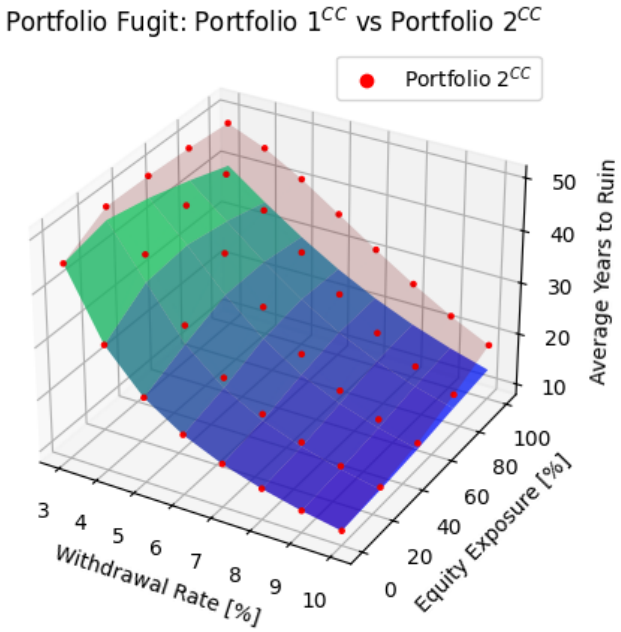

Figure 4.19: Portfolio Fugit - Portfolio 2^{CC} vs Portfolio 1^{CC}.

As a final case, we consider Portfolio 2^{SC} and investigate the impact of stochastic correlation on the portfolio fugit by comparing it to Portfolio 2^{CC}, which assumes a constant correlation. A breakdown of the fugit for

different portfolio compositions and the respective surface plots can be found in Table 4.10 and Figure 4.20, respectively.

Introducing stochastic correlation in future portfolio modelling increases the fugit compared to the constant correlation portfolio for all portfolio compositions. It is important to note that an increase is now observed on portfolios that consist of T-bill only, due to the stochastic correlation incorporated in the stochastic risks factor modelling. The fugit of a retiree who invests 50% into equity and a 7% withdrawal rate is approximately 29 years for Portfolio 2^{SC} compared to 24 years and 20 years for Portfolio 2^{CC} and Portfolio 1^{CC}, respectively.

Table 4.10: Portfolio 2^{SC} Fugit (Years) at Varying Withdrawal Rates and Equity Exposures

Equity Exposure	**3%**	**4%**	**5%**	**6%**	**7%**	**8%**	**9%**	**10%**	**11%**	**12%**
0%	45.0	32.0	24.3	19.5	16.2	13.9	12.1	10.7	9.6	8.7
25%	49.4	42.6	31.3	23.5	18.7	15.6	13.3	11.7	10.3	9.3
50%	49.3	45.7	38.6	30.5	23.5	18.7	15.3	13.0	11.3	10.0
75%	48.8	45.7	40.8	34.7	28.6	23.2	18.8	15.6	13.1	11.3
100%	48.0	45.0	40.9	36.0	31.1	26.4	22.2	18.6	15.7	13.3
Average	48.1	42.2	35.2	28.8	23.7	19.6	16.4	13.9	12.0	10.5

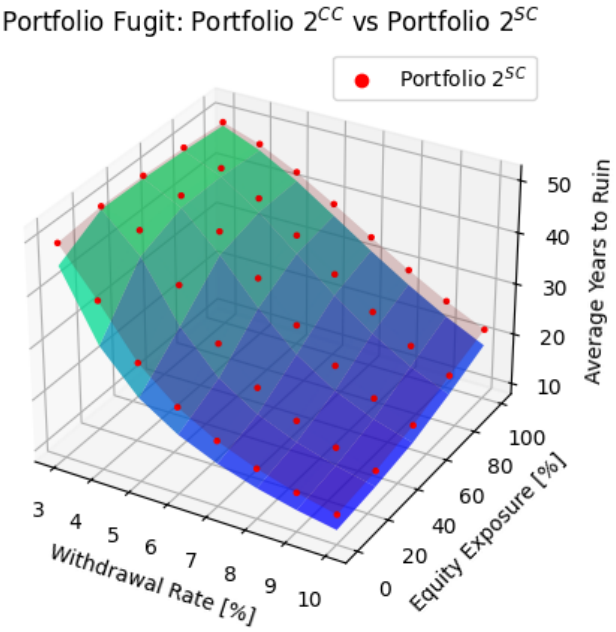

Figure 4.20: Portfolio Fugit – Portfolio 2^{CC} vs Portfolio 2^{SC}.

4.9 Concluding Comments

If I had to summarize money success in a single word it would be 'survival'. (Housel, 2020)

Generally, the risk premia in South Africa is higher compared to the United States. In South Africa, we expect higher returns, but this is coupled with higher inflation rates and greater risk. Inflation is one of the primary risks that threaten a 'safe' retirement by deteriorating a retiree's capital base faster than the investment growth it attempts to maintain in a dwindling economy. Seeking returns in foreign markets with a lower risk premium will diversify a retiree's portfolio and protect against adverse local market conditions.

Our calibration period for the stochastic retirement portfolio modelling was based on 20 years of historical data that included two significant stress

events, which contribute to the low success rates observed when only investing in local equities and T-bill compared to those obtained by Maré (2016) and Van Appel et al. (2021) which are based on over 100 years of historical data.

Diversifying a retirement portfolio by including foreign equity exposure results in a dramatic increase in both the success rates and fugit of a retirement portfolio, and a retiree is on average 27% more likely to have a 'safe' retirement. Our results indicate that retirees requiring higher withdrawal rates have to include a greater portion of equity exposure to have a chance of not outliving their retirement savings due to the lower returns offered from T-bill.

Stochastic correlation modelling provides a more accurate approach to modelling portfolios over long periods, where correlations between assets tend to change through cycles. Introducing stochastic correlation in retirement portfolio modelling also resulted in an increase in both the success rates and the fugit of approximately 9.26% and 13.03% on average, respectively.

We note that this research is based on the assumption that withdrawal rates are constant. According to the Pension Fund Act, a retiree can set/change their withdrawal rate from a living annuity once a year. Siegel (2015) disapproved of the notion of withdrawing a fixed amount from an inherently volatile portfolio. Our results indicate the same, that is, a careful and vigilant approach is needed to sustain a successful portfolio over a long period of time. Seeking both local and foreign equity exposure might increase the success of a retirement portfolio. However, there is no guarantee that historical returns will be mimicked in future returns.

To conclude, we concur with Cooley et al. (1998) and Maré (2016) that withdrawal rates of 4% or less are deemed to be 'safe'; however, including both foreign and local equities results in a diversification benefit that increases the success rates and fugit.

In this chapter, we addressed research questions 6 and 7, further refining our understanding of factors that enhance retirement portfolio performance. The sixth research question investigates the success rates and fugit outcomes for living annuities that incorporate foreign exposure. As demonstrated

in the results section, for the calibration period used, introducing foreign exposure – specifically through the S&P 500 – provides a clear diversification benefit, reducing risk and improving overall portfolio resilience. This highlights the potential for global market participation to enhance long-term retirement outcomes.

The seventh research question examines the potential gains from incorporating stochastic correlation into our modelling framework. Our results indicate that stochastic correlation positively impacts both success rates and fugit, offering a more dynamic and realistic representation of market behaviour by allowing asset class relationships to evolve over time. This approach more accurately reflects the interconnected nature of global markets, providing retirees with a strategy that adapts to shifting economic conditions and further bolsters the robustness of living annuity portfolios.

Chapter 5

Conclusion

'The general message here is that the more complex the environment, the greater the perils of complex control. The optimal response to a complex environment is often not a fully state-contingent rule. Rather, it is to simplify and streamline. In complex environment, decision rules based on one, or a few, good reasons can trump sophisticated alternatives. Less may be more.' (Haldane, 2012)

From our results and analysis, it becomes evident that every retiree is unique and requires a tailored approach to retirement planning. There is no one-size-fits-all solution; instead, retirement strategies must be specifically designed to meet the individual needs and circumstances of each retiree. This is particularly significant in the South African context, where only 6% of economically active individuals are projected to retire comfortably, leaving the majority at risk of a reduced standard of living compared to their pre-retirement years (ASISA, 2022). These statistics emphasise the critical importance of creating structured, secure, and sustainable retirement solutions to address the challenges faced by South African retirees.

Chapter 2 addresses the first aim of the thesis. The chapter introduced the process of constructing and simulating a retirement portfolio. The findings reveal a significant decline in portfolio success rates as retirement spending increases, measured as an annual, inflation-adjusted percentage. Additionally, the concept of a portfolio's expected life offers valuable insights

into the expected time to failure or the time to portfolio ruin.

The results clearly illustrate the impact of asset allocation on portfolio success. For instance, a 30-year portfolio composed entirely of bonds achieves only a 1% success rate with an annual withdrawal rate of 8%. In contrast, a portfolio consisting solely of equities significantly improves the success rate to 54% under the same conditions. This indicates that sustaining higher withdrawal rates over prolonged periods requires sufficient equity exposure. Our analysis also demonstrates that lower withdrawal rates significantly extend the expected time to ruin for living annuities, regardless of equity exposure. Portfolios with higher equity allocations tend to last longer due to the potential for greater growth, as illustrated by the 44.1-year ruin time for a 70% equity allocation compared to 31.1 years for a 10% allocation at a 5% withdrawal rate. However, at high withdrawal rates, even portfolios with substantial equity exposure face rapid depletion, reinforcing the need for careful balance between withdrawal rates and asset allocation.

In essence, Chapter 2 illustrates the importance of equity exposure in living annuities when trying to sustain high withdrawal rates over a prolonged period.

Chapter 3 addresses the second and third aims of the thesis. The chapter demonstrated that a hybrid retirement strategy allows retirees to sustain higher withdrawal rates compared to a pure living annuity. For retirees withdrawing less than 8% annually, which accounts for approximately 50% of the annuitised population, the hybrid strategy significantly increases the probability of maintaining a sustainable portfolio. While portfolio management fees have a notable impact on success rates, the hybrid approach consistently outperforms a pure living annuity, even when such costs are considered. Additionally, the living annuity portion of the hybrid strategy retains a higher average value after 30 years (depending on portfolio composition), offering a greater potential inheritance for heirs.

The findings suggest that a hybrid strategy can sustain ‘safe’ withdrawal rates of up to 6% when fees are included, a notable improvement over the 4% ‘safe’ withdrawal rate recommended by Maré (2016) for South African retirees using pure living annuities. This highlights the hybrid strategy’s

potential for greater income flexibility and sustainability.

Chapter 4 addresses the fourth and fifth aims of the thesis. The chapter used 20 years of historical data that included two significant stress events (GFC and Covid), for the calibration of stochastic retirement portfolio modelling. This shorter calibration period resulted in lower success rates for portfolios invested solely in local equities and T-bill compared to the findings of Maré (2016) and Van Appel et al. (2021), which were based on over 100 years of historical data. These findings emphasise the importance of selecting data for the calibration of stochastic processes, which might understate or overstate results depending on the choice of the duration of data.

Diversifying retirement portfolios by incorporating foreign equity exposure significantly improves both success rates and fugit. On average, retirees are 8.5% more likely to achieve a 'safe' retirement when foreign equities are included. Furthermore, retirees with higher withdrawal rates need greater equity exposure to offset the comparatively lower returns of T-bill. This highlights the critical role of diversification and growth-oriented investments in maintaining portfolio sustainability over extended periods.

Stochastic correlation modelling offers a more accurate method for simulating portfolios over long horizons, capturing the dynamic changes in asset correlations through market cycles. This approach resulted in an average increase of 9.26% in success rates and 13.03% in fugit. While withdrawal rates of 4% or less remain 'safe', as supported by Maré (2016) and Cooley et al. (1998), the inclusion of both local and foreign equities provides a diversification benefit that further enhances portfolio outcomes. However, it is essential to note that historical returns may not predict future performance, and vigilance in managing withdrawal rates and portfolio composition remains crucial for a sustainable retirement.

There are a few areas of future research that could extend the analysis presented in this thesis:

1. Further research may include determining the 'optimal' portfolio composition that increases the success rate for a given withdrawal rate. Further, there may be merit in investigating the 'optimal' time to

convert a living annuity (or a part thereof) to a life annuity, as a life annuity becomes cheaper the older a retiree becomes.

2. Investigating varying withdrawal rates or employing utility functions as withdrawal rates. Withdrawal rates vary over time, as retirees age, they generally have lower expenditures and may reinvest gains back into a living annuity; hence, a more flexible withdrawal strategy is often needed to balance income needs with the sustainability of the portfolio.

3. Extended research could also include the investigation of success rates in a hybrid strategy that is exposed to foreign exposures and stochastic correlation as well as dynamic investing strategy that shifts the weights of the retirement portfolio throughout the retirement period to comply with regulation 28. Regulation 28, as set out by the South African government, indicates that a retiree may invest a maximum of 45% of their retirement savings in foreign assets, 25% in property, 15% in private equity, 10% in commodities, 10% in hedge funds, and 2.5% in other excluded assets. Regulation 28 also has a limit on the total equity exposure a retiree may have in their portfolio.

4. Derivative strategies can be employed to hedge the composition exposure of a living annuity by mitigating risks associated with fluctuations in asset values, such as equities or bonds. Instruments like options or futures allow retirees to protect their portfolio against downside risks while maintaining potential for growth. By incorporating these strategies, a living annuity can achieve a more stable income stream, which safeguards the sustainability of retirement savings against market volatility.

5. Analyse the tax efficiency of hybrid retirement strategies compared to pure life or living annuities, while accounting for South African tax laws and possible international investments.

6. Develop a volatility-targeting asset allocation strategy that dynamically adjusts portfolio compositions over the lifespan of a living annuity, and evaluate the associated success rates and fugit outcomes. This approach aims to manage the volatility experienced by living annuities by establishing an initial volatility threshold, with the portfolio adapting as needed to maintain volatility within a predefined range around the set parameter.

Bibliography

Abramowitz, M. and Stegun, I. (1964), *Handbook of Mathematical Functions with Formulas, Graphs, and Mathematical Tables*, Dover Publications, New York.

Africa, S. S. (2024), *Statistics South Africa on official unemployment rate in third quarter of 2024 | South African Government gov.za*. Viewed 20 January 2025. https://www.gov.za/news/media-statements/statistics-south-africa-official-unemployment-rate-third-quarter-2024-12-nov.

Allianz (2023), 'Americans facing a new retirement reality'. Viewed 20 June 2024. https://www.allianzlife.com/about/newsroom/2023-Press-Releases/Americans-Facing-a-New-Retirement-Reality.

Anarkulova, A., Cederburg, S., O Doherty, M. and Sias, R. (2023), 'The safe withdrawal rate: Evidence from a broad sample of developed markets', *SSRN* . Viewed 20 June 2024. https://papers.ssrn.com/sol3/papers.cfm?abstract_id=4227132.

Andersen, L., Andreasen, J. and Eliezer, D. (1999), 'Jump-diffusion processes: Volatility smile fitting and numerical methods for option pricing', *Review of Derivatives Research* **3**(3), 231–262.

Andrews, G., Askey, R. and Roy, R. (1999), *Special Functions*, Cambridge University Press.

ASISA (2022), *The Association for Savings and Investment South Africa*. Viewed 20 June 2024. https://www.asisa.org.za/media/hfvhoous/20231128_asisa-living-annuities-drawdown-survey-statistics-report-2017-to-2022.xlsx.

Auret, C. and Vivian, R. (2014), *A comparative analysis of returns of various financial asset classes in South Africa: A triumph of bonds?*, *Southern African Business Review*, South Africa. 18(3), Pages 175-195.

Bailey, W. (1935), 'Generalized hypergeometric series', *Cambridge Tracts in Mathematics and Mathematical Physics* **32**.

Bank, S. A. R. (2024), *Risk-free rates - 2023*. Viewed 6 February 2024. `https://www.resbank.co.za/en/home/publications/publication-detail-pages/prudential-authority/pa-insurers/Insurance-Sector-Data/pa-risk-free-rates/2023/Risk-free-rates-2023`.

Bansal, R., Gallant, A., Hussey, R. and Tauchen, G. (1995), 'Nonparametric estimation of structural models for high-frequency currency market data', *Journal of Econometrics* **66**(1-2), 251–287.

Beinash, L. (2008), *Living Annuities: The Advisory Process*. Presented at the South African Actuarial Convention 2008.

Bengen, W. (1994), *Determining withdrawal rates using historical data*, Vol. 7, *Journal of Financial Planning*.

Bjork, T. (2009), *Arbitrage Theory in Continuous Time*, 3rd edn, Oxford University Press, Oxford, UK. Comprehensive coverage of arbitrage pricing and stochastic calculus in finance.

Black, F. and Scholes, M. (1973), 'The pricing of options and corporate liabilities', *Journal of Political Economy* **81**(3), 637–654.

Blake, D., Cairns, A. J. and Dowd, K. (2006), 'On asset-liability modeling for pension funds in south africa', *Pensions: An International Journal* **11**(3), 180–195.

Blanchett, D. (2014), *Addressing Key Retirement Risks*, Vol. 2, The Journal of Retirement.

Bodie, Z., Hammond, M. D. and Mitchell, O. S. (2004), *Retirement Income Redesigned: Master Plans for Distribution: An Adviser's Guide for Funding Boomers' Best Years*, John Wiley & Sons, New York.

Buraschi, A. and Porchia, P. (2009), 'Correlation risk and optimal portfolio choice', *The Journal of Finance* **64**(1), 359–402.

BusinessTech (2024), *96% of South Africans know the two-pot system will hurt them – they take out anyway.* Viewed 2 December 2024. https://businesstech.co.za/news/business/802362/96-of-south-africans-know-the-two-pot-system-will-hurt-them-they/-take-out-anyway/.

Butler, M. and Van Zyl, C. (2012), *Retirement adequacy goals for South African households*, Vol. 12, South African Actuarial Journal.

Cooley, P. L., Hubbard, C. M. and Daniel, T. (1999), *Sustainable withdrawal rates from your retirement portfolio*, Vol. 10, Financial Counselling and Planning.

Cooley, P. L., Hubbard, C. M. and Walz, D. T. (1998), *Retirement savings: Choosing a withdrawal rate that is sustainable*, Vol. 20, Journal of the American Association of Individual Investors.

Cox, J., Ingersoll, J. and Ross, S. (1985), 'A theory of the term structure of interest rates', *Econometrica* **53**(2), 385–407.

Daraei, D. and Sendova, K. (2024), 'Determining safe withdrawal rates for post-retirement via a ruin-theory approach', *Risks* **12**(4), 1–24.

Dimson, E., Marsh, P. and Staunton, M. (2014), *Credit Suisse Global Investment Returns Sourcebook 2014*, Credit Suisse Research Institute.

Dorrington, R. E. and Tootla, S. (2007), *South African Annuitant Standard Mortality Tables 1996 to 2000 (SAIML98 and SAIFL98)*, Vol. 7, South African Actuarial Journal.

Duffie, D. and Singleton, K. (1993), 'Simulated moments estimation of markov models of asset prices', *Econometrica* **61**(4), 929–952.

Dybvig, P. H. and Liu, H. (1999), 'Portfolio allocation for long-term investors', *Review of Financial Studies* **12**(1), 99–127.

Efron, B. (1979), *Bootstrap Methods: Another Look at the Jackknife*, Vol. 7, The Annals of Statistics.

Feller, W. (1951), *An Introduction to Probability Theory and Its Applications*, 1st edn, Wiley, New York.

Finke, M., Pfau, W. and Williams, D. (2012), 'Spending flexibility and safe withdrawal rates', *Journal of Financial Planning* .

Firer, C. and Staunton, M. (2002), '102 years of south african financial market history', **31**(56), 57–65.

Fokker, A. (1914), 'Die mittlere energie rotierender elektrischer dipole im strahlungsfeld', *Annalen der Physik* **348**(5), 810–820.

Gallant, A. and Nychka, D. (1987), 'Semi-nonparametric maximum likelihood estimation', *Econometrica* **55**(2), 363–390.

Gallant, A. and Tauchen, G. (1996), 'Which moments to match?', *Econometric Theory* **12**(4), 657–681.

Gardiner, C. (2009), *Stochastic Methods: A Handbook for the Natural and Social Sciences*, Springer, Berlin, Heidelberg.

Garman, M. B. (1989), Fugit: A concept for option pricing models, *in* J. Smith and A. Jones, eds, 'Advances in Financial Modelling', Springer, New York, pp. 55–70.

Golub, G. and Van Loan, C. (2013), *Matrix Computations*, Johns Hopkins University Press, Baltimore.

Haldane, A. G. (2012), The dog and the frisbee, *in* 'Federal Reserve Bank of Kansas City Economic Policy Symposium', Jackson Hole, Wyoming. Viewed 8 October 2024. `https://www.bankofengland.co.uk/-/media/boe/files/paper/2012/the-dog-and-the-frisbee.pdf`.

Heston, S. (1993), 'A closed-form solution for options with stochastic volatility with applications to bond and currency options', *The Review of Financial Studies* **6**(2), 327–343.

Higham, D. (2001), 'An algorithmic introduction to numerical simulation of stochastic differential equations', *SIAM Review* **43**(3), 525–546.

Higham, N. (1988), 'Computing a nearest symmetric positive semidefinite matrix', *Linear Algebra and its Applications* **103**, 103–118.

Higham, N. J. (1989), 'Matrix nearness problems and applications', *Proceedings of the Royal Society of London. Series A, Mathematical and Physical Sciences* **431**(1884), 151–170.

Housel, M. (2020), *The Psychology of Money: Timeless lessons on wealth, greed, and happiness*, Harriman House, London. Viewed 25 October 2024. https://www.harriman-house.com/thepsychologyofmoney.

Hull, J. (2018), *Futures, and Other Derivatives*, 10th edn, Pearson, London.

Karatzas, I. and Shreve, S. E. (1991), *Brownian Motion and Stochastic Calculus*, Springer, New York.

Klein, S. and Sapra, S. (2020), *Optimal asset allocation, asset location and drawdown in retirement*, Quantitative Research and Analytics.

Kloeden, P. and Platen, E. (1992), *Numerical Solution of Stochastic Differential Equations*, Springer, Berlin, Heidelberg.

Koepf, W. (1998), 'Hypergeometric summation: An algorithmic approach to summation and special function identities', *Vieweg+Teubner Verlag* pp. 1–234.

Levendis, A. and Maré, E. (2023), 'On the calibration of stochastic volatility models to estimate the real-world measure used in option pricing', *ORiON* **39**(1), 65–91. Viewed 27 June 2024. https://orion.journals.ac.za/pub/article/download/747/632.

Long-Term Insurance Act, 1998: Regulation 39 (1998), Government Printer, South Africa. Published by the Department of Justice and Constitutional Development.

Maré, E. (2016), 'Safe spending rates for south african retirees', *South African Journal of Science* **112**(1/2), 4.

Markus, A. and Kumar, S. (2020), 'Social media marketing gains importance after covid-19', *Cogent Business & Management* **7**(1). Viewed 27 June 2024. https://www.tandfonline.com/doi/pdf/10.1080/23311975.2020.1870797.

Merton, R. C. (1969), 'Lifetime portfolio selection under uncertainty: The continuous-time case', *The Review of Economics and Statistics* **51**(3), 247–257.

Metropolis, N. and Ulam, S. (1949), 'The monte carlo method', *Journal of the American Statistical Association* **44**(247), 335–341.

Milevsky, M. A. (2013), *Life Annuities: An Optimal Product for Retirement Income*, Research Foundation of CFA Institute.

Milevsky, M. A. and Haung, H. (2011), *Spending retirement on planet Vulcan: The impact of longevity risk aversion on optimal withdrawal rates*, Vol. 67, Financial Analyst Journal.

National Treasury (2012), *Enabling a Better Income in Retirement: Technical Discussion Paper B for public comment by The South African National Treasury.* Viewed 30 June 2024. http://www.treasury.gov.za/publications/other/retirement/Enabling%20a%20Better%20Income%20in%20Retirement.pdf.

National Treasury (2013), *Charges in South African Retirement Funds: Technical Discussion Paper A for public comment by The South African National Treasury.* Viewed 1 July 2024. http://www.treasury.gov.za/publications/other/retirement/Charges%20in%20South%20African%20Retirement%20Funds.pdf.

Olver, F., Lozier, D., Boisvert, R. and Clark, C. (2010), *NIST Handbook of Mathematical Functions*, Cambridge University Press, Cambridge.

Pfau, W. D. (2011), 'Capital market expectations, asset allocation, and safe withdrawal rates', *SSRN* . Viewed 27 June 2024. https://papers.ssrn.com/sol3/papers.cfm?abstract_id=2544656.

Risken, H. (1996), *The Fokker-Planck Equation: Methods of Solution and Applications*, Springer, Berlin, Heidelberg.

Rusconi, R. (2020), *Regulating South African retirement funds: The case for clearer objectives.* Presented at the Actuarial Society of South Africa's 2020 Virtual Convention.

Samuelson, P. A. (1965), 'Rational theory of warrant pricing', *Industrial Management Review* **6**(2), 13–31.

Siegel, L. B. (2015), 'The only spending rule article you will ever need', *Financial Analysts Journal* **71**(1), 91–107.

Slater, L. (1966), 'Generalized hypergeometric functions', *Cambridge University Press* pp. 1–240.

South African National Treasury (2024), 'Introduction of the Two-Pot Retirement System in South Africa'. Viewed on 24 November 2024. https://www.sars.gov.za/two-pot-retirement-system/.

South African Revenue Service (SARS) (2024), 'Two-Pot Retirement System: Early Uptake and Challenges'. Viewed on 24 November 2024. https://www.sars.gov.za/two-pot-retirement-system/.

Swart, N. (2012), *Personal Financial Planning: South African Perspective*, Juta and Company Ltd, Cape Town.

Teng, Z., Ehrhardt, M. and Günther, M. (2016), 'Modelling stochastic correlation', *Journal of Mathematics in Industry* **6**(1), Article 4. Viewed 2 June 2024. https://mathematicsinindustry.springeropen.com/articles/10.1186/s13362-016-0018-4.

Van Appel, V., Maré, E. and Van Niekerk, A. (2021), *Quantitative guidelines for retiring (more safely) in South Africa*, Vol. 21, *South African Actuarial Journal*.

Van Emmerich, C. (2006), 'Modelling correlation as a stochastic process'. Preprint 06/03, Department of Mathematics, University of Wuppertal, Viewed 25 March 2024. https://www.imacm.uni-wuppertal.de/fileadmin/imacm/preprints/amna_06_03.pdf.

Van Heerden, G. and Koekemoer, R. (2008), 'Optimal asset allocation for retirement funds in south africa', *South African Journal of Economic and Management Sciences* **11**(4), 424–444.

Van Niekerk, A. J. and Maré, E. (2020), 'Optimale ontrekkingskoerse vir aftreebeleggings in suid-afrika', *Suid-Afrikaanse Tydskrif vir Natuurwetenskap en Tegnologie* **139**(1).

Van Niekerk, A. J., Moutzouris, V. and Maré, E. (2024), 'Hybrid retirement strategy in south africa', *South African Journal of Economic and Management Sciences* **27**(1), a5681. Viewed 20 November 2024. https://doi.org/10.4102/sajems.v27i1.5681.

Visser, J. (2024), *Uptick in demand for blended living annuities*. Viewed 9 March 2024. https://citywire.com/za/news/uptick-in-demand-for-blended-living-annuities/a2445263.

Warring, M. B. and Siegel, L. B. (2015), *The only spending rule article you will ever need*, Vol. 71, *Financial Analysts Journal*.

World Health Organization (2019), *World Health Organization: The Global Health Observatory*. Viewed 23 June 2024. `https://data.who.int/countries/710`.

World Health Organization (2021), *World Health Organization: The Global Health Observatory*. Viewed 23 January 2024. `https://data.who.int/countries/710`.

Wright, S. (2015), 'Coordinate descent algorithms for matrix problems', *SIAM Journal on Matrix Analysis and Applications* **57**(2), 319–341.

Index

Appendix A

'Optimal' Portfolio per Withdrawal Rate

Retirement modelling for optimal solutions requires fixing key variables and making essential assumptions to manage the complexity inherent in these problems. While asset allocations to equities, bonds, and cash may remain fixed in our research, other factors – such as withdrawal rates, longevity projections, and annuity proportions – introduce multiple degrees of freedom. Without constraining certain variables, the search for an 'optimal' solution becomes intractable due to the expansive range of possible scenarios. By setting specific withdrawal rates and defining the allocation between living and life annuities, we reduce the dimensionality of the problem, allowing for a more focused and practical optimisation process. This structured approach simplifies the modelling process while still capturing the key trade-offs involved in retirement planning.

The necessity of fixing variables reflects the reality that retirees face–decisions must be made within the context of personal preferences, risk tolerance, and financial goals. Optimal solutions in this setting are not universal but rather conditional on the retiree's profile and the assumptions made during the modelling process. For example, the level of exposure to equities or the chosen withdrawal rate directly influences the portfolio's longevity and performance. By establishing these parameters, we can simulate different

market conditions and derive insights that guide retirees toward sustainable and reliable strategies. Ultimately, this approach balances the need for flexibility with the requirement for actionable solutions, ensuring that the models are both rigorous and applicable to real-world retirement scenarios.

A.1 'Optimal' Portfolio for Hybrid Strategy (Section 3.6)

The analysis of the five graphs below reveals critical insights into the sustainability of various withdrawal rates over a 30-year period for portfolios with differing allocations between life annuities and living annuities. Each portfolio demonstrates how varying equity exposure and withdrawal rates interact to impact success probabilities, helping to identify optimal strategies for long-term financial planning. Starting from the base case of 100% living annuities and progressively reducing their allocation in favour of life annuities, the analysis highlights the interplay between portfolio composition and withdrawal sustainability.

In the base case of 100% living annuities FigureA.1, the graphs show that withdrawal rates of 3% and 4% can be sustained with high success probabilities across most equity exposures. This outcome reflects the flexibility of living annuities, particularly for retirees with conservative withdrawal needs. However, for withdrawal rates of 5% and above, success probabilities drop significantly, especially at higher equity exposures. This indicates that a higher allocation to bonds (lower equity exposure) provides more stable outcomes in this scenario, reinforcing the need for caution with aggressive withdrawals in purely living annuity portfolios. More aggressive withdrawal strategies would require significant risky asset holdings to increase the chances of long term sustainability.

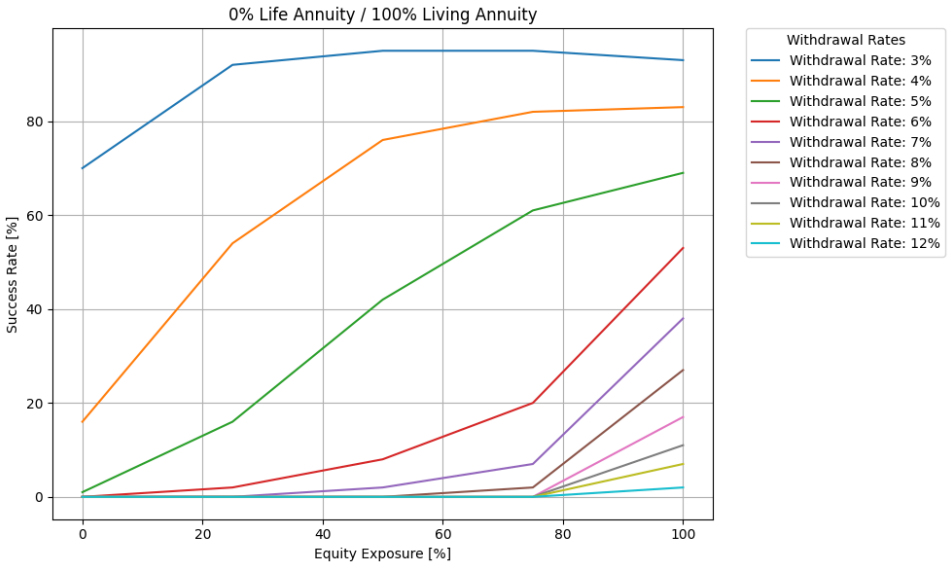

Figure A.1: 100% Living Annuity and 0% Life Annuity, Success Rates per Withdrawal Rate.

As the allocation shifts to include a portion of life annuities (e.g., 75% living annuity), withdrawal rates of up to 5% can be sustained with over 80% success probability, even at moderate equity exposures. The inclusion of life annuities introduces an element of guaranteed income, reducing reliance on market performance and improving overall portfolio stability. At a 50% life and 50% living annuity allocation, similar results are observed, with withdrawal rates up to 5% being easily sustainable. This balance between guaranteed income and market-driven growth provides a robust structure for retirees with moderate withdrawal needs.

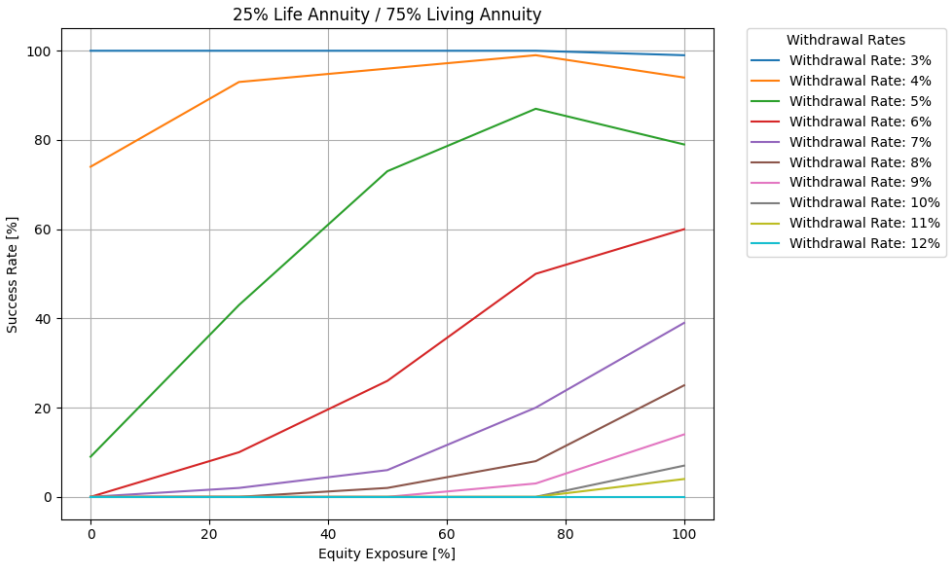

Figure A.2: 75% Living Annuity and 25% Life Annuity, Success Rates per Withdrawal Rate.

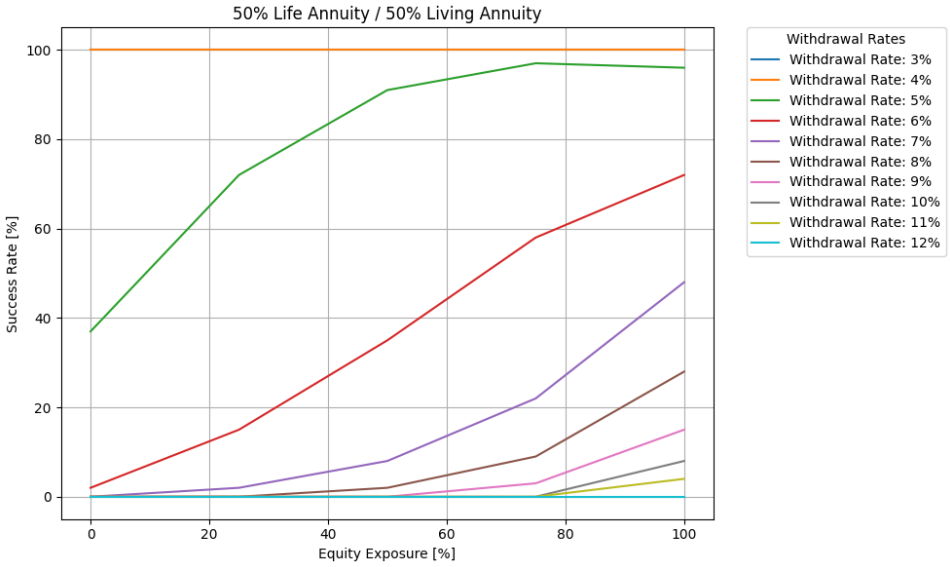

Figure A.3: 50% Living Annuity and 50% Life Annuity, Success Rates per Withdrawal Rate.

For portfolios with smaller living annuity allocations, such as 25% and 10%, higher withdrawal rates become more sustainable. The 25% living annuity

portfolio supports withdrawal rates up to 6% with sufficient equity exposure, highlighting the role of high-growth assets in complementing life annuity stability. In the case of the 10% living annuity portfolio, withdrawal rates of up to 7% can be supported, with a 60% equity exposure achieving an 80% success rate. These results demonstrate that as the life annuity allocation increases, the portfolio becomes more resilient to higher withdrawal rates, provided that sufficient equity exposure is maintained and can meet growth demands over the long term. This progressive allocation to life annuities highlights a clear trade-off between guaranteed stability and the need for equity-driven growth in managing aggressive withdrawal scenarios.

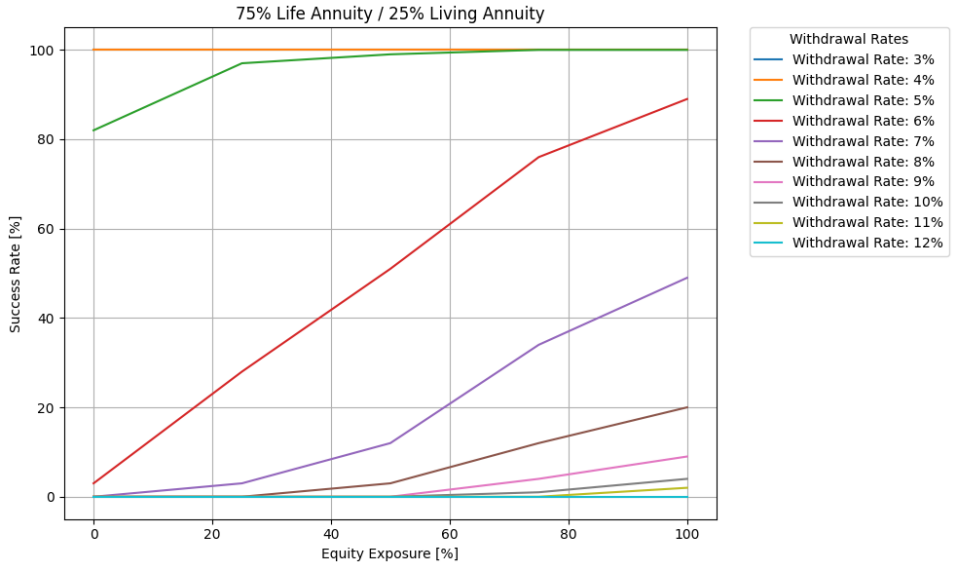

Figure A.4: 25% Living Annuity and 75% Life Annuity, Success Rates per Withdrawal Rate.

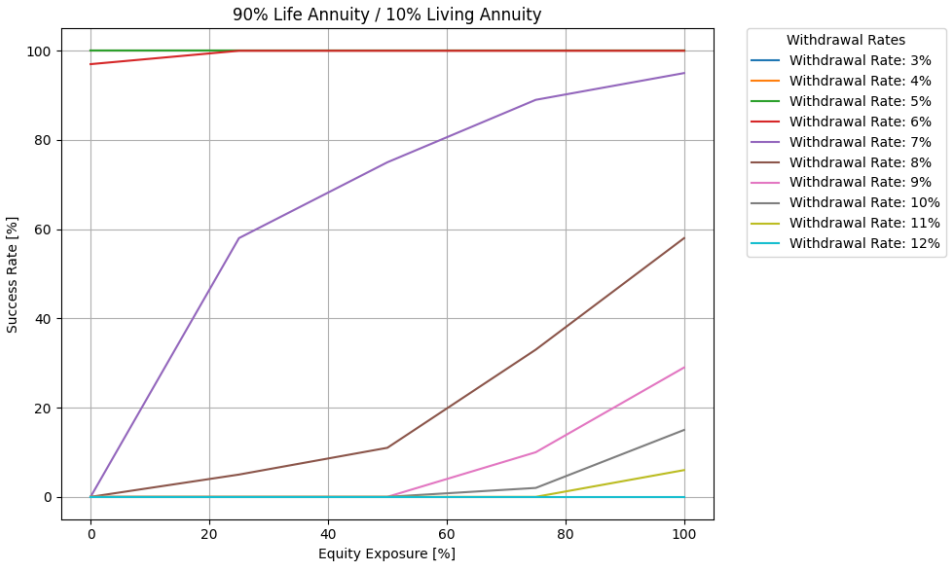

Figure A.5: 10% Living Annuity and 90% Life Annuity, Success Rates per Withdrawal Rate.

While certain general patterns emerge–such as the ability of portfolios with higher life annuity allocations to sustain higher withdrawal rates due to their guaranteed income component–there is no universal solution that applies to all retirees. Each retiree's circumstances, risk tolerance, and financial goals are unique, requiring a bespoke approach to retirement planning. Some may prioritise stability and guaranteed income, favouring higher allocations to life annuities, while others may seek higher growth potential, necessitating greater equity exposure and living annuity flexibility. Ultimately, crafting an optimal retirement portfolio demands a careful assessment of individual needs, preferences, and market conditions, ensuring a tailored solution that aligns with the retiree's long-term sustainability and peace of mind.

A.2 'Optimal' Portfolio including Foreign Exposure and Stochastic Correlation (Section 4.8)

In retirement planning, selecting the optimal portfolio composition is a delicate balance between minimising risk and maximising success rates over

a long time horizon, such as 30 years. The minimum variance portfolio, often considered the most stable option, is constructed to reduce the impact of market fluctuations by prioritising low-volatility assets such as Tbill. This approach ensures a steady stream of returns, making it particularly suitable for retirees with lower withdrawal rates, where preserving capital is paramount. However, as withdrawal rates increase, the focus shifts towards maximising success rates by incorporating higher-yielding, growth-oriented assets like equities. This trade-off reflects the necessity of generating sufficient returns to sustain higher withdrawal demands, even at the expense of increased portfolio volatility. The interplay between minimising risk and optimising long-term success rates forms the foundation of selecting a portfolio strategy that aligns with both financial needs and risk tolerance in retirement

The analysis of the graphs below reveals key insights into the success rates of living annuities under different portfolio compositions and withdrawal rates over a 30-year period. Portfolio 1^{CC}, which consists of RSA T-bill and JSE equities under constant correlation, demonstrates that for lower withdrawal rates such as 3%, the optimal portfolio composition is entirely T-bill-based, with 100% allocation to Tbills and 0% equities. This portfolio composition minimises risk and ensures stability and longevity of the portfolio, as T-bill are less volatile than equities. As the withdrawal rate increases, however, the reliance on equities begins to rise. At a 4% withdrawal rate the optimal portfolio composition would be 25% JSE and 75% Tbills. As withdrawal rates increase, so does the necessity for equity exposure. For example, any withdrawal rate larger than 6% would require 100% equity allocation to maximise the relevant success rate over the 30-year horizon. This reflects the need for higher growth potential in more aggressive withdrawal scenarios.

A.2. 'Optimal' Portfolio including Foreign Exposure and Stochastic Correlation (Section 4.8)

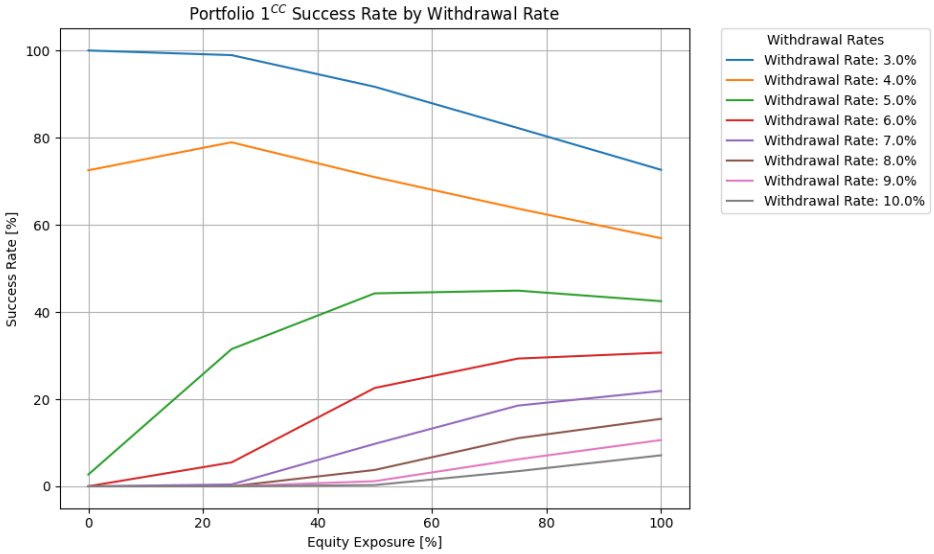

Figure A.6: Portfolio 1^{CC} Success Rates per Withdrawal Rate.

Portfolio 2^{CC} incorporates RSA T-bill, JSE equities, and S&P 500 equities with a constant correlation structure. Similar to Portfolio 1^{CC}, lower withdrawal rates such as 3% achieve optimal success with a 100% Tbill allocation. As withdrawal rates increase, to 5% for example, we observe that the optimal portfolio composition would be at 75% equities exposure(37.5% JSE and 37.5% S&P 500) and 15% T-bill. Higher than 5% withdrawal rates would require 100% equity exposre to ensure long term survivability of the living annuity. This portfolio shows that international diversification under constant correlation allows for more sustainable withdrawal rates by capturing growth opportunities in global markets while still retaining some stability.

A.2. 'Optimal' Portfolio including Foreign Exposure and Stochastic Correlation (Section 4.8)

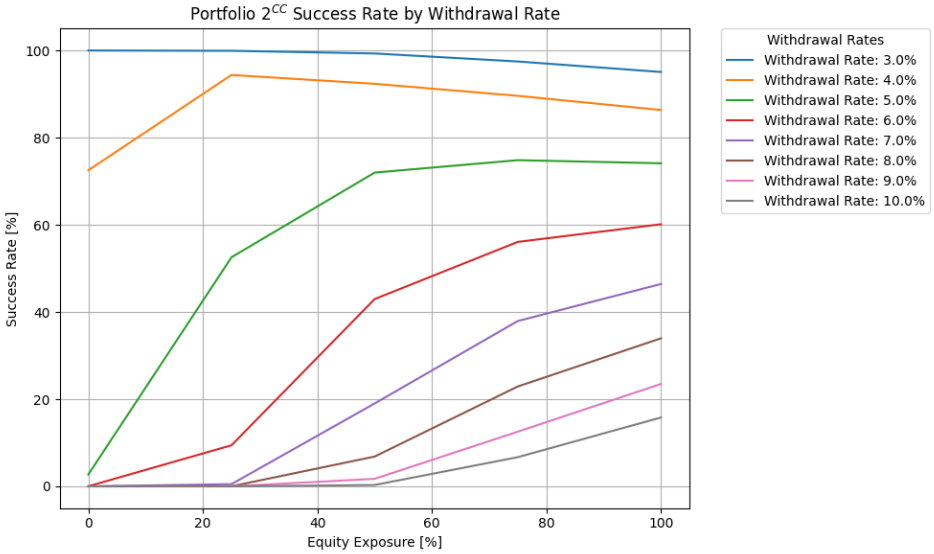

Figure A.7: Portfolio 2^{CC} Success Rates per Withdrawal Rate.

Portfolio 2^{SC}, which incorporates stochastic correlation, introduces more realistic market variability into the simulations. At a 3% withdrawal rate, the optimal allocation remains 100% T-bills, as the stability of these assets offsets the variability introduced by stochastic correlations. For higher withdrawal rates, for example 6%, the optimal portfolio composition would be 75% equities exposure (37.5% JSE and 37.5% S&P 500) and 25% T-bill. For withdrawal rates that are 7% and higher it would be prudent to allocate the portfolio fully to equities to ensure long term survavibility. While stochastic correlation introduces additional challenges, the data clearly indicate that the growth potential of equities is indispensable for sustaining higher withdrawals in volatile market conditions.

A.2. 'Optimal' Portfolio including Foreign Exposure and Stochastic Correlation (Section 4.8)

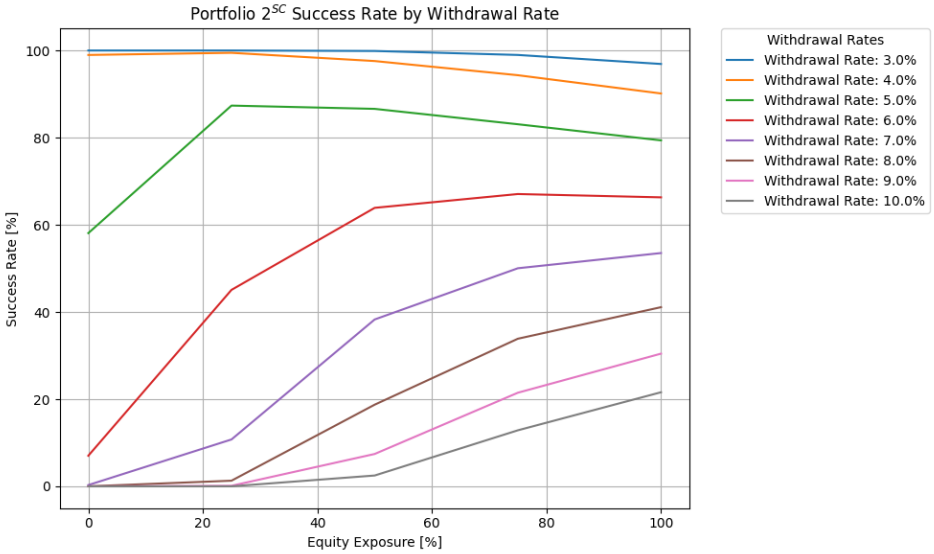

Figure A.8: Portfolio 2^{SC} Success Rates per Withdrawal Rate.

Across all three portfolio scenarios, the consistent theme is that bonds outweigh the optimal portfolio composition at lower withdrawal rates, providing stability and reducing volatility. However, at higher withdrawal rates such as 10%, equities become critical for achieving sufficient growth to sustain the portfolio over the long term. The need for 100% equities at higher withdrawal rates is evident in all three scenarios, underscoring the necessity of shifting toward growth-oriented assets as withdrawal demands increase.

Appendix B

Theory

B.1 Fokker-Planck Equation

Refer to Section 4.6.1 for context of the use of the Fokker-Planck equation. The Fokker-Planck equation describes the time evolution of the probability density function $p(x,t)$ of a stochastic process. It is particularly useful for processes governed by random diffusion and drift. Risken (1996) provides a comprehensive overview of the derivation and applications of this equation. The general form is:

$$\frac{\partial p(x,t)}{\partial t} = -\frac{\partial}{\partial x}[A(x,t)p(x,t)] + \frac{\partial^2}{\partial x^2}[B(x,t)p(x,t)],$$

where:

1. $A(x,t)$: Drift coefficient, describing deterministic motion.
2. $B(x,t)$: Diffusion coefficient, describing the magnitude of stochastic fluctuations.
3. $p(x,t)$: Probability density function.

B.2 Euler-Maruyama Scheme

Refer to Sections 4.5.2 and 4.3.2 for context of the use of the Euler-Maruyama Scheme. The Euler-Maruyama scheme is a numerical method for approximating the solution of stochastic differential equations (SDEs). It is an extension of the Euler method for ordinary differential equations (ODEs) to incorporate stochastic terms. The method and its convergence properties are well-explored in the literature (Kloeden and Platen, 1992; Higham, 2001; Gardiner, 2009).

SDE Formulation

Consider an SDE of the form:

$$dX_t = f(X_t, t)\,dt + g(X_t, t)\,dW_t,$$

where:

1. X_t is the stochastic process of interest,
2. $f(X_t, t)$ is the drift term (deterministic part),
3. $g(X_t, t)$ is the diffusion term (stochastic part), and
4. W_t is a Wiener process (standard Brownian motion).

The solution X_t is defined in an Itô sense, meaning the stochastic integral respects Itô's calculus (Kloeden and Platen, 1992):

$$X_t = X_0 + \int_0^t f(X_s, s)\,ds + \int_0^t g(X_s, s)\,dW_s.$$

Discretisation Scheme

The Euler-Maruyama scheme approximates the SDE by discretising the time interval $[0, T]$ into N subintervals, each of length $\Delta t = \frac{T}{N}$. Let $t_n = n\Delta t$ for

$n = 0, 1, \ldots, N$. The discrete approximation $X_n \approx X_{t_n}$ evolves according to:

$$X_{n+1} = X_n + f(X_n, t_n)\Delta t + g(X_n, t_n)\Delta W_n,$$

where:

$$\Delta W_n = W_{t_{n+1}} - W_{t_n},$$

is the increment of the Wiener process over $[t_n, t_{n+1}]$. Under Itô calculus, ΔW_n is a Gaussian random variable:

$$\Delta W_n \sim \mathcal{N}(0, \Delta t).$$

Derivation of the Scheme

From the SDE, over a small time increment $[t_n, t_{n+1}]$, the exact evolution is:

$$X_{t_{n+1}} = X_{t_n} + \int_{t_n}^{t_{n+1}} f(X_s, s)\, ds + \int_{t_n}^{t_{n+1}} g(X_s, s)\, dW_s.$$

The Euler-Maruyama scheme approximates this integral using:

$$\int_{t_n}^{t_{n+1}} f(X_s, s)\, ds \approx f(X_n, t_n)\Delta t,$$

and:

$$\int_{t_n}^{t_{n+1}} g(X_s, s)\, dW_s \approx g(X_n, t_n)\Delta W_n,$$

where the approximations are based on the assumption that $f(X_s, s)$ and $g(X_s, s)$ do not vary significantly over the small time interval (Higham, 2001).

Key Properties

1. First-Order Strong Convergence:

The scheme is accurate to $\mathcal{O}(\Delta t^{1/2})$ in the *strong sense*, meaning the mean-

square error $\mathbb{E}[|X_{t_n} - X_n|^2]$ scales as $\mathcal{O}(\Delta t)$.

2. First-Order Weak Convergence:

The scheme is accurate to $\mathcal{O}(\Delta t)$ in the *weak sense*, meaning the error in expectations of smooth functions $\phi(X_t)$ scales as $\mathcal{O}(\Delta t)$.

3. Stability:

Stability depends on the drift and diffusion terms. For stiff SDEs, more advanced schemes may be necessary (Gardiner, 2009).

Limitations

1. Accuracy degrades for large Δt, requiring small step sizes for reliable results.
2. It may produce unstable solutions for stiff problems unless Δt is extremely small.
3. Higher-order schemes, such as the Milstein method, may be preferable for problems requiring high accuracy.

B.3 Higham's Eigenvalue Raising Framework

Refer to subsection 4.6.2 for context of the use of the Higham's Eigenvalue Raising Framework. Higham's Eigenvalue Raising is a method designed to improve the numerical stability and spectral properties of a symmetric (or Hermitian) matrix by shifting its eigenvalues. This technique is particularly useful for ensuring positive definiteness or mitigating the effects of ill-conditioning in numerical computations. The fundamental concepts and applications of eigenvalue modification are thoroughly discussed in the works of Higham (1988); Golub and Van Loan (2013); Wright (2015).

Problem Setup

Let $A \in \mathbb{R}^{n\times n}$ (or $A \in \mathbb{C}^{n\times n}$) be a symmetric (or Hermitian) matrix with eigenvalues:

$$\lambda_1 \leq \lambda_2 \leq \cdots \leq \lambda_n.$$

The Eigenvalue Raising method modifies A by adding a scaled identity matrix, αI, where $\alpha > 0$. The modified matrix is:

$$\tilde{A} = A + \alpha I,$$

where I is the identity matrix of size $n \times n$ (Higham, 1988).

Effect on Eigenvalues

By the properties of matrix addition, the eigenvalues of $\tilde{A}$ are:

$$\tilde{\lambda}_i = \lambda_i + \alpha, \quad \forall i = 1, 2, \ldots, n.$$

This implies that each eigenvalue of A is shifted upwards by α (Golub and Van Loan, 2013).

Properties of the Modified Matrix

1. Positive Definiteness: If $\alpha > -\lambda_1$, then all eigenvalues of $\tilde{A}$ are positive:

   $$\tilde{\lambda}_i > 0 \quad \forall i.$$

   Hence, $\tilde{A}$ becomes positive definite.

2. Improved Conditioning: The condition number of A with respect to the eigenvalues is:

   $$\kappa(A) = \frac{\lambda_{\max}}{|\lambda_{\min}|},$$

   where $\lambda_{\min}$ is the smallest eigenvalue. For $\tilde{A}$, the condition number becomes:

   $$\kappa(\tilde{A}) = \frac{\lambda_{\max} + \alpha}{\lambda_{\min} + \alpha}.$$

By choosing $\alpha > 0$, the denominator increases, reducing $\kappa(\tilde{A})$, thus improving the conditioning (Wright, 2015).

3. Spectral Norm Bound: Using Weyl's theorem for eigenvalue perturbation, the change in each eigenvalue satisfies:

$$|\tilde{\lambda}_i - \lambda_i| \leq \|\alpha I\|_2 = \alpha.$$

Therefore, the eigenvalue shift is precisely controlled by α (Golub and Van Loan, 2013).

4. Preservation of Symmetry: Since the identity matrix I is symmetric (or Hermitian), the modified matrix $\tilde{A}$ retains the same structure as A.

5. Stability for Numerical Computations: Adding αI ensures that the smallest eigenvalue moves away from zero or becomes positive, reducing the risk of numerical instability in algorithms that rely on matrix inversion or eigenvalue decomposition (Higham, 1988).

Perturbation Analysis

The perturbation introduced by αI has a spectral norm:

$$\|\alpha I\|_2 = \alpha.$$

By Weyl's perturbation theorem, the eigenvalues of $\tilde{A}$ satisfy:

$$\lambda_i + \alpha = \tilde{\lambda}_i \quad \forall i.$$

The perturbation does not change the eigenvectors of A, ensuring that the eigenspace remains aligned (Wright, 2015).

Choosing α

The choice of α depends on the application and desired properties:

1. For ensuring positive definiteness, choose:

$$\alpha > -\lambda_1.$$

2. For improving conditioning, α should be sufficiently large to increase $\lambda_{\min}$, but not so large as to distort the spectrum.

B.4 Pochhammer Symbol

The *Pochhammer symbol*, denoted as $(x)_n$, represents the rising factorial of x. It is defined as follows:

$$(x)_n = \begin{cases} 1, & \text{if } n = 0, \\ x(x+1)(x+2)\cdots(x+n-1), & \text{if } n > 0. \end{cases}$$

Equivalently, it can be written as:

$$(x)_n = \prod_{k=0}^{n-1} (x+k), \quad n \geq 1.$$

The Pochhammer symbol plays a key role in combinatorics and special functions, as detailed by Abramowitz and Stegun (1964); Koepf (1998); Olver et al. (2010).

The Pochhammer symbol can also be expressed using the Gamma function:

$$(x)_n = \frac{\Gamma(x+n)}{\Gamma(x)},$$

where $\Gamma(x)$ is the Gamma function (Abramowitz and Stegun, 1964).

B.5 Derivation of solution in Equation 4.45

We start with the integral:

$$I = \int_{-1}^{1} (1+\bar{\rho})^{a+b}(1-\bar{\rho})^{a-b} d\bar{\rho}.$$

Step 1: Transformation of the Variable

Let $\bar{\rho} = 2x - 1$, so $d\bar{\rho} = 2dx$. Transforming the integral gives:

$$I = 2\int_{0}^{1} (2x)^{a+b}(2-2x)^{a-b} dx.$$

Simplifying:

$$I = 2^{2a+1}\int_{0}^{1} x^{a+b}(1-x)^{a-b} dx.$$

Step 2: Expressing the Integral as a Beta Function

The Beta function is defined as:

$$B(p,q) = \int_{0}^{1} x^{p-1}(1-x)^{q-1} dx.$$

Setting $p = a + b + 1$ and $q = a - b + 1$, the integral becomes:

$$I = 2^{2a+1} B(a+b+1, a-b+1).$$

The properties of the Beta and Gamma functions are thoroughly covered by Abramowitz and Stegun (1964); Andrews et al. (1999); Olver et al. (2010).

Step 3: Relating the Beta Function to the Gamma Function

Using the relationship between the Beta and Gamma functions:

$$B(p,q) = \frac{\Gamma(p)\Gamma(q)}{\Gamma(p+q)},$$

we substitute $p = a + b + 1$ and $q = a - b + 1$:

$$B(a+b+1, a-b+1) = \frac{\Gamma(a+b+1)\Gamma(a-b+1)}{\Gamma(2a+2)}.$$

Thus:

$$I = 2^{2a+1}\frac{\Gamma(a+b+1)\Gamma(a-b+1)}{\Gamma(2a+2)}.$$

Step 4: Expansion Using the Hypergeometric Function

The integral result can also be expressed in terms of the hypergeometric function F as:

$$M = \Gamma(1+a-b)\frac{F(1-a-b, 2+a-b, -1)}{\Gamma(2+a-b)} + \Gamma(1+a+b)\frac{F(-a-b, 2+a+b, -1)}{\Gamma(2+a+b)}.$$

Here, $F(a, b; c; z)$ is the hypergeometric function defined as:

$$F(a, b; c; z) = \sum_{n=0}^{\infty} \frac{(a)_n (b)_n}{(c)_n} \frac{z^n}{n!}.$$

Hypergeometric functions and their properties are extensively discussed by Bailey (1935); Slater (1966).

B.6 Derivation of the Stationary Density Function: Eqaution 4.37

In this proof, we derive the stationary density function $f(\tilde{\rho})$ by solving the Fokker-Planck equation governing the evolution of the transition density of a stochastic process. The solution takes the form of a hypergeometric function, which provides insight into the long-term behaviour of the system.

The method follows the standard approach of reducing the Fokker-Planck

equation to an elliptic form and applying an appropriate ansatz, as described by Cox et al. (1985) and Karatzas and Shreve (1991).

The Fokker-Planck Equation

The transition density function $f(t, \tilde{\rho})$ satisfies the following Fokker-Planck equation (Karatzas and Shreve, 1991):

$$\frac{\partial}{\partial t} f(t, \tilde{\rho}) + \frac{\partial}{\partial \tilde{\rho}} \left(a(t, \tilde{\rho}) f(t, \tilde{\rho}) \right) = \frac{1}{2} \frac{\partial^2}{\partial \tilde{\rho}^2} \left(b(t, \tilde{\rho})^2 f(t, \tilde{\rho}) \right), \tag{B.1}$$

where the drift and diffusion coefficients are given by:

$$a(t, \tilde{\rho}) = \kappa^*(\mu^* - \tilde{\rho})(1 - \tilde{\rho}^2), \quad b(t, \tilde{\rho}) = (1 - \tilde{\rho}^2)\sigma^*. \tag{B.2}$$

Stationary Solution

To obtain the stationary density $f(\tilde{\rho})$ as $t \to \infty$, the time derivative term vanishes:

$$f(\tilde{\rho}) = \lim_{t \to \infty} f(t, \tilde{\rho}). \tag{B.3}$$

Thus, the Fokker-Planck equation simplifies to:

$$\frac{\partial}{\partial \tilde{\rho}} \left((1 - \tilde{\rho}^2)\kappa^*(\mu^* - \tilde{\rho}) f(\tilde{\rho}) \right) = \frac{1}{2} \frac{\partial^2}{\partial \tilde{\rho}^2} \left((1 - \tilde{\rho}^2)\sigma^{*2} f(\tilde{\rho}) \right). \tag{B.4}$$

Simplification of the Stationary Equation

Expand the Left-Hand Side (LHS)

$$\frac{\partial}{\partial \tilde{\rho}} \left[(1 - \tilde{\rho}^2)\kappa^*(\mu^* - \tilde{\rho}) f(\tilde{\rho}) \right] = \kappa^* \frac{\partial}{\partial \tilde{\rho}} \left[(\mu^* - \tilde{\rho})(1 - \tilde{\rho}^2) f(\tilde{\rho}) \right]. \tag{B.5}$$

Applying the product rule:

$$= \kappa^* \left[(\mu^* - \tilde{\rho}) \frac{\partial}{\partial \tilde{\rho}} \left((1 - \tilde{\rho}^2) f(\tilde{\rho}) \right) - (1 - \tilde{\rho}^2) f(\tilde{\rho}) \right]. \tag{B.6}$$

Expand the Right-Hand Side (RHS)

$$\frac{1}{2}\frac{\partial^2}{\partial\tilde{\rho}^2}\left[(1-\tilde{\rho}^2)\sigma^{*2}f(\tilde{\rho})\right]. \tag{B.7}$$

First, compute the first derivative:

$$\frac{\partial}{\partial\tilde{\rho}}\left[(1-\tilde{\rho}^2)f(\tilde{\rho})\right] = -2\tilde{\rho}f(\tilde{\rho}) + (1-\tilde{\rho}^2)\frac{df(\tilde{\rho})}{d\tilde{\rho}}. \tag{B.8}$$

Second derivative:

$$\frac{\partial^2}{\partial\tilde{\rho}^2}\left[(1-\tilde{\rho}^2)f(\tilde{\rho})\right] = -2f(\tilde{\rho}) - 2\tilde{\rho}\frac{df(\tilde{\rho})}{d\tilde{\rho}} + (1-\tilde{\rho}^2)\frac{d^2f(\tilde{\rho})}{d\tilde{\rho}^2}. \tag{B.9}$$

Applying an Ansatz

Assume a solution of the form:

$$f(\tilde{\rho}) = C(1-\tilde{\rho}^2)^m. \tag{B.10}$$

Substituting this ansatz and solving for m yields a recurrence relation, leading to the form of a hypergeometric function.

Hypergeometric Solution:

To transform the equation into standard hypergeometric form, apply the variable change:

$$x = \frac{1+\tilde{\rho}}{2}. \tag{B.11}$$

This results in:

$$x(1-x)\frac{d^2F}{dx^2} + [c-(a+b+1)x]\frac{dF}{dx} - abF = 0, \tag{B.12}$$

where $F(a,b;c;x)$ is the hypergeometric function.

Final Solution

The general solution is:

$$f(\tilde{\rho}) = A(1+\tilde{\rho})^p + B(1-\tilde{\rho})^q F(a,b,c;x), \tag{B.13}$$

where:

$$a = 1, \quad b = \frac{2\sigma^2 - 2\kappa^*}{\sigma^2}, \quad c = \frac{(-\mu^* - 1)\kappa^* + 2\sigma^2}{\sigma^2}, \tag{B.14}$$

$$p = \frac{\kappa^* - 2\sigma^2}{\sigma^2}, \quad q = 0, \tag{B.15}$$

$$A = \frac{m}{2^{\frac{\kappa^*}{\sigma^2}}}, \quad B = \frac{n}{1 - \tilde{\rho}^2} \left(\frac{1}{2}\right)^{\frac{2\sigma^2 - \kappa^*}{\sigma^2}}. \tag{B.16}$$

Appendix C

Python Code Appendix

C.1 BootStrapping and Portfolio Modelling

We include our Bootstrapping and portfolio modelling code, as seen in Chapter 3 of this document. This code leverages bootstrap methodology to simulate the future performance of a retirement portfolio by resampling historical financial data. Bootstrap sampling is applied to create multiple random paths of asset returns (equity, bonds, cash, and inflation), preserving the inherent characteristics of the original data while introducing variability. By generating numerous bootstrap samples, the model constructs a diverse set of possible return scenarios, capturing a wide range of market conditions. This allows the simulation to account for uncertainty in future returns, providing a robust framework for evaluating portfolio sustainability over different investment horizons. The actuarial present value (APV) functions further introduce mortality rates and risk charges, reflecting the real-life complexity of retirement planning by modelling the cost of future liabilities.

Once bootstrap samples are generated, the code simulates portfolio growth and depletion across multiple scenarios. For each simulation, the portfolio is rebalanced over time, blending equity and bond returns while deducting regular withdrawals to mimic retirement income needs. The portfolio's ability to sustain withdrawals is assessed by tracking its value over time and recording instances of depletion. Key metrics, such as the success rate

(probability of portfolio survival) and the average time to depletion, are computed for different combinations of withdrawal rates and asset allocations. This comprehensive simulation process offers valuable insights into the likelihood of portfolio longevity, enabling better-informed decisions for retirees seeking to balance income needs with the risk of outliving their savings.

```
# -*- coding: utf-8 -*-
"""
Created on Mon Jan 29 11:13:50 2024

@author: dries
"""
import cupy as cp
import scipy.stats as ss
from numpy import log as ln
import numpy as np
from matplotlib import pyplot as plt
import pandas as pd
import matplotlib.pyplot as plt
import seaborn as sns
from scipy.stats import ks_2samp
import time

# Define global
init_value = 1000000
no_sims =10000              # number of simulations
m = 12                      # Number of grid points for 1 year
upfront=0
int_rate = 0.1125
Risk_charge=0.1

# Life portfolio
dfm = pd.read_excel(r'C:\Users\dries\OneDrive\Retirement
    research\SAJS Publication\Hybrid retirement strategy\
    SA_tables.xlsx', sheet_name='Male')
dff = pd.read_excel(r'C:\Users\dries\OneDrive\Retirement
    research\SAJS Publication\Hybrid retirement strategy\
    SA_tables.xlsx', sheet_name='Female')

df =pd.read_excel(r'C:\Users\dries\OneDrive\Retirement research
    \SAJS Publication\Hybrid retirement strategy\
    SA_Data_from_Firer_updated.xlsx', sheet_name='
    SeasonalFillIn')
```

```
31
32
33 def bootstrap(data, num_samples, num_returns):
34     # Ensure data is a DataFrame
35     if not isinstance(data, pd.DataFrame):
36         raise ValueError("Data must be a pandas DataFrame.")
37
38     # Number of rows in the data
39     n_rows = data.shape[0]
40
41     # Initialize an empty list to store the bootstrap samples
42     bootstrap_samples = []
43
44     for _ in range(num_samples):
45         # Generate a list of row indices for the bootstrap
               sample
46         sample_indices = np.random.choice(range(n_rows), size=
               num_returns, replace=True)
47         # Retrieve the rows corresponding to the indices
48         bootstrap_sample = data.iloc[sample_indices, :]
49         # Append the bootstrap sample DataFrame to the list
50         bootstrap_samples.append(bootstrap_sample)
51
52     # Combine all bootstrap samples into a single DataFrame
53     combined_samples = pd.concat(bootstrap_samples, keys=range(
           num_samples))
54
55     return combined_samples
56
57
58
59 def APv(pv,qx,int1,Risk_charge):
60     Amount_pa_bought=(pv/((1-(qx/(qx+int1)))/(int1/(1+int1))
           *(1+Risk_charge)))/init_value
61     return Amount_pa_bought
62
63 def APv_def(qx,int1,Risk_charge,investment_amt):
64     APV= (1-qx/(qx+int1))/(int1/(1+int1))*(1+Risk_charge)*
           investment_amt
65     return APV
66
67 success_rate1 = {}
68 fudgit1 = {}
69 start = time.time()
```

```
70
71
72  for T in range(15,35,5):
73      # Create time vector for simulations
74      t = np.linspace(0, T, num = int(np.round(T/(1/m))) ,
            endpoint = True)
75      N = len(t)      # length of time vector
76      deltat = t[1] - t[0]             #Time steps
77
78      # Parameters for bootstrapping
79      num_bootstrap_samples = no_sims
80      num_returns = N
81      bsm = bootstrap(df, num_bootstrap_samples, num_returns)
82      equity_df = bsm[['Equity']]
83      bonds_df = bsm[['Bonds']]
84      cash_df = bsm[['Cash']]
85      infl_df = bsm[['Inflation']]
86      # Reshape the equity return data
87      num_columns = N
88      equity_return = equity_df.values.reshape(-1, num_columns)
89      bonds_return = bonds_df.values.reshape(-1, num_columns)
90      cash_return = cash_df.values.reshape(-1, num_columns)
91      infl_return = infl_df.values.reshape(-1, num_columns)
92
93      ############################################################
94      # Portfolio Modelling
95      ############################################################
96      success_rate = np.zeros([6,11])
97      fudgit = np.zeros([6,11])
98      default_perc = np.zeros([6,11])
99      Time_to_def_life= np.zeros([6,11])
100
101     success_rate1[T] = np.zeros([6,11])
102     fudgit1[T] = np.zeros([6,11])
103     for eq in range(0,5,1):
104         for withd in range(3,13,1):
105             left_over=init_value*(1-upfront)
106             w_e = eq/4
107             w_b = 1-w_e
108
109             cum_Amount_pa_bought= np.zeros([no_sims,N])
110
111             Amount_pa_bought = np.zeros([no_sims,N])
112             Amount_pa_bought[:] = APv(upfront*init_value,dfm.qx
```

```
        [20],int_rate,Risk_charge)

    withdraw_rate_annual = (withd)/100-Amount_pa_bought
    withdraw_period = 12 # number of days between
        withdrawals
    withdraw_frequency = int(12/withdraw_period)
    withdraw_rate=np.zeros([no_sims,N])
    withdraw_rate[:]=  withdraw_rate_annual/
        withdraw_frequency

    Amount_pa=left_over*withdraw_rate_annual
    print('Total_withd=',  withdraw_rate_annual+
        Amount_pa_bought)

    port_value = np.zeros([no_sims,N])
    port_value[:,0] = left_over   * (1-withdraw_rate
        [:,0])

    PtT = np.zeros([N,N])

    # Coupon Modelling
    bond_frequency = withdraw_period/2
    bond_period = m/bond_frequency

    profit = np.zeros([no_sims,N])
    def_count=0
    print(T)

    for j in range(1,N):
        port_value[:,j] = w_e*port_value[:,j-1]*(1+
            equity_return[:,j])*(1-infl_return[:,j]) +
            w_b*port_value[:,j-1]*(1+bonds_return[:,j])
            *(1-infl_return[:,j])

        if  np.mod(j,withdraw_period) == 0:
            port_value[:,j] = port_value[:,j] -
                withdraw_rate[:,j] * init_value
        idzz = np.where(port_value[:,j] <= 0)[0]
        port_value[idzz,j:] = 0

    #Fudgit and portfolio success
    idx = np.zeros(no_sims)
    idy = np.zeros(no_sims)
    for i in range(no_sims):
```

```
148                 if np.where(port_value[i,:] == 0)[0].size==0:
149                     idx[i] = 0
150                     idy[i] = N
151                 else:
152                     idx[i] = np.where(port_value[i,:] == 0)
                            [0][0]
153                     idy[i] = np.where(port_value[i,:] == 0)
                            [0][0]
154
155             kk=int(eq)
156             jj=int(withd-3)
157             print(kk)
158             print(jj)
159             success_rate1[T][kk,jj] = 1-np.count_nonzero(idx)/
                    no_sims
160             fudgit1[T][kk,jj] = np.mean(idy)/m
161
162 end = time.time()
163 print(round(end-start,2))
```

Listing C.1: Data Processing Script

C.2 Efficient Method of Moments

We include our calibration code for EMM as detailed in Chapter 4 of this document. This code implements the Efficient Method of Moments (EMM) to calibrate a Heston stochastic volatility model, a widely-used approach in financial modelling for capturing volatility dynamics in asset prices. The script begins by importing historical price data from an Excel sheet and calculating log returns. The first stage of the process involves fitting an ARIMA (0,0,1) model to remove the mean from the return series, leaving behind residuals that are used to fit a Generalised Autoregressive Conditional Heteroskedasticity (GARCH) model. The GARCH model estimates time-varying volatility, capturing the clustering effect often observed in financial returns. These residuals and conditional volatility serve as inputs for calibrating the Heston model parameters by maximising the likelihood function through numerical optimisation techniques, such as the Nelder-Mead method or basin-hopping to avoid local minima.

The script proceeds to simulate asset paths using the calibrated Heston model by applying Monte Carlo methods. Simulations generate multiple paths of stock prices and variance processes, incorporating stochastic volatility to reflect realistic market behaviour. The variance process evolves through a mean-reverting square root diffusion, while asset prices follow a stochastic differential equation influenced by correlated Brownian motions. The calibration step minimises the discrepancy between simulated and historical return distributions by adjusting key parameters of the Heston model. Visualization tools, including KDE plots and percentile bands, illustrate the distribution of simulated returns compared to historical data. The final output assesses the accuracy of the calibration by comparing statistical moments (mean, variance, skewness, and kurtosis) of the simulated returns with actual market data, ensuring that the Heston model accurately reflects the empirical properties of asset returns.

```
# -*- coding: utf-8 -*-
"""
Created on Fri Apr 26 13:31:10 2024

@author: dries
"""

import numpy as np
import pandas as pd
from matplotlib import pyplot as plt
from scipy.stats import skew, kurtosis
import statsmodels.api as sm
from arch import arch_model
from scipy import integrate
from scipy.stats import norm
from scipy.optimize import minimize, basinhopping
import seaborn as sns
import sys

import warnings
warnings.filterwarnings("ignore")

directory = r'C:\Users\dries\OneDrive\Retirement research\SAAJ - DO NOT TOUCH\Data'
# directory = r'C:\Users\dries\OneDrive\Retirement research\SAAJ - Vasili'

```

```
filename = '\\Dataset.xlsx'
# filename = '\\data.xlsx'

# prices = pd.read_excel(directory + filename)['S&P500(Adj Close)'].dropna().values
prices = pd.read_excel(directory + filename, sheet_name = 'JSE')['Price'].values
returns_orig = np.log(prices[1:]/prices[0:-1])
returns = np.log(prices[1:]/prices[0:-1])
# returns = pd.read_excel(directory + filename)['Return'].dropna().values
# returns_orig = pd.read_excel(directory + filename)['Return'].dropna().values
pltflg = 0
#%% Statistics on data
data_stats = {}
data_stats['mean'] = np.mean(returns)
data_stats['std dev'] = np.std(returns)
data_stats['skew'] = skew(returns)
data_stats['kurtosis'] = kurtosis(returns, fisher = False)
data_stats['min return'] = min(returns)
data_stats['max return'] = max(returns)

# Plot daily returns from data
plt.figure()
plt.plot(returns)
plt.title('Daily returns from data')
plt.ylabel('Return [%]')

#%% Fit ARIMA (0,0,1) to remove mean from data
mod = sm.tsa.ARIMA(returns, order=(0, 0, 1))
# residuals of fitted ARIMA (0,0,1)
ARIMA_results = mod.fit()
residuals = ARIMA_results.resid
# Make prediction from fitted ARIMA (0,0,1)
ARIMA_prediction = ARIMA_results.predict()
# Parameters of ARIMA model
ARIMA_params = ARIMA_results.params

# Plot ARIMA to see consitency with historical data?
plt.figure()
plt.plot(residuals)
plt.title('Residuals of ARIMA (0,0,1)')
plt.ylabel('Residuals')
```

```
66
67  # Statistics on fitted ARIMA
68  ARIMA_stats = {}
69  ARIMA_stats['mean'] = np.mean(residuals)
70  ARIMA_stats['std dev'] = np.std(residuals)
71  ARIMA_stats['skew'] = skew(residuals)
72  ARIMA_stats['kurtosis'] = kurtosis(residuals, fisher = False)
73  ARIMA_stats['min return'] = min(residuals)
74  ARIMA_stats['max return'] = max(residuals)
75
76  #%% Fit GARCH model with zero mean since removed mean from data
77  garch_mSPX = arch_model(np.multiply(residuals,100),mean='zero')
78  garch_fit = garch_mSPX.fit()
79
80  # Plot GARCH fit
81  fig=garch_fit.plot()
82
83  # Residuals of GARCH model
84  residual_garch = garch_fit.std_resid
85  # Volatility of GARCH scaled down since returns were scaled up
86  vol_garch = garch_fit.conditional_volatility * 0.01
87
88  # Convert back to Normal RV from Standard normal RV
89  returns = residual_garch * vol_garch + ARIMA_params[0]
90
91  # Plot returns of transformed data
92  plt.figure()
93  plt.plot(returns)
94  plt.ylabel('Returns [%]')
95  plt.title('Transformed Data: Returns')
96
97  # Statistics of fitted GARCH
98  GARCH_stats = {}
99  GARCH_stats['mean'] = np.mean(returns)
100 GARCH_stats['std dev'] = np.std(returns)
101 GARCH_stats['skew'] = skew(returns)
102 GARCH_stats['kurtosis'] = kurtosis(returns, fisher = False)
103 GARCH_stats['min return'] = min(returns)
104 GARCH_stats['max return'] = max(returns)
105
106 #%% Define Loglikelihood function
107 def neg_loglike(param_vec, returns):
108
109     v=0.01
```

```
110     # Fit GARCH model
111     garch_mSPX = arch_model(np.multiply(returns,100),mean='zero
            ')
112     # Fix parameters of GARCH model?
113     fixed_res=garch_mSPX.fix([param_vec[0],param_vec[1],
            param_vec[2]])
114     # Residuals of GARCH model
115     res=fixed_res.std_resid
116     # Scaled conditional volatility of GARCH model
117     cond_vol=np.multiply(fixed_res.conditional_volatility,0.01)
118
119     # Define density function as in Gallant
120     density_func_int = lambda u: ((1+param_vec[3]*u+param_vec
            [4]*(u**2-1)+param_vec[5]*(u**3-3*u)+param_vec[6]*(u
            **4-6*u**2+3)+param_vec[7]*(u**5-10*u**3+15*u)+
            param_vec[8]*(u**6-15*u**4+45*u**2-15))**2)*norm.pdf(u,
            loc=0,scale=1)
121     # Integrate density function from -infty to infty
122     integr=integrate.quad(density_func_int,-np.infty,np.infty)
123
124     # Log-likelihood function
125     density_func = lambda u: np.log((v+(1-v)*(((1+param_vec[3]*
            u+param_vec[4]*(u**2-1)+param_vec[5]*(u**3-3*u)+
            param_vec[6]*(u**4-6*u**2+3)+param_vec[7]*(u**5-10*u
            **3+15*u)+param_vec[8]*(u**6-15*u**4+45*u**2-15))**2)/
            integr[0]))*norm.pdf(res,loc=0,scale=1)/cond_vol)
126     ll= density_func(res)
127     # Mean of log-likelihood function
128     ll2=-np.mean(ll)
129
130     return ll2
131
132 # init_params =
        [0.0127,0.08,0.9555,-0.0064,-0.2426,-0.0220,0.1227,-0.0036,-0.0559]

133 init_params = [garch_fit.params['omega'],garch_fit.params['
        alpha[1]'],garch_fit.params['beta[1]'
        ],-0.0064,-0.2426,-0.0220,0.1227,-0.0036,-0.0559]
134 init_log_likelihood = neg_loglike(init_params, returns)
135 print('Initial Log Likelihood = ', init_log_likelihood)
136
137 bnds=[(0,None),(0,1),(0,1),(None,None),(None,None),(None,None)
        ,(None,None),(None,None),(None,None)]
138 minimized_log_likelihood = minimize(neg_loglike, x0 =
```

```
    init_params, args = (returns))
min_value = minimized_log_likelihood.fun
# minimized_log_likelihood = minimize(neg_loglike,  x0 =
    init_params, args = (returns, ), method = 'Powell',\
                  # bounds=bnds, options={'disp': False, 'xtol
                      ': 1e-12, 'ftol': 1e-12},tol=1e-12)
# min_value = minimized_log_likelihood.fun


# minimized_log_likelihood = basinhopping(neg_loglike,
    init_params, minimizer_kwargs = {'args': (returns,)})
# min_value = minimized_log_likelihood.fun
print('Minimized Log Likelihood = ', min_value)

#%% Plot conditional volatility vs GARCH conditional volatility

# Minimised parameters
exo=minimized_log_likelihood.x
v=0.01
# Fit GARCH model
garch_mSPX = arch_model(np.multiply(returns,100),mean='zero')
# Fix GARCH parameters
final_res=garch_mSPX.fix([exo[0],exo[1],exo[2]])
# Residuals of GARCH model
res=final_res.std_resid
# Conditional volatility of GARCH model
cond_vol=final_res.conditional_volatility*0.01

plt.figure()

plt.plot(cond_vol, label = 'Conditional Vol')
plt.plot(np.multiply(garch_fit.conditional_volatility,0.01),
    label = 'GARCH Conditional Vol')
plt.ylabel('Volatility')
plt.legend()
plt.title('GARCH conditional volatility')

#%% Derivatives - differ slightly compares to Alexis probably
    due to optimization technique
def get_deriv(returns, idx, exo, pltflg):
    dx = 1e-3 #(sys.float_info.epsilon)**(1/3)
    exo1 = np.ones(len(exo)) * exo
    exo2 = np.ones(len(exo)) * exo
    exo1[idx] = exo1[idx] - dx
```

```
177     exo2[idx] = exo2[idx] + dx
178     v=0.01
179
180     garch_mSPX = arch_model(np.multiply(returns,100),mean='zero
            ')
181     final_res=garch_mSPX.fix([exo1[0],exo1[1],exo1[2]])
182     final_res2=garch_mSPX.fix([exo2[0],exo2[1],exo2[2]])
183     res=final_res.std_resid
184     res2=final_res2.std_resid
185     cond_vol=final_res.conditional_volatility*0.01
186     cond_vol2=final_res2.conditional_volatility*0.01
187     def density_func_int(u, exo):
188         test = ((1+exo[3]*u+exo[4]*(u**2-1)+exo[5]*(u**3-3*u)+
                exo[6]*(u**4-6*u**2+3)+exo[7]*(u**5-10*u**3+15*u)+
                exo[8]*(u**6-15*u**4+45*u**2-15))**2)*norm.pdf(u)
189         return test
190
191     integr1=integrate.quad(density_func_int,-np.infty,np.infty,
             args= (exo1,))
192     integr2=integrate.quad(density_func_int,-np.infty,np.infty,
             args= (exo2,))
193
194     def density_func(exo, res, cond_vol, integr, v):
195         test = np.log((v+(1-v)*((1+exo[3]*res+exo[4]*(res**2-1)
                +exo[5]*(res**3-3*res)+exo[6]*(res**4-6*res**2+3)+
                exo[7]*(res**5-10*res**3+15*res)+exo[8]*(res**6-15*
                res**4+45*res**2-15))**2/integr[0]))*norm.pdf(res)/
                cond_vol)
196         return test
197
198     ll = density_func(exo1, res, cond_vol, integr1, v)
199     ll2 = density_func(exo2, res2, cond_vol2, integr2, v)
200
201     dfx0=(ll2-ll)/(2*dx)
202
203     if pltflg == 1:
204         plt.figure()
205         plt.plot(dfx0)
206         plt.title('Derivative x' + str(idx))
207
208     return dfx0
209
210 derivatives = {}
211 mean_derivatives = {}
```

```
212
213 for i in range(len(exo)):
214     derivatives['x'+str(i)] = get_deriv(returns, i, exo, pltflg
        )
215     mean_derivatives['x'+str(i)] = np.mean(get_deriv(returns, i
        , exo, pltflg))
216
217 #%% Compute outer product
218 dfmatrix = np.zeros([len(derivatives['x0']),9])
219 for i in range(len(exo)):
220     dfmatrix[:,i] = derivatives['x'+str(i)]
221
222 # convert 2-D array to 3-D
223 df_matrix3d = dfmatrix[:,:,np.newaxis]
224 # compute outer product
225 outer_prod = df_matrix3d[:,:,None]*df_matrix3d[:,None]
226 # reshape into 2-D array
227 outer_prod = outer_prod.reshape(-1, int(outer_prod.shape[-2] *
    outer_prod.shape[-3]))
228 # Compute mean across rows, results in 1-D array
229 mean_outer_prod = np.mean(outer_prod, axis = 0)
230 # Reshape array to be 2-D variance covariance matrix
231 VCV = mean_outer_prod.reshape((9,9))
232 # Compute inverse of matrix
233 VCV_inv = np.linalg.pinv(VCV)
234
235 # %% Define Monte Carlo Simulation
236 def MC(params, returns, VCV_inv, exo):
237
238     numsims = 10
239     timelength = int(10*len(returns))
240     dt= 1/2520
241
242     np.random.seed(0)
243
244     W1 = np.random.normal(loc = 0, scale = 1, size = [int(
        timelength/2),numsims])
245     Z1 = np.vstack([W1,-W1])
246     W1 = 0
247     W2 = np.random.normal(loc = 0, scale = 1, size = [int(
        timelength/2),numsims])
248     Z2 = np.vstack([W2,-W2])
249     W2 = 0
250     Z3 = params[4]*Z1 + np.sqrt(1-params[4]**2)*Z2
```

```
251
252     Z2 = 0
253     v = np.zeros([timelength,numsims])
254     s = np.zeros([timelength,numsims])
255     v[0,:] = 0.01
256     s[0,:] = np.log(100)
257
258     for j in range(1,timelength):
259         s[j,:] = s[j-1,:] + (params[0]-0.5*np.maximum(v[j
                -1,:],0)) * dt + np.sqrt(np.maximum(v[j-1,:],0)*dt)
                 * Z1[j,:]
260         v[j,:] = v[j-1,:] + (params[1]-params[2]*np.maximum(v[j
                -1,:],0)) * dt + params[3]*np.sqrt(np.maximum(v[j
                -1,:],0)*dt) * Z3[j,:]
261
262     Z1 = 0
263     Z3 = 0
264     v = 0
265
266     s = s[int(0.1*timelength):,:]
267     log_ret = (s[1:,:]-s[0:-1,:])
268
269     # Remove first few simulations to remove bias from initial
        parameters
270     # log_ret2 = log_ret[int(0.1*timelength):,:].flatten()
271     log_ret3 = np.zeros([int(len(log_ret)/10)-1,numsims])
272     for i in range(1,int(len(log_ret)/10)-1):
273         log_ret3[i,:] = np.sum(log_ret[(i-1)*10:i*10,:], axis =
                0)
274
275     log_ret3 = log_ret3[1:,:]
276     log_ret3 = log_ret3.flatten()
277
278     derivatives = np.zeros([len(log_ret3), len(exo)])
279     mean_derivatives = np.zeros([len(exo),1])
280
281     for i in range(len(exo)):
282         derivatives[:,i] = get_deriv(log_ret3, i, exo, pltflg)
283         mean_derivatives[i] = np.mean(derivatives[:,i])
284
285     ret=np.matmul(np.transpose(mean_derivatives),VCV_inv)
286     ret2=np.matmul(ret,mean_derivatives)[0][0]
287     print(ret2)
288     return ret2
```

```
289
290 sim_params = [ 0.0756,  0.0438,  3.2508,  0.1850, -0.5877]
291 MC(sim_params, returns, VCV_inv, exo )
292
293 #%% Perform minimization to get optimal parameters
294 # param_start =   [ 0.2,  0.1137,  4.9395,  0.3747, -0.8801]
295 param_start = [ 0.0856,  0.1438,  5.2508,  0.3, -0.8877]
296 bnds=[[0,0.5],[0,1],[0,10],[0,1],[-1,1]]
297 # bpc = minimize(MC, param_start, args = (returns, VCV_inv, exo
        , ), method = 'Powell',\
298                  # bounds=bnds, options={'disp': False, 'xtol
                       ': 1e-12, 'ftol': 1e-12},tol=1e-12)
299 bpc = minimize(MC, param_start, args = (returns, VCV_inv, exo,
        ),bounds=bnds)#, method = 'L-BFGS-B', options={'disp':
        False, 'xtol': 1e-12, 'ftol': 1e-12},tol=1e-12)
300
301 params = bpc.x
302 # params = param_start
303
304
305 #%% Simulate daily
306 # params = [0.11431662511904605584, 0.16079327838335100154,
        5.2534239602091759025, 0.27593034497201140987,
        -0.87111041721236370794]
307
308 numsims = 10
309 timelength = int(10*len(returns))
310 dt= 1/2520
311
312 s = 0
313 v = 0
314
315 np.random.seed(0)
316
317 W1 = np.random.normal(loc = 0, scale = 1, size = [int(
        timelength/2),numsims])
318 Z1 = np.vstack([W1,-W1])
319 W1 = 0
320 W2 = np.random.normal(loc = 0, scale = 1, size = [int(
        timelength/2),numsims])
321 Z2 = np.vstack([W2,-W2])
322 W2 = 0
323 Z3 = params[4]*Z1 + np.sqrt(1-params[4]**2)*Z2
324
```

```
Z2 = 0

v = np.zeros([timelength,numsims])
s = np.zeros([timelength,numsims])
v[0,:] = 0.01
s[0,:] = np.log(100)

for j in range(1,timelength):
    s[j,:] = s[j-1,:] + (params[0]-0.5*np.maximum(v[j-1,:],0))
        * dt + np.sqrt(np.maximum(v[j-1,:],0)*dt) * Z1[j,:]
    v[j,:] = v[j-1,:] + (params[1]-params[2]*np.maximum(v[j
        -1,:],0)) * dt + params[3]*np.sqrt(np.maximum(v[j
        -1,:],0)*dt) * Z3[j,:]
Z1 = 0
Z3 = 0

v = 0

s = s[int(0.1*timelength):,:]
log_ret = (s[1:,:]-s[0:-1,:])

# Remove first few simulations to remove bias from initial
    parameters
# log_ret2 = log_ret[int(0.1*timelength):,:].flatten()
log_ret3 = np.zeros([int(len(log_ret)/10)-1,numsims])
for i in range(1,int(len(log_ret)/10)-1):
    log_ret3[i,:] = np.sum(log_ret[(i-1)*10:i*10,:], axis = 0)

log_ret3 = log_ret3[1:,:]
log_ret_sim = log_ret3.flatten()

#%% Statistics of simulated returns
simulated_stats = {}
simulated_stats['mean'] = np.mean(log_ret_sim)
simulated_stats['std dev'] = np.std(log_ret_sim)
simulated_stats['skew'] = skew(log_ret_sim.flatten())
simulated_stats['kurtosis'] = kurtosis(log_ret_sim.flatten(),
    fisher = False)
simulated_stats['min return'] = np.min(log_ret_sim)
simulated_stats['max return'] = np.max(log_ret_sim)

#%% Plot density of returns
hist_returns = returns_orig

```

```
364 plt.figure()
365 sns.kdeplot(hist_returns, color = 'red')
366 sns.kdeplot(log_ret_sim.flatten(), color = 'blue')
367 plt.legend(['JSE', 'Simulated'])
368
369 plt.xlabel('Daily Log Returns')
370 plt.title('Heston EMM Fit')
371
372 #%% Simulate daily
373
374 numsims = 1000
375 timelength = int(len(returns))
376 dt= 1/252
377
378 s = 0
379 v = 0
380
381 np.random.seed(0)
382
383 W1 = np.random.normal(loc = 0, scale = 1, size = [int(
        timelength/2),numsims])
384 Z1 = np.vstack([W1,-W1])
385 W1 = 0
386 W2 = np.random.normal(loc = 0, scale = 1, size = [int(
        timelength/2),numsims])
387 Z2 = np.vstack([W2,-W2])
388 W2 = 0
389 Z3 = params[4]*Z1 + np.sqrt(1-params[4]**2)*Z2
390
391 Z2 = 0
392
393 v = np.zeros([timelength,numsims])
394 s = np.zeros([timelength,numsims])
395 v[0,:] = np.std(returns_orig*100)**2*0.01
396 s[0,:] = prices[0]
397
398 for j in range(1,timelength):
399     v[j,:] = v[j-1,:] + (params[1]-params[2]*np.maximum(v[j
            -1,:],0)) * dt + params[3]*np.sqrt(np.maximum(v[j
            -1,:],0)*dt) * Z3[j,:]
400     s[j,:] = s[j-1,:] * np.exp((params[0] - 0.5*np.maximum(v[j
            -1,:],0))*dt + np.sqrt(np.maximum(v[j-1,:],0)*dt) * Z1[
            j,:])
401     # s[j,:] = s[j-1,:] + (params[0]-0.5*np.maximum(v[j-1,:],0)
```

```
        ) * dt + np.sqrt(np.maximum(v[j-1,:],0)*dt) * Z1[j]

Z1 = 0
Z3 = 0

p_5 = np.percentile(v,5, axis = 1)
p_50 = np.percentile(v,50, axis = 1)
p_95 = np.percentile(v, 95, axis = 1)

plt.figure()
plt.plot(p_5)
plt.plot(p_50)
plt.plot(p_95)
plt.title('Variance')

# v = 0

# s = s[int(0.1*timelength):,:]
# s = s[100:,:]

p_5 = np.percentile(s,5, axis = 1)
p_50 = np.percentile(s,50, axis = 1)
p_95 = np.percentile(s, 95, axis = 1)

plt.figure()
plt.plot(prices)
plt.plot(p_5)
plt.plot(p_50)
plt.plot(p_95)
plt.title('Stock Price')

log_ret = np.log(s[1:,:]/s[0:-1,:])

log_ret_sim = log_ret.flatten()

#%% Statistics of simulated returns
simulated_stats = {}
simulated_stats['mean'] = np.mean(log_ret_sim)
simulated_stats['std dev'] = np.std(log_ret_sim)
simulated_stats['skew'] = skew(log_ret_sim.flatten())
simulated_stats['kurtosis'] = kurtosis(log_ret_sim.flatten(),
    fisher = False)
simulated_stats['min return'] = np.min(log_ret_sim)
simulated_stats['max return'] = np.max(log_ret_sim)
```

```
444
445 #%% Plot density of returns
446 hist_returns = returns_orig
447
448 plt.figure()
449 sns.kdeplot(hist_returns, color = 'red')
450 sns.kdeplot(log_ret_sim.flatten(), color = 'blue')
451 plt.legend(['JSE', 'Simulated'])
452
453 plt.xlabel('Daily Log Returns')
454 plt.title('Heston EMM Fit')
```

Listing C.2: Data Processing Script

C.3 US CPI Modelling

We include our calibration code for US CPI as detailed in Chapter 4 of this document. This code simulates inflation dynamics based on historical US Consumer Price Index (CPI) data using a combination of Brownian Bridge interpolation and Geometric Brownian Motion. The script first extracts monthly log returns from the CPI series and applies a Brownian Bridge to smooth the inflation path, generating finer daily estimates from monthly data. The Brownian Bridge function constructs paths that interpolate between known data ensuring the simulated values align at the beginning and end of each period. This approach maintains realistic short-term variations and preserves the long-term trend of inflation data. Visualisations display the interpolated inflation paths and compare them against the original CPI data, highlighting the smoothing effect of the Brownian Bridge process.

Following the interpolation, the code performs Monte Carlo simulations to project future CPI paths based on drift and volatility estimates derived from historical inflation rates. The gBm model, a common choice for simulating asset prices and economic indicators, introduces stochasticity to the inflation projections. Simulated CPI paths are calculated for 10 000 iterations, generating percentiles (5th, 50th, and 95th) to capture the range of possible future inflation trajectories. These results are plotted against the historical CPI, providing insight into potential inflation scenarios. The script concludes by

comparing the distribution of simulated inflation returns to historical returns through kernel density estimation (KDE), demonstrating the robustness of the model in capturing inflation dynamics. This analysis is valuable for risk management, pension planning, and economic forecasting, as it offers probabilistic projections of inflation, essential for long-term financial modelling.

```
# -*- coding: utf-8 -*-
"""
Created on Tue Apr  2 19:00:00 2024

@author: dries
"""

import pandas as pd
import numpy as np
import matplotlib.pyplot as plt
import seaborn as sns

file_path_inf = r'C:\Users\dries\OneDrive\Retirement research\SAAJ - DO NOT TOUCH\Data\Dataset.xlsx'
inflation_data = pd.read_excel(file_path_inf, sheet_name = 'US CPI')
CPI = inflation_data['Price'].values
inf_rate = np.log(CPI[1:]/CPI[0:-1])
np.random.seed(0)

def brownian_bridge(steps, start, end, sims, start_time, end_time):
    dt = (end_time/30)
    W = np.zeros((sims, steps+1))
    s2=end_time
    s1=start_time
    x1=start
    x2=end
    W[:,0] = x1
    for s in range(1, steps+1):
        t = s * dt
        mean = ((s2-t)*x1+(t-s1)*x2)/(s2-s1)
        var = (s2-t)*(t-s1)/(s2-s1)
        W[:, s] = np.random.randn(sims) * np.sqrt(var)*np.sqrt(dt)+mean
        s1 = t
        x1 = W[:, s]
```

```
    W[:,-1] = end
    return W

test = np.zeros(int(len(inf_rate)*30))
k = 0
i = 0
while i < len(test)+1:
    if np.mod(i,30) == 0:
        test[i] = inf_rate[k]
        k += 1
        i += 1
        if k == len(inf_rate):
            break
    else:
        test[i:i+30] = np.mean(brownian_bridge(30, inf_rate[k
            -1], inf_rate[k], 1, 0, 1/30), axis = 0)[1:]
        i = i+29

abcd = brownian_bridge(30, inf_rate[k-2], inf_rate[k-1], 100,
    0, 1/30)
plt.figure()
for i in range(len(abcd)):
    plt.plot(abcd[i,:])
plt.plot(np.mean(abcd, axis = 0), color = 'black')

x = np.array(range(0, len(test)))
x2 = np.array(range(0,len(test),30))

plt.figure()
plt.plot(x,test, color = 'black', linewidth = 0.5)
plt.plot(x2, inf_rate, marker = '.', linestyle = 'none', color
    = 'red')

plt.figure()
plt.plot(x[:91],test[:91], color = 'black', linewidth = 0.5)
plt.scatter(x2[:4],inf_rate[:4], color = 'red')

# inf_rate = test



N = 12 #len(CPI)-1
M = 10000
dt = 1/N
```

```
drift = np.mean(inf_rate)
vol = np.std(inf_rate)

sig = vol/np.sqrt(dt)
mu = drift/dt + 0.5*sig**2

S = np.zeros([N,M])
S[0,:] = CPI[0]

Z = np.random.normal(0, 1, size = [N,M])

for i in range(1, N):
    S[i,:] = S[i-1,:] * np.exp((mu-0.5*sig**2)*dt + np.sqrt(dt)
        *sig*Z[i-1,:])

S_5 = np.percentile(S, 5, axis = 1)
S_50 = np.percentile(S, 50, axis = 1)
S_95 = np.percentile(S, 95, axis = 1)
plt.figure()
plt.plot(CPI, label = 'historical')
plt.plot(S_5, label = '5th percentile')
plt.plot(S_50, label = '50th percentile')
plt.plot(S_95, label = '95th percentile')
plt.legend()

inf_returns_sim = np.log(S[1:,:]/S[0:-1,:])

plt.figure()
plt.hist(inf_rate, density=True, bins=100, facecolor="LightBlue
    ", label="Historical")
sns.kdeplot(inf_returns_sim.flatten(), color = 'red', label = '
    Simulated', linestyle = '--')
plt.legend()

plt.xlabel('Daily Log Returns')
plt.title('US CPI')
```

Listing C.3: US CPI

C.4 RSA CPI Modelling

We include our calibration code for RSA CPI as detailed in Chapter 4 this document. This script simulates and forecasts South African inflation dynamics using historical Consumer Price Index (CPI) data. It applies a Brownian Bridge technique to interpolate monthly inflation rates into daily estimates, creating a smoother and continuous inflation path. The interpolated values are used to construct a gBm model, projecting future CPI values through Monte Carlo simulations. By generating 10 000 simulated paths, the model produces percentile bands (5th, 50th, and 95th), offering a probabilistic view of future inflation trajectories. The results are visualized alongside historical CPI, highlighting the alignment between simulated and real-world inflation trends. The comparison of simulated and historical inflation returns through kernel density plots provides insights into the accuracy and robustness of the model, essential for economic forecasting and financial planning in the South African context.

```
# -*- coding: utf-8 -*-
"""
Created on Tue Apr  2 19:00:00 2024

@author: dries
"""

import pandas as pd
import numpy as np
import matplotlib.pyplot as plt
import seaborn as sns

file_path_inf = r'C:\Users\dries\OneDrive\Retirement research\SAAJ - DO NOT TOUCH\Data\\Dataset.xlsx'
inflation_data = pd.read_excel(file_path_inf, sheet_name = 'ZAR CPI')
CPI = inflation_data['Price'].values
inf_rate = np.log(CPI[1:]/CPI[0:-1])

np.random.seed(0)
def brownian_bridge(steps, start, end, sims, start_time, end_time):
    dt = (end_time/30)
    W = np.zeros((sims, steps+1))
```

```
    s2=end_time
    s1=start_time
    x1=start
    x2=end
    W[:,0] = x1
    for s in range(1, steps+1):
        t = s * dt
        mean = ((s2-t)*x1+(t-s1)*x2)/(s2-s1)
        var = (s2-t)*(t-s1)/(s2-s1)
        W[:, s] = np.random.randn(sims) * np.sqrt(var)*np.sqrt(
            dt)+mean
        s1 = t
        x1 = W[:, s]
    W[:,-1] = end
    return W

test = np.zeros(int(len(inf_rate)*30))
k = 0
i = 0
while i < len(test)+1:
    if np.mod(i,30) == 0:
        test[i] = inf_rate[k]
        k += 1
        i += 1
        if k == len(inf_rate):
            break
    else:
        test[i:i+30] = np.mean(brownian_bridge(30, inf_rate[k
            -1], inf_rate[k], 1, 0, 1/30), axis = 0)[1:]
        i = i+29

abcd = brownian_bridge(30, inf_rate[k-2], inf_rate[k-1], 100,
    0, 1/30)
plt.figure()
for i in range(len(abcd)):
    plt.plot(abcd[i,:])
plt.plot(np.mean(abcd, axis = 0), color = 'black')

x = np.array(range(0, len(test)))
x2 = np.array(range(0,len(test),30))

plt.figure()
plt.plot(x,test, color = 'black', linewidth = 0.5)
plt.plot(x2, inf_rate, marker = '.', linestyle = 'none', color
```

```
    = 'red')

plt.figure()
plt.plot(x[:91],test[:91], color = 'black', linewidth = 0.5)
plt.scatter(x2[:4],inf_rate[:4], color = 'red')

# inf_rate = test



N = 12 #len(CPI)-1
M = 10000
dt = 1/12
drift = np.mean(inf_rate)
vol = np.std(inf_rate)

sig = vol/np.sqrt(dt)
mu = drift/dt + 0.5*sig**2

S = np.zeros([N,M])
S[0,:] = CPI[0]

Z = np.random.normal(0, 1, size = [N,M])

for i in range(1, N):
    S[i,:] = S[i-1,:] * np.exp((mu-0.5*sig**2)*dt + np.sqrt(dt)
        *sig*Z[i-1,:])


S_5 = np.percentile(S, 5, axis = 1)
S_50 = np.percentile(S, 50, axis = 1)
S_95 = np.percentile(S, 95, axis = 1)
plt.figure()
plt.plot(CPI, label = 'historical')
plt.plot(S_5, label = '5th percentile')
plt.plot(S_50, label = '50th percentile')
plt.plot(S_95, label = '95th percentile')
plt.legend()

inf_returns_sim = np.log(S[1:,:]/S[0:-1,:])

plt.figure()
plt.hist(inf_rate, density=True, bins=100, facecolor="LightBlue
    ", label="Historical")
```

```
104 sns.kdeplot(inf_returns_sim.flatten(), color = 'red', label = '
        Simulated', linestyle = '--')
105 plt.legend()
106
107 plt.xlabel('Daily Log Returns')
108 plt.title('ZAR CPI')
```

Listing C.4: RSA CPI

C.5 FX Rate Modelling

We include our calibration code for FX Rate as detailed in Chapter 4 of this document. This code simulates the USD/ZAR exchange rate using a Geometric Brownian Motion model, projecting future FX rate paths based on historical data. The model uses historical monthly FX rates from a dataset, calculating log returns to estimate the drift and volatility of the process. Monte Carlo simulations (10 000 iterations) are performed to generate potential future exchange rate paths, with the simulated FX rates plotted alongside historical data. Percentile bands (shaded areas) visualise the distribution of simulated outcomes, capturing the uncertainty and variability in future projections. Additionally, kernel density estimates (KDE) compare the distribution of simulated returns against historical returns to assess the accuracy of the model.

A Kolmogorov-Smirnov (KS) test is performed to evaluate the goodness-of-fit between the simulated and historical return distributions, with the resulting p-value indicating the similarity between the two datasets. A higher p-value suggests that the simulated data closely follow the historical distribution, validating the effectiveness of the gBm model in capturing exchange rate dynamics. The visualisation component provides a clear representation of the simulated FX paths, allowing for intuitive comparison with real-world data. This model is valuable for risk management, financial forecasting, and evaluating potential exchange rate scenarios in the context of retirement or investment planning.

```
1 # -*- coding: utf-8 -*-
2 """
```

```
Created on Tue Apr  2 19:00:00 2024

@author: dries
"""

import pandas as pd
import numpy as np
import matplotlib.pyplot as plt
import seaborn as sns
from scipy.stats import kstest

file_path_inf = r'C:\Users\dries\OneDrive\Retirement research\SAAJ FINAL\Data\FINAL DATASET MONTHLY.xlsx'
CPI = pd.read_excel(file_path_inf, sheet_name = 'Prices')['FX'].values
inf_rate = np.log(CPI[1:]/CPI[0:-1])

dates  = pd.read_excel(file_path_inf, sheet_name = 'Prices')['Unnamed: 0'].values

dates_plot = [pd.to_datetime(x) for x in dates]

dt = 1/12

N = len(CPI)
M = 10000

drift = np.mean(inf_rate)
vol = np.std(inf_rate)

sig = vol/np.sqrt(dt)
mu = drift/dt + 0.5*sig**2

S = np.zeros([N,M])
S[0,:] = CPI[0]

Z = np.random.normal(0, 1, size = [N,M])

for i in range(1, N):
    S[i,:] = S[i-1,:] * np.exp((mu-0.5*sig**2)*dt + np.sqrt(dt)*sig*Z[i-1,:])

inf_returns_sim = np.log(S[1:,:]/S[0:-1,:])

```

```
plt.figure()
# plt.hist(inf_rate, density=True, bins=100, facecolor="LightBlue", label="Historical")
sns.kdeplot(inf_returns_sim.flatten(), color = 'red', label = 'Simulated')
sns.kdeplot(inf_rate, color = 'blue', label = 'Historical')
plt.legend()
plt.xlabel('Daily Log Returns')
plt.title('USD/ZAR FX rate')

plt.figure()
ax = plt.subplot(111)
for i in range(1,49):
    plt.plot(dates_plot, np.percentile(S,50+i,axis=1), 'r', alpha = 1-i/50)
    plt.plot(dates_plot, np.percentile(S,50-i, axis=1), 'r', alpha = 1-i/50)
    plt.fill_between(dates_plot, np.percentile(S,50+i,axis=1), np.percentile(S,50+i-1,axis=1), facecolor = 'r', alpha = 1-i/75)
    plt.fill_between(dates_plot, np.percentile(S,50-i,axis=1), np.percentile(S,50-i-1,axis=1), facecolor = 'r', alpha = 1-i/75)
# plt.plot(dates_plot, np.percentile(rho_new,50,axis=0), color = 'white', label = '50 percentile')
plt.plot(dates_plot, np.mean(S, axis=1), color = 'white', label = 'Simulated mean')
plt.plot(dates_plot, CPI, color = 'black', label = 'Historical')

# Shrink current axis's height by 10% on the bottom
box = ax.get_position()
ax.set_position([box.x0, box.y0 + box.height * 0.1,
                 box.width, box.height * 0.9])
# Put a legend below current axis
ax.legend(loc='upper center', bbox_to_anchor=(0.5, -0.15),
          fancybox=True, shadow=True, ncol=3, facecolor = 'lightgrey')
# plt.legend(facecolor = 'lightgrey', location = 'outside')
plt.xlabel('Date')
plt.ylabel('USD/ZAR')
plt.title('USD/ZAR FX Simulation')


```

```
#%% Run goodness of fit test
ks_test = kstest(inf_returns_sim.flatten(), inf_rate)
print('KS-Test p-value = ', ks_test.pvalue)
```

Listing C.5: ZAR USD FX

C.6 ZAR T-bill modelling

We include our calibration code for ZAR T-bill as detailed in Chapter 4 of this document. This code simulates the ZAR 90-day Treasury bill rates using the Cox-Ingersoll-Ross (CIR) model, a popular stochastic process for modelling interest rates. The script begins by importing historical T-bill price data and calculating returns. Ordinary Least Squares (OLS) regression estimates the CIR model parameters: the speed of mean reversion (kappa), the long-term mean (theta), and volatility (sigma). These estimates are used to simulate future paths of the Tbill rate through Monte Carlo simulations, incorporating random shocks via the Brownian motion. The simulation outputs percentile bands around the mean rate, visually comparing simulated paths against historical data to assess the model's ability to capture interest rate dynamics.

The density function of the CIR process is also computed and plotted, illustrating the theoretical distribution of rates based on the estimated parameters. Kernel Density Estimation (KDE) overlays the distribution of simulated returns with the actual historical returns, providing a graphical assessment of fit. A Kolmogorov-Smirnov (KS) test quantitatively evaluates the similarity between simulated and historical return distributions, with the resulting p-value indicating the model's accuracy. This analysis is crucial for financial forecasting, risk management, and pricing fixed-income securities, offering insights into future interest rate movements and their uncertainty.

```
# -*- coding: utf-8 -*-
"""
Created on Mon May 13 16:17:29 2024

@author: dries
"""

```

```
8
9  import numpy as np
10 import scipy as scp
11 import scipy.stats as ss
12 import matplotlib.pyplot as plt
13 from statsmodels.graphics.gofplots import qqplot
14 from scipy.special import iv
15 from scipy.optimize import minimize
16 import pandas as pd
17 from sklearn.linear_model import LinearRegression
18 import seaborn as sns
19 from scipy.stats import kstest
20
21 file_path = r'C:\Users\dries\OneDrive\Retirement research\SAAJ
       FINAL\Data\test_data2.csv'
22 tbill_data = pd.read_csv(file_path)
23 sample = np.flip(tbill_data['Price'].values)/100
24
25 dates  = pd.read_csv(file_path)['DATE'].values
26
27 dates_plot = [pd.to_datetime(x) for x in dates]
28
29 sample_ret = sample[1:] / sample[:-1] - 1
30
31
32 plt.figure(figsize=(10, 5))
33 plt.plot(sample, label="CIR process")
34 plt.legend(loc="upper right")
35 plt.title("Historical Data")
36 plt.xlabel("Date")
37 plt.show()
38
39 def CIR_pdf(x, x0, T, k, t, sig):
40     """
41     Density of the CIR process
42     x: array value
43     x0: starting point,
44     T: terminal time,
45     k,t,s: kappa, theta, sigma
46     """
47     c = 2 * k / ((1 - np.exp(-k * T)) * sig**2)
48     q = 2 * k * t / sig**2 - 1
49     u = c * x0 * np.exp(-k * T)
50     v = c * x
```

```
51
52      return c * np.exp(-u - v) * (v / u) ** (q / 2) * iv(q, 2 *
            np.sqrt(u * v))
53
54  N = len(sample)  # time steps
55  paths = 10000  # number of paths
56  T = N/12
57  T_vec, dt = np.linspace(0, T, N, endpoint = True, retstep=True)
58
59  # formulas for the OLS estimators kappa and theta
60  num = (
61      N**2
62      - 2 * N
63      + 1
64      + sum(sample[1:]) * sum(1 / sample[:-1])
65      - sum(sample[:-1]) * sum(1 / sample[:-1])
66      - (N - 1) * sum(sample[1:] / sample[:-1])
67  )
68  den = (N**2 - 2 * N + 1 - sum(sample[:-1]) * sum(1 / sample
        [:-1])) * dt
69  kappa_OLS = (num / den)
70  theta_OLS = ((N - 1) * sum(sample[1:]) - sum(sample[1:] /
        sample[:-1]) * sum(sample[:-1])) / num
71
72  # residuals of the regression
73  YY = (sample[1:] - sample[:-1]) / np.sqrt(sample[:-1])  #
        response variable
74  XX1 = 1 / np.sqrt(sample[:-1])  # regressor 1
75  XX2 = np.sqrt(sample[:-1])  # regressor 2
76  sigma_OLS = np.std(YY - theta_OLS * kappa_OLS * dt * XX1 + dt *
         kappa_OLS * XX2, ddof=2) / np.sqrt(dt)
77
78  print("kappa OLS: ", kappa_OLS)
79  print("theta OLS: ", theta_OLS)
80  print("sigma OLS: ", sigma_OLS)
81
82  xxx = np.linspace(0.1, 2, 100)
83
84  r = np.zeros([N,paths])
85  r[0,:] = sample[0]
86
87  W1 = np.random.normal(loc = 0, scale = 1, size = [int(N/2)+1,
        paths])
88  Z = np.vstack([W1, -W1])
```

```
89
90  for j in range(1,N):
91      r[j,:] = r[j-1,:] + kappa_OLS * (theta_OLS - np.maximum(r[j
            -1,:],0)) * dt + np.sqrt(np.maximum(r[j-1,:],0)*dt)*
            sigma_OLS * Z[j,:]
92
93  ret_sim = r[1:,:] / r[0:-1,:] -1
94
95  plt.figure()
96  ax = plt.subplot(111)
97  for i in range(1,49):
98      plt.plot(dates_plot, np.percentile(r,50+i,axis=1), 'r',
            alpha = 1-i/50)
99      plt.plot(dates_plot, np.percentile(r,50-i, axis=1), 'r',
            alpha = 1-i/50)
100     plt.fill_between(dates_plot, np.percentile(r,50+i,axis=1),
             np.percentile(r,50+i-1,axis=1), facecolor = 'r', alpha
             = 1-i/75)
101     plt.fill_between(dates_plot, np.percentile(r,50-i,axis=1),
             np.percentile(r,50-i-1,axis=1), facecolor = 'r', alpha
             = 1-i/75)
102 # plt.plot(dates_plot, np.percentile(rho_new,50,axis=0), color
        = 'white', label = '50 percentile')
103 plt.plot(dates_plot, np.mean(r, axis=1), color = 'white', label
         = 'Simulated mean')
104 plt.plot(dates_plot, sample, color = 'black', label = '
        Historical')
105
106 # Shrink current axis's height by 10% on the bottom
107 box = ax.get_position()
108 ax.set_position([box.x0, box.y0 + box.height * 0.1,
109                  box.width, box.height * 0.9])
110 # Put a legend below current axis
111 ax.legend(loc='upper center', bbox_to_anchor=(0.5, -0.15),
112           fancybox=True, shadow=True, ncol=3, facecolor = '
                lightgrey')
113 # plt.legend(facecolor = 'lightgrey', location = 'outside')
114 plt.xlabel('Date')
115 plt.ylabel('90-day Tbill')
116 plt.title('ZAR 90-day T-Bill Simulation')
117
118 # x = np.sort(sample)
119 x = np.linspace(0, sample.max()*1.5, num = 10000)
120
```

```
density_line = np.zeros(len(x))
for i in range(1,len(x)):
    density_line[i] = CIR_pdf(x[i], x[i-1], 1, kappa_OLS,
        theta_OLS, sigma_OLS)

plt.figure()
# plt.hist(inf_rate, density=True, bins=100, facecolor="
    LightBlue", label="Historical")
sns.kdeplot(ret_sim.flatten(), color = 'red', label = '
    Simulated')
sns.kdeplot(sample_ret, color = 'blue', label = 'Historical')
plt.legend()
plt.xlabel('Monthly Returns')
plt.title('ZAR 90-day T-Bill')

#%% Run goodness of fit test
ks_test = kstest(ret_sim.flatten(), sample_ret)
print('KS-Test p-value = ', ks_test.pvalue)
```

Listing C.6: ZAR TBILL SARB DATA